1966

# Static tests on longitudinally stiffened plate girders, June 1966, Publication No. 310 (66-16)

M. A. D'Apice

D. J. Fielding

P. B. Cooper

Submitted to the Welding Research Council Subcommittee
on Lehigh University Welded Plate Girder Project

# STATIC TESTS ON

# LONGITUDINALLY STIFFENED PLATE GIRDERS

by

Michael A. D'Apice

David J. Fielding

Peter B. Cooper

Lehigh University

Fritz Engineering Laboratory Report No. 304.8

May 1966

# TABLE OF CONTENTS

## ABSTRACT

Two series of static tests on longitudinally stiffened plate girders are described. The first series consisted of six static bending tests on six longitudinally stiffened specimens. The experimental variables were the panel size and the longitudinal stiffener size. The primary objectives of this series were: (1) to determine to what extent longitudinal stiffeners can contribute to the resistance of the web to vertical buckling of the compression flange, (2) to determine how the stress redistribution at loads above the theoretical web buckling load is affected by the presence of a longitudinal stiffener and (3) to determine to what extent lateral web deflections can be reduced by the use of a longitudinal stiffener.

The second test series consisted of eight static shear tests on four longitudinally stiffened plate girders. The experimental variables were the panel aspect ratio and the longitudinal stiffener location and size. The primary objectives of these tests were to determine the effect of longitudinal stiffeners on the static behavior of plate girder panels subjected to high shear and to determine the contribution of longitudinal stiffeners to the static shear strength of plate girders.

The test setups and test procedures are described and the results are analyzed and discussed. For the bending tests the longitudinal stiffeners were effective in retarding stress redistribution and in controlling web deflections. However, the longitudinal stiffeners which were used in these tests had no significant effect upon the observed ultimate loads, except for one test where an 11% increase in the ultimate load was realized. From the shear tests it is concluded that the longitudinal stiffeners were effective in controlling web deflections, forcing separate tension fields to develop in the subpanels formed by the longitudinal stiffeners. The shear strengths of the test girders were increased from 6% to 38% due to the longitudinal stiffeners.

## FOREWARD

Prior to 1961 the provisions for the design of steel plate girders in most specifications were based on the theoretical buckling strength of the web. Theoretical and experimental research on transversely stiffened plate girders at Lehigh University has shown that there is no consistent relationship between the ultimate strength and the theoretical buckling strength of a steel girder.[1,2,3,4] Specifications based on this work for transversely stiffened plate girders for buildings are now being used in this country.[5]

In 1963 a new plate girder research project was started at Lehigh University with the general objective of determining the contribution of longitudinal stiffeners to the static load-carrying capacity of plate girders. The experimental phase of this research consisted of six static bending tests on six specimens and eight static shear tests on four girders. The purpose of this report is to describe the testing techniques, to present the test results and to offer the conclusions of the experimental investigation. The results of parallel theoretical studies have been presented separately in another report.[6]

# PART 1: TEST PROGRAM

## 1.1 Introduction

The purpose of Part 1 is to present data on the dimensions and material properties of the test girders and to establish reference loads computed using this data. Before presenting the data, a general description of the test program will be given.

Two different loading conditions were investigated. Using the test setup shown schematically in Fig. 1.1, static bending tests were conducted on six specimens. In these tests only the portion of a girder in the center, pure moment region, was considered to be the test section. Eight static shear tests were conducted on four girders using the test arrangement shown in Fig. 1.2. For these tests the flanges were designed conservatively so that the shear loading would govern the behavior and strength of the girders.

For the bending tests the web slenderness ratio $\beta$ (ratio of web depth to web thickness) and the longitudinal stiffener position $\eta$ (distance from compression flange to stiffener divided by web depth) were kept essentially constant so that the principal variables were the aspect, ratio $\alpha$ (ratio of panel width to web depth) and the size of the longitudinal stiffener. Since structural carbon steel was specified for all the specimens, the material properties did not vary greatly.

The web slenderness ratio was also kept essentially the same for the shear tests so that the main variables were the aspect ratio and the longitudinal stiffener position and size. By using structural carbon steel for all of the shear girders, the material properties were again nearly constant.

The values of the principal geometric parameters for the two series of tests are summarized in Table 1.1. Further details on the design of the specimens and the selection of the values of these parameters will be presented in Parts 2 and 3 of this report.

## 1.2 Girder Dimensions

The cross sections of the test specimens are shown in Fig. 1.3. Since the actual, as-delivered dimensions of the component plates were expected to vary considerably from the nominal sizes shown in the figure, the true dimensions were measured. These measured dimensions were then used to compute the cross-sectional properties used in establishing reference loads.

The actual dimensions of the component plates of the test specimens were obtained from measurements of coupons cut from the various plates prior to fabrication. Figure 1.4 shows the typical locations of these coupons in the specimen component plates for one of the shear girders. Widths and thicknesses of the flange and longitudinal stiffener coupons and the thcikness of the web coupons were measured at the points indicated in Fig. 1.5. In all subsequent

calculations the average values of thicknesses and widths obtained from these measurements, were used. These average values are listed in Table 1.2 for all test specimens.

For specimens LB2 to LB5, where the longitudinal stiffener plates were cut from the web plates, the nominal widths of the longitudinal stiffeners were used and the average thicknesses obtained from measurements on the web coupons were assumed to apply to the longitudinal stiffeners. In all cases nominal values were used for the web depth and the width and thickness of the transverse stiffeners.

## 1.3 Material Properties

Standard tensile tests were conducted to determine the mechanical properties of the component plates. On the coupons in Fig. 1.4 are sketched the locations of the tensile specimens. Two tensile specimens were taken from each web plate coupon (one perpendicular and one parallel to the direction of rolling) and the average values of the measured properties from tests on these two specimens were used to represent the properties of the web plate material. Only specimens parallel to the direction of rolling could be obtained from the flange and longitudinal stiffener coupons. For girders LB1 to LB5, where the longitudinal stiffener plates were cut from the web plates, the material properties determined for the webs were assumed to represent the properties of the stiffeners also.

Since the yield stress is the property used in calculating the reference values, the main emphasis was placed on determining this property. Static yield stress was measured in all the tensile tests.[4] In addition, the percent elongation over an eight inch gage length was determined to provide an indication of the ductility of the material. These properties are listed in Table 1.3 for the components of all the test girders, along with the ladle compositions obtained from the mill test reports. For the web plates, the static yield stress $\sigma_y$ varied from 33.3 ksi to 48.6 ksi while for the flange plates the variation was from 29.4 ksi to 37.6 ksi. The web plates for the bending specimens (LB1-LB6) were ASTM A245 grade C steel and all other plates were ASTM A36 steel.

## 1.4 Reference Loads

Four reference loads were calculated for each test, using the measured dimensions and material properties. These reference loads were used to decide on the load increments for the tests and were later compared with the experimentally obtained ultimate loads. The four reference loads $P_{cr}$, $P_w$, $P_y$ and $P_o$ are listed in Table 1.4 for each of the tests along with the value of the buckling coefficient used in computing $P_{cr}$. They will be referred to in Parts 2 and 3 when the test results are discussed and evaluated.

The first reference load, the theoretical web buckling load $P_{cr}$, was computed from the critical buckling stress[4]

$$\left.\begin{matrix}\sigma_{cr}\\ \tau_{cr}\end{matrix}\right\} = k\,\frac{\pi^2 E}{12(1-\nu^2)}\cdot\frac{1}{\beta^2}$$

where $\sigma_{cr}$ and $\tau_{cr}$ are the critical normal and shearing stresses, respectively. The web buckling coefficient k is dependent on the loading, panel boundary conditions, aspect ratio $\alpha$ and the longitudinal stiffener size. Assuming the web panels to be simply supported on all edges, the k-values for the bending tests were obtained from Ref. 7 while those for the shear tests were taken from Ref. 8. $P_{cr}$ for the bending tests was obtained from

$$P_{cr} = \sigma_{cr}\, S_a/120,$$

where $S_a$ is the section modulus obtained by dividing the moment of inertia of the entire section, including the longitudinal stiffener, by the distance from the neutral axis to the extreme fiber of the compression flange, and 120 is the length of the shear span in inches. For the shear tests, $P_{cr}$ is given by

$$P_{cr} = 2V_{cr} = 2\,\tau_{cr}\, A_w,$$

where $A_w$ is the area of the web.

The working load $P_w$ was calculated using allowable bending stresses $\sigma_w$ and shear stresses $\tau_w$ obtained from the AISC Specification.[5] For these calculations, the presence of a longitudinal stiffener was neglected and nominal values of the cross section dimensions were used, as would be the situation in actual design calculations. For the bending tests $P_w = \sigma_w S_a/120$ and for the shear tests $P_w = 2V_w = 2\tau_w A_w$.

The yield load $P_y$ is defined as the load which causes initiation of yielding in the cross section according to beam theory. $P_y$ for the bending tests was obtained from the expression $P_y = \sigma_y S_a/120$. For the shear tests,

$$P_y = 2V_y = 2\tau_y It/Q,$$

where $\tau_y$ is the yield stress in shear, I is the moment of inertia of the section, Q is the static moment of the area above the neutral axis and t is the web thickness. The yield stress in shear was computed using Mises' yield condition, $\tau_y = \sigma_y/\sqrt{3}$.

The final reference load is the theoretical ultimate strength of a girder without the longitudinal stiffener, $P_o$. For the bending tests this was computed according to Ref. 1, while for the shear tests $P_o$ was computed using tension field theory as described in Ref. 2.

# PART 2: BENDING TESTS

## 2.1 Introduction

The purpose of Part 2 is to describe and discuss the specimens, testing procedure, general girder behavior and the test results for each of the six bending tests.

The primary objectives of the bending tests were to determine:

1) to what extent longitudinal stiffeners can contribute to the resistance of the web to vertical buckling of the compression flange,
2) how the stress redistribution at loads above the theoretical web buckling load is affected by the presence of a longitudinal stiffener and
3) to what extent lateral web deflections can be reduced by the use of a longitudinal stiffener.

In the following discussion points of importance on the test specimens are identified by a coordinate system. The origin of this system is at the geometric center of the web of each specimen, with the x-axis in the longitudinal direction, the y-axis upward in the transverse direction and the z-axis in a direction perpendicular to the plane of the web (see Nomenclature). The side of the specimen in the positive z direction will be called the near

side of the specimen and the side in the negative z direction will be referred to as the far side. Thus all the longitudinal stiffeners were on the near side and all the transverse stiffeners were on the far side.

## 2.2 Test Specimens

Six specimens were tested under pure bending, with one test being conducted on each specimen. Both the specimen and the test on the specimen are identified by the same designation.

For Tests LB1 to LB5, the setup considted of three major sections, two identical end sections (end fixtures) and the test specimen itself (Fig. 2.1). The end fixtures and the test specimens were designed so that they could be bolted together thus permitting the same end fixtures to be used with all five test specimens.

Test specimens LB1 to LB5 were 11 ft. 3 in. long. For each specimen the web was 1/8 in. thick and 55 in deep, the flanges and the end bolting plates were 12 in. wide and 3/4 in. thick and the transverse stiffeners were 3 in. wide and 1/4 in. thick. Both the longitudinal stiffener and the transverse stiffeners were one-sided. The longitudinal stiffener size and the test panel size (spacing between transverse stiffeners) were varied for each individual test specimen (Fig. 2.2) such that the longitudinal stiffener size was the only variable for the first three

test specimens (LB1, LB2, and LB3) and the panel size was the only variable for test specimens LB2, LB4 and LB5 (Table 1.1).

The following criteria were used in designing the first five test specimens. The web was selected so as to have a high web slenderness ratio ($\beta$ range of 400 to 500) while selecting a web plate thickness such that practical size welds could be used. The flanges were designed according to Reference 1, ensuring that neither lateral buckling nor torsional buckling of the compression flange would occur before the yield stress was reached in the flange. The transverse stiffeners were designed conservatively, exceeding the requirements of both the AISC Specification[5] and the AASHO Specification.[9] Longitudinal stiffener sizes were chosen so as to have a low value of stiffener rigidity ratio ($\gamma_s$ = 0, Specimen LB1), an intermediate value ($\gamma_s$ = 33.8, Specimens LB2, LB4 and LB5) and a high value ($\gamma_s$ = 66.2, Specimen LB3), where $\gamma_s$ is the ratio of the stiffener moment of inertia to the moment of inertia of the web and is given by $\gamma_s = 12(1-\nu^2)I_s/bt^3$. These stiffener rigidity ratios are shown in Fig. 2.3. Also plotted in this figure for comparison purposes are the recommended values of stiffener rigidity ratio according to the German Specifications,[10] the British Specifications[11] and the AASHO Specifications[9] (note that the AASHO Specification has been extended above the minimum allowable aspect ratio of 1.0).

The results of the first five tests indicated that another test was needed to provide additional data on the influence of longitudinal stiffener size on the bending strength of a panel. Accordingly, Specimen LB6 was designed and tested. In designing LB6, the nominal web depth and thickness were kept the same as in the first five specimens and square panels ( $\alpha = 1.0$) were used in the test section as in Specimens LB1, LB2, and LB3. The shear spans were designed to be an integral part of the specimen instead of utilizing the end fixtures from tests LB1 to LB5, and the flange plates were reduced from 12" x 3/4" to 10" x 5/8" to make the web behavior more critical to the performance of the girder (Fig. 2.4). The longitudinal stiffener was selected to have the same width as that of Specimen LB2 and a thickness twice as large. The actual stiffener rigidity ratio $\gamma_s$ for Specimen LB6 is plotted in Fig. 2.3.

## 2.3 Test Setup

As previously explained, the setup for Tests LB1 to LB5 consisted of two identical end fixtures bolted to a test specimen. The end fixtures were designed to resist the combined effects of the shear forces and bending moments present (See References 2 and 3 for design criteria), and their function was to transverse the bending stresses from the loading system to the test specimen. These end fixtures are shown in Fig. 2.5. The location of the end supports and loading points for test LB6 was the same as for the

other tests, however, Specimen LB6 was a continuous girder with integral shear spans serving the purpose of end fixtures (Fig. 2.4).

In the joints between the test specimens and end fixtures in Tests LB1 to LB5 (Fig. 2.5), 1 in. diameter high strength steel bolts were tightened to a tensile stress of approximately 10,000 psi except for the bottom eight bolts in each joint which were tightened to approximately 50,000 psi (approximate yield stress of the bolts). This pattern of tightening the bolts permitted the reuse of the top ten bolts of each joint.

Specimens LB1 through LB4 had one test panel (center panel) and two adjacent side panels (Fig. 2.2) while Specimen LB5 had two test panels and two side panels (Fig. 2.2). The function of these side panels was to further distribute the bending stresses throughout the depth of the girder. Specimen LB6 had two identical test panels and two side panels in the center, pure moment region (Fig. 2.4).

The only measurements taken outside of the test panels were level readings at the supports which were used to correct the center line deflection readings for support settlement. All other test data was obtained from the test panels only. Therefore any portion of the test setup outside of the test panels was considered to be part of the loading system and any failure in these sections was not considered as a failure of the test specimen.

The loading system consisted of two 220 kip Amsler hydraulic jacks. These jacks were supplied with oil fed through a common distributor by an Amsler Pendulum Dynamometer which measured the load (P) that was present on one hydraulic jack only. The loading system and the test setup are shown in Fig. 2.6.

Intermittent lateral support of the compression flange was provided by 2 ½ in. diameter pipes which were pinned to the test specimen and the loading fixtures at one end and to a lateral support beam at the other end. This pinned arrangement allowed the test specimen to move in a vertical direction only, restraining lateral movement in either direction. The lateral supports were located at the transverse stiffeners which bounded the test panels, at the bolted joints and at the loading points.

During the testing of the first five specimens certain modifications of the loading fixtures were required to obtain a satisfactory transfer of stress to the center test panel. Reinforcing plates were required at the bottom of the bolted joint (Fig. 2.7) to prevent excessive deformation of the end plates of the test specimen. This excessive deformation caused additional bending stresses in the bottom bolts and led to a failure of the bottom two bolts in the first test of the series. Reinforcement was also required at the compression flange in the side panels (Fig. 2.7) to prevent yielding of the compression flange in this zone (side panels) before yielding was obtained in the test panel compression flange.

After this additional reinforcement was added no further difficulties were experienced and all failures occurred in the center panels of the test specimens.

## 2.4 General Girder Behavior

The testing history and general behavior of any one test specimen can be traced with the aid of the load-versus-center line deflection curve for the particular specimen (Figs. 2.8 through 2.13). The applied load P on each hydraulic jack was measured as explained in Sect. 2.3 and the vertical deflection at the center line of the specimen ($v_{\mathbb{C}}$) was measured with a dial gage mounted on the floor of the test bed. The dial gage readings provided a control on the testing speed, gave an indication of the behavior of the specimen during testing and were also used to determine when the ultimate load had been attained. Scales mounted on the bearing stiffeners at the supports were read with an engineer's level to determine the support settlements. These support settlement readings were used to correct the center line deflection readings which are plotted in Figs. 2.8 through 2.13.

In the P-$v_{\mathbb{C}}$ curves (see for example Fig. 2.10) the load P is plotted as the ordinate and the corrected center line deflection is plotted as the absissa. Also shown in the figure is a sketch of the girder before and after the application of the two applied loads (P). The numbered circles indicate positions on the curve where the loading was stopped and measurements taken. These

positions are referred to by the load numbers next to the circles. The values of the reference loads $P_w$ and $P_{cr}$ are also plotted together with the observed ultimate load $P_u^{ex}$.

The first loading cycle consisted of loading the test specimen until inelastic behavior was observed (indicated by more rapid increase in deflection per unit load) and then returning to zero load. A second cycle was then started and continued until the ultimate load of the test specimen was attained. In any welded structure residual stresses are present which affect measurements to the extent that readings taken during an initial loading cycle may be misleading.[12] The first loading cycle was intended to partially relieve the effects of residual stresses on the measurements taken during the second cycle.

Initially (Fig. 2.10, load Nos. 1 through 14), web deflections and strain measurements were taken at load increments which were selected to insure that at least seven such sets of readings were obtained. In the inelastic range (Fig. 2.10, load Nos. 15 through 20) the procedure was to load the specimen until a certain predetermined center line deflection was obtained and then to allow the load to stabilize as the deflection was held constant. All measurements were taken after the load had stabilized. This same procedure was followed in all the test specimens except Specimen LB2. For this specimen the load was held constant in the inelastic range and the center line deflection was allowed to increase until

it stabilized (Fig. 2.9, load Nos. 15 through 18). However, this procedure required an excessive waiting period and therefore it was not used in testing the other specimens.

## 2.5 Strain Distribution

Strain measurements were taken at the center line of the test panel ($x = 0$) for various load points, using electrical resistance strain gages. The measured strains at four different loads are plotted to show the strain distribution throughout the depth of each test specimen (Figs. 2.14 through 2.19). Using Specimen LB3 as an example (Fig. 2.16) a typical strain distribution plot will be explained.

The various strain gage positions are shown in Fig. 2.16. At each of these positions is plotted the strain at the center of the web, obtained by averaging strain readings from two gages located opposite each other on the web surface, for loads of $0^k$ (second load cycle), $80^k$, $120^k$ and the ultimate load. The plotted points have been connected by straight lines. In a separate graph (same figure) the variation in strain at two points (labeled A and B) can be traced from a load of $0^k$ (second cycle) to the ultimate load. In this plot the strain is plotted as the absissa and the load P as the ordinate.

## 2.6 Web Deflection

Lateral web deflections were measured using a specially designed device. This device consisted of a portable rigid truss to which dial gages were attached at certain y-coordinate points (Fig. 2.20). By placing the measuring device at x-coordinate stations and reading the gages, the deflected configuration of the test panel web was obtained. Reference measurements were taken after every set of readings using a milled steel surface to check against accidental movement of the dial gages. Measurements were taken at several cross sections in the test panels.

The deflected web shapes are given for the six test specimens in Figs. 2.21 through 2.26. Specimen LB3 (Fig. 2.23) will again be used to explain a typical web deflection plot. The measured deflections were plotted at the y-coordinate points and then connected with straight lines. The deflected shapes shown in Fig. 2.23 are for load Nos. 8, 12, 14 and 20 ($0^k$, $80^k$, $120^k$ and the ultimate load). The inserted sketch of the test panel indicates the cross sections A and B where the web deflections were taken. In the two graphs on the right the lateral deflections at the longitudinal stiffener during the second load cycle (load Nos. 8 through 20) are plotted as the absissa and the load P as the ordinate.

## 2.7 Ultimate Load and Mode of Failure

### Specimen LB1

Two separate tests were conducted on this specimen. In the first test, which was also the first test in the program, a failure occurred outside the test panel (center panel), at the bolted joint. The second test, which was the fifth test in the series, consisted of testing the same specimen after it had been reinforced as previously explained. In this test, yielding of the compression flange was first observed between load Nos. 36 and 37 and the ultimate load attained was 156.5 kips. General yielding of the compression flange (yielding throughout the entire flange thickness) was the factor which determined the ultimate load. There were also indications of possible torsional buckling of the compression flange.

Figure 2.27 shows the completely yielded compression flange in the test panel area after the second test, as viewed from below the compression flange on the near side. The tilting of the compression flange in Fig. 2.28 indicates the tendency toward torsional buckling of the compression flange and it also clearly shows that yielding had penetrated through the thickness of the flange. The yield line patterns across the width of the compression flange can be seen in Fig. 2.29. The effectiveness of the reinforcement outside of the test panel is demonstrated in this figure by the absence of yield lines in the reinforced area.

Specimen LB2

This specimen was reinforced in the bolted joint area before testing to prevent a bolt failure similar to that which occurred in the first test on Specimen LB1. Yielding of the compression flange was first observed at load No. 15 and yielding of the longitudinal stiffener started at load No. 17. The ultimate load of this specimen was 152.0$^{k}$ with the controlling factor again being general yielding of the compression flange at both ends of the test section. This yielding developed outside of the test panel (in the side panels) however, and when the specimen was strained beyond the ultimate load vertical buckling of the compression flange occurred in the yielded portion. A second test was attempted after reinforcing the compression flange in the side panel areas but the reinforced specimen was unable to sustain loads as high as those in the first test.

Figure 2.30 shows the vertical buckle as viewed from the near side of the specimen. Buckles in the longitudinal stiffener are also evident in this photo. Figures 2.31 and 2.32 show the extent of yielding in the compression flange and also the damage to the web of the specimen. Figure 2.31 was taken from the near side of the specimen and Fig. 2.32 was taken from the far side.

Specimen LB3

As a result of the behavior of the first two specimens, Specimen LB3 was reinforced at both the compression flange (in the side panel zones) and the bolted joint before it was tested. The compression flange was first observed to yield at load No. 15. Yielding and buckling of the longitudinal stiffener took place at load No. 19. The ultimate load for the specimen was $150^{k}$ with general yielding of the compression flange being the controlling factor.

In Fig. 2.33 the extent of yielding in the compression flange after the test is clearly shown. Buckling of the longitudinal stiffener is also evident in this figure (view is from the near side of the specimen). Figures 2.34 and 2.35 show the yield patterns present across the width of the compression flange and also the buckled shape of the longitudinal stiffener (Fig. 2.34).

Specimen LB4

Specimen LB4 was reinforced before testing in the same manner as Specimen LB3. First yielding of the compression flange occurred at load No. 15; deformation of the longitudinal stiffener began between load Nos. 15 and 16 with the longitudinal stiffener buckling at load No. 18. The ultimate load attained for this specimen was $147^{k}$ with general yielding of the compression flange being the controlling factor. The specimen was then strained beyond the ultimate load until vertical buckling of the compression flange took place in the test panel.

Figures 2.36 and 2.37 show the yielded compression flange after the ultimate load was reached. Also visible in Fig. 2.36 are the buckles in the longitudinal stiffener. In Fig. 2.37 a tendency toward lateral buckling can be seen from the distribution of yield lines. Figures 2.38 and 2.39 show the specimen after vertical buckling. Extensive damage to the web is clearly shown in each figure. Figure 2.38 is a view from the near side and Fig. 2.39 from the far side.

Specimen LB5

Specimen LB5 was reinforced in the same manner as Specimens LB3 and LB4. First yielding of the compression flange was observed at load No. 15 and noticeable bending of the longitudinal stiffener began between load Nos. 17 and 18. At load No. 21 the longitudinal stiffener was severely buckled. The ultimate load of the specimen was $150.8^{k}$ with general yielding of the compression flange in the two test panels controlling.

Figure 2.40 shows the yielded compression flange and the severely buckled longitudinal stiffener as seen from the near side of the specimen. Figure 2.41 shows the compression flange as viewed from the far side. The two test panels are also clearly shown by this photo. Figure 2.42 shows the yield line pattern present across the width of the compression flange in both test panels.

Specimen LB6

Specimen LB6 was designed and tested after the completion of the other five tests to provide additional data on the influence of the size of the longitudinal stiffener on the bending strength. The specimen was a continuous girder without a bolted joint between end fixtures and test section (Fig. 2.4). In the test on Specimen LB6, yield lines on the top of the compression flange were first observed at load No. 4, and by load No. 5 yielding on the bottom surface of the compression flange was detected. Some yielding in the web adjacent to the compression flange was visible at load No. 12. Just prior to load No. 13, a loud rumble was heard accompanied by a slight drop in load.* Yielding on the longitudinal stiffener was first observed at load No. 13. The ultimate load of 112.8$^{k}$ was attained at load No. 14 with general yielding of the compression flange being the controlling factor.

After the ultimate load test had been completed (load No. 16), the specimen was subjected to additional straining until a failure occurred. The P vs. $v_{\mathbb{E}}$ curve for this "destructive test" is plotted in Fig. 2.13. A much higher strain rate was used, causing a slight increase in the measured load during the first portion of the destruction test. Beyond this point the load gradually decreased as the deflection increased and, at an additional centerline

* It was later determined from strain and web deflection readings that the longitudinal stiffener buckled at this point.

deflection of about one inch, failure occurred due to vertical buckling of the compression flange in one of the test panels.

The extent of yielding in the compression flange at the end of the ultimate load test (load No. 16) is shown in Fig. 2.43, while the buckling of the longitudinal stiffener and yielding in the near side of the web at the same load are evident in Fig. 2.44. The deformations which developed when the compression flange buckled into the web, terminating the "destruction test", are shown in Fig. 2.45, taken from the near side after testing had been completed.

## 2.8 Discussion

One of the strongest impressions left by the tests was the similarity in the behavior of the first four specimens which had longitudinal stiffeners (Specimens LB2, LB3, LB4 and LB5). For each of these specimens a definite sequence of events leading to the attainment of ultimate load can be traced. Local yielding of the compression flange was the first observed event. As the applied load was increased, yielding and then local buckling of the longitudinal stiffener occurred. Finally, the compression flange became completely yielded and at this stage the ultimate load was reached.

Because the longitudinal stiffener of Specimen LB6 had a lower width-thickness ratio than the longitudinal stiffeners of the other specimens (8 as opposed to 16 for Specimens LB2, LB4, and LB5 and 20 for Specimen LB3), the resistance to local buckling was higher and a somewhat different sequence of events was observed during the test. Yielding of the compression flange was observed first, as was the case in the four tests discussed above. However, no yielding was evident on the longitudinal stiffener until after the stiffener had buckled. Also, overall buckling of the stiffener of Specimen LB6 was observed while the stiffeners of Specimens LB2 to to LB5 buckled locally, and this buckling occurred suddenly rather than in a gradual manner as was the case in Specimens LB2 to LB5. The ultimate load was reached as a result of general yielding of the compression flange; however, unlike the other four specimens, the magnitude of the ultimate load was affected by the longitudinal stiffener as discussed below.

Previous research has demonstrated that the bending strength of a transversely stiffened plate girder is not directly related to the theoretical web buckling load[1,2,3,4]. The tests described in this report show that there is no rational correlation between the theoretical web buckling load the bending strength of a longitudinally stiffened plate girder. $P_{cr}$ for the four longitudinally stiffened specimens with the same web thickness (LB2 to LB5) ranged from 81.1 kips to 81.7 kips, more than five times the 15.1 kip value computed for Specimen LB1, which had no longitudinal

stiffener (Table 2.1). However, the experimentally obtained ultimate loads for these same five specimens ranged from 147.0 kips to 156.5 kips, with little difference between $P_u^{ex}$ for the longitudinally stiffened specimens and $P_u^{ex}$ for LB1.

One of the main objectives of the tests was to determine to what extent longitudinal stiffeners can contribute to the resistance of the web to vertical buckling of the compression flange. Vertical buckling of the compression flange did occur in three of the specimens (LB2, LB4 and LB6), but only after the ultimate load had been attained and the compression flange had been subjected to additional straining. Thus the tests indicate that longitudinal stiffeners have no direct influence on the resistance to vertical buckling. They can have an indirect influence, however, by increasing the ultimate load through control of web deflections and reduction of the stress redistribution from the web to the compression flange.*

In the last column of Table 2.1, the ratio of the experimentally obtained ultimate load to the theoretical ultimate load for the girder without longitudinal stiffeners is listed for each test. A comparison of this $P_u^{ex}/P_y$ ratio for the first five tests indicates that the longitudinal stiffeners had little, if any, influence on the magnitude of the ultimate loads. For the test on Specimen LB6, the longitudinal stiffener resulted in an 11% increase in the ultimate load.

* This topic is discussed in more detail in Ref. 6.

It has been observed in tests on transversely stiffened plate girders[1,4] that, at loads above the theoretical web buckling load, a redistribution of stress from the compressed portion of the web to the compression flange takes place. As is evident from the strain distribution plots in Fig. 2.14, this stress redistribution was also present in the specimen without a longitudinal stiffener, Specimen LB1. The effect of the longitudinal stiffeners of Specimens LB2 to LB6 on the strain distribution can be seen in Figs. 2.15 through 2.19. At loads up to $P_w$ and above, the measured strain distributions were quite close to the linear distribution predicted by beam theory. Only after a longitudinal stiffener had buckled did any significant redistribution of strain to the compression flange occur, and even at this point, the strain at the stiffener was markedly higher than it would have been at the same position if no stiffener were present. In most cases the strain at the stiffener reached or exceeded the yield strain by by the time that the ultimate load was reached.

Because of the stress redistribution described in the previous paragraph, the ultimate load of a plate girder will generally be below that required to initiate yielding in the extreme fiber according to beam theory. The values of the ratio $P_u^{ex}/P_y$ in Table 2.1 indicate that, with the exception of Test LB6, predictions of ultimate loads based on beam theory would overestimate the bending strength of the test specimens by 10 to 12%.

Another objective of the test program was to determine to what extent lateral web deflections can be reduced by the use of a longitudinal stiffener. The effectiveness of the longitudinal stiffeners of Specimens LB2 through LB6 can be judged qualitatively with the aid of Figs. 2.21 through 2.26, but a more accurate evaluation of the stiffener's ability to control web deflections can be made with the information presented in Table 2.2. In the fourth column of the table, listed for each girder, is the maximum value of lateral web deflection which was measured at the longitudinal stiffener at the working load, $(w_w)_{max}$. In the next column is listed the deflection measured at the same position when the applied load was zero, $w_o$. The percent increase in lateral web deflection between zero load and the working load is given by $\Delta_w = \left[(w_{w_{max}} - w_o)/w_o\right] \times 100$ and is listed in the last column of Table VI. Since $\Delta w$ for Specimen LB1 with no longitudinal stiffener is 140% while the largest value of $\Delta w$ for the five girders with longitudinal stiffeners is only 40%, it is evident that the stiffeners were very effective in controlling web deflections at the working load. As can be seen from Figs. 2.21 through 2.26, the web deflections increased rapidly only after the longitudinal stiffener had buckled.

The effect of the principal test variables, aspect ratio ($\alpha$) and stiffener rigidity ratio ($\gamma_s$), can also be evaluated from Table 2.2. From the data for the four specimens with a constant aspect ratio of 1.0 and with varying stiffener rigidities (Specimens

LB1, LB2, LB3, and LB6) it is seen that larger stiffener rigidities result in more effective web deflection control. For girders of the same depth, the aspect ratio influences the effectiveness of a stiffener since it determines the distance the stiffener must span between transverse stiffeners. Thus, for Specimens LB2, LB4 and LB5, which had the same stiffener rigidity but different aspect ratios, the specimen with the largest aspect ratio was least effective in controlling web deflections.

In summary, the tests demonstrated that longitudinal stiffeners can be very effective in controlling lateral web deflections and in maintaining a linear strain distribution up to the point where local buckling of the stiffener occurs. However, for the stiffener sizes used in these tests, no significant effect on the magnitude of the ultimate load was apparent except for Specimen LB6 where an 11% increase in the ultimate load was observed. A discussion of the proportioning of longitudinal stiffeners and of predicting the bending strength of longitudinally stiffened plate girders has been presented in a separate report.[6]

## 2.9 Summary

It can be concluded from the six bending tests described in Part I that there is no rational correlation between the theoretical web buckling load and the bending strength of a longitudinally stiffened plate girder. The test results can be summarized as follows:

1. In all of the tests, the ultimate load was reached as a result of general yielding of the compression flange.
2. Vertical buckling of the compression flange was observed in three tests; in all cases this occurred when the specimen was strained beyond the ultimate load.
3. The longitudinal stiffeners which were used in these tests had no significant effect upon the observed ultimate loads, except for Specimen LB6 where an 11% increase in the ultimate load was realized.
4. The longitudinal stiffeners had a significant effect upon the strain redistribution in the girders, causing the strain distribution to remain approximately linear until the longitudinal stiffener buckled.
5. The longitudinal stiffeners were very effective in controlling web deflections up to the loads at which the stiffeners buckled, but doubling the moment of inertia of the longitudinal stiffener did not decrease the web deflection by any significant amount.

# PART 3: SHEAR TESTS

## 3.1 Introduction

It has been shown both analytically and experimentally that for transversely stiffened plate girders subjected to high shear, a significant post-buckling strength is available through the development of tension field action.[2,4] Anchored by the flanges and transverse stiffeners, a field of diagonal tensile stresses forms in each panel so that the girder behaves in a manner similar to a Pratt truss. The introduction of a longitudinal stiffener in such a shear panel could result in a considerable rearrangement of the distribution of forces in the panel and in an increase in the shear strength. Accordingly, the objectives of this part of the investigation were to determine the effect of longitudinal stiffeners on the static behavior of plate girder panels subjected to high shear and to determine the contribution of longitudinal stiffeners to the static shear strength of plate girders.

## 3.2 Test Specimens and Setup

In Fig. 3.1 the sketches of test girders LS1 to LS4 show the plate sizes and stiffener locations. Overall girder length was 27 feet 6 inches. The basic design criterion was that the material properties and panel geometry should be the same or similar to those of the transversely stiffened plate girders previously tested in

shear (Girders G6 and G7, Ref. 4). Practical ranges of the aspect ratio ($0.75 \leq \alpha \leq 1.5$) and longitudinal stiffener position ($0.2 \leq \eta \leq 0.5$) were used. Longitudinal, transverse, and bearing stiffeners were designed according to available theory.[6,13] The longitudinal stiffeners and the transverse stiffeners were one-sided, but the bearing stiffeners, located at the end supports and at the point of load application, were symmetrical with respect to the plane of the web. To ensure that the girders would fail in shear, the flange plates were designed conservatively.

One end of Girder LS1 (the first test girder) had no longitudinal stiffener; the test on this part of LS1 was referred to as T1, a control test. The other half of this same girder had a longitudinal stiffener which made it stronger than the tested portion, and this end was tested as LS1-T2, the second test on Girder LS1. A test on Girder LS2 further investigated the effect of stiffener size, three tests on Girder LS3 checked the effect of aspect ratio, and two tests on LS4 investigated the effect of two stiffener locations different from that of LS1, LS2 and LS3.

The girders were tested in a hydraulic universal testing machine. As shown in Fig. 3.2 the girders were simply supported at their ends by rollers, and the load was applied at midspan. Load was transferred from the machine crosshead to a girder through a spherical bearing block which also supplied lateral bracing to the compression flange at this point. Additional lateral bracing was

provided at the quarter points by steel pipes. This bracing was designed to permit sufficient vertical deflection of the girder by pinning the pipes to the girder and to a rigid beam connected to the testing machine.

## 3.3 Test Procedure

A convenient record of the testing history and general behavior of the shear girders is presented in the load-versus-center line deflection curves (Figs. 3.3 to 3.6), similar to those for the bending girders.

The test procedure was the same as that used for the bending girders (see Sect. 2.4). The first loading cycle consisted of loading the girder until inelastic behavior was observed, then returning to zero load (for example, Load Nos. 1 to 7, Fig. 3.3). A second loading cycle started with zero load (Load No. 7) and was terminated when the ultimate load was attained, as indicated by a substantial increase in deflection with no accompanying increase in load. At predetermined load increments in the elastic range and at predetermined center line deflection increments in the inelastic range, the load was stabilized and web deflection and strain measurements were taken.

Failure occurred in the first test on Girder LS1, test LS1-T1, in the three panels which were not longitudinally stiffened. The three panels with longitudinal stiffeners were not damaged at this stage. To permit a test on these undamaged panels, the failed

panels were reinforced by welding stiffeners along the tension diagonals. This repair is indicated on the P vs. $v_{\mathbb{C}}$ curve (Fig. 3.3) by a weld symbol at Load No. 19 and is shown in detail in Fig. 3.7a. For Girders LS3 and LS4, as well as Girder LS1, this method of repair proved to be an excellent means of reinforcing damaged panels so that tests of undamaged panels could be conducted.

The second test on Girder LS1 (Load Nos. 19 to 35) was conducted in a manner similar to that of the first test. At the end of test T2, the girder was subjected to a destruction test (Load Nos. 35 to 38) which was terminated after the load-carrying capacity was reduced by about ten percent. This destruction test was carried out only to observe the deformation capacity of the girder and thus the only readings taken after Load No. 35 were centerline deflection readings using an engineer's level and a scale mounted on the web at mid height.

The procedure used in testing Girders LS2, LS3 and LS4 was similar to that described above for Girder LS1. A record of the testing history of these girders is provided by their respective P vs. $v_{\mathbb{C}}$ curves shown in Figs. 3.4 to 3.6. The repairs for Girders LS3 and LS4 are shown in Fig. 2.7b, c and d. Since all six panels of Girder LS2 failed during the first test, a second test on this girder was not possible.

## 3.4 Behavior and Ultimate Loads

### Girder LS1

There were two tests on Girder LS1. The first one was a control test on the end of the girder which had three square panels with no longitudinal stiffeners. Between Load Nos. 13 and 14 (refer to Fig. 3.3) yielding began along the tension diagonals, starting in the end panel. When Load No. 14 was reached, yielding was evident along the diagonals of all three panels, as shown in Fig. 3.8. This yielding became more pronounced by the time the ultimate load of 363.5 kips was reached. The girder was unloaded to zero kips at Load No. 18 to complete test T1.

The repairs (diagonal stiffeners) after test LS1-T1 are shown in Fig. 3.9, a photograph taken after the destruction test. Test LS1-T2 began with Load No. 19, and the load-deflection curve (Fig. 3.3) indicates that the linear portion between Load Nos. 19 and 26 is steeper than the unloading line for test T1. This is the result of strengthening the failed panels with the diagonal repair stiffeners. For this test, as in test T1, the aspect ratio was 1.0, but a longitudinal stiffener was present at $\eta = 0.33$ in the test panels. Diagonal yield patterns formed in the subpanels as distinctly separate diagonal strips, as shown in Fig. 3.10, taken at Load No. 35. In the upper subpanels, horizontal and vertical yield lines formed. The ultimate load was 414.0 kips (Load No. 29). The appearance of the girder after the destruction

test (Figs. 3.9 and 3.11) provides visual evidence of the effectiveness of the repair stiffeners on one end of the girder and the development of separate tension fields in the six subpanels at the other end of the girder.

Girder LS2

Girder LS2 had 4 in. x 1/2 in. longitudinal stiffeners at $\eta = 0.33$ in three square panels at one end and 5 ½ in. x 1 in. stiffeners at $\eta = 0.33$ in the three square panels at the other end. The three panels with stronger stiffeners began yielding before the other three panels had failed, so only one test was obtained from the specimen. Figure 3.12 shows the extent of yielding in the stronger end and Fig. 3.13 shows the weaker end at the same load (Load No. 18). In both figures separate tension diagonals in the subpanels are evident, with more pronounced yielding in the outermost panels. The ultimate load was 315.5 kips (Load No. 17). The appearance of the specimen after the destruction test is shown in Fig. 3.14. Note the white unyielded strips on the web at the location of the longitudinal stiffeners. These stiffeners are on the side of the web which is not visible in Fig. 3.14.

Girder LS3

One end of Girder LS3 had two panels with $\alpha = 1.5$ while the other end had four panels with $\alpha = 0.75$. A continuous longitudinal stiffener was located at $\eta = 0.33$ throughout the girder length. Test T1 was conducted on the end panel with an aspect ratio of 1.5

and a 2 in. x ½ in. longitudinal stiffener. The ultimate load, 278.5 kips, was reached at Load No. 13 after the longitudinal stiffener had failed and the web had buckled together with it. Figure 3.15 shows the buckled stiffener. After Load No. 15 this end panel was reinforced with a diagonal stiffener.

Test T2 was conducted on the other panel with $\alpha = 1.5$. This panel had a 3 ½ in. x ½ in. longitudinal stiffener. Again the horizontal and vertical yield line patterns were observed with a tension diagonal forming in the lower subpanel (Fig. 3.16). The test was ended when extensive yielding had developed along the tension diagonal at an ultimate load of 296.0 kips (Load No. 21). The girder was unloaded (Load No. 25) and a diagonal stiffener was placed in the failed panel.

In test LS3-T3 the four panels on the + x end of Girder LS3 had an aspect ratio of 0.75 and a longitudinal stiffener equal in size to that of LS3-T2 (3 ½ in. x ½ in.). The ultimate load was 338.0 kips (Load No. 35). Figure 3.17 shows the yield patterns and deformations in the girder after the destruction test. In this photograph the effectiveness of the repair stiffeners is again evident from the lack of yielding in the reinforced panels.

Girder LS4

The two halves of Girder LS4 were identical except that the longitudinal stiffener on one end was at $\eta = 0.2$ while on the other end it was at $\eta = 0.5$. Because of this single difference, it was

not known which end would fail first. After test T1 had been completed it was obvious that the end with $\eta = 0.5$ had failed; this occurred at an ultimate load of 380.5 kips (Load No. 18). Figure 3.18 shows the familiar yield patterns, and again the end panels had the most advanced yielding. This photograph was taken at the end of test T1 (Load No. 19) after the girder was unloaded. Diagonal stiffeners were welded along the tension diagonals to prepare for test T2.

The stronger end of the girder with $\eta = 0.5$ reached its ultimate load at 405.5 kips (Load No. 28) when tension diagonals could be seen in all six subpanels. This is shown in Fig. 3.19, a photograph taken after the destruction test had been completed. As in the other tests, the effectiveness of the repair stiffeners and the development of separate tension diagonals in the subpanels are well illustrated in this photograph.

## 3.5 Web Deflections

Lateral web deflections were measured at selected cross sections in the test panels, using the device described in Sect. 2.6 (Fig. 2.20). In tests LS1-T1 and T2, LS2-T1, and LS3-T1 and T2 web deflections were measured at the fifth-points (x-coordinates) of each panel. Measurements for LS3-T3 were made at the third-points of each panel, and for LS4-T1 and T2 they were made at the panel mid-points. Reference measurements on a milled steel surface were taken after each set of readings to check against accidental

movement of the dial gages. Figures 3.20 to 3.27 shows girder cross sections with the measured out-of-plane web deflection superimposed.

The web deflections were plotted relative to the reference surface at the various y-coordinate points and then connected with straight lines. Figure 3.23, a typical web deflection plot, shows deflected shapes for Load Nos. 7, 10, and 13 ($0^k$, $180^k$, and $278.5^k$). At x = - 140, there is a valley in the upper subpanel; at x = - 125, the valley is lower in the cross section and it is deeper; the valley is still lower in the x = - 110 cross section; and finally, at x = - 95 the valley has reached the tension flange. These valleys will be discussed later.

## 3.6 Web Strains

For LS1-T2 and LS2-T1 strain rosettes were placed in the end panels, one gage on each side of the web at the center of each of the two subpanels. Their purpose was to measure three strains, thereby making possible the calculation of principal strains and stresses and their inclinations.

Figures 3.28 and 3.29 show the principal stresses for the various Load Nos. indicated. Tensile stresses are shown as arrows directed away from the point at which the gage was located, and compressive stresses are shown as arrows directed toward it. The solid arrows show measured strain results and the dashed arrows

represent the stresses which were calculated from beam theory. A discussion of these figures and a comparison between measured and computed stresses is presented in Sect. 3.8.

## 3.7 Strains in Longitudinal and Transverse Stiffeners

Strains were measured on the longitudinal stiffeners midway between the transverse stiffeners. Four strain gages were located around the stiffeners as indicated in Fig. 3.30. On the transverse stiffeners, strains were measured midway between the longitudinal stiffener and the flanges, using the same locations as in Fig. 3.30. The purpose of these measurements was to provide a means of estimating the axial forces carried by the stiffeners. Some of the data obtained from gages on the longitudinal stiffeners in four tests is plotted in Fig. 31. The plotted points for several Load Nos. are connected with straight lines in this figure to indicate the strain distribution across the stiffener section.

The results of a few tests indicate that an effective width of about twenty thicknesses of the web acts with the stiffener in resisting lateral bending.[14] Using this approximation, the location of the neutral axis at Section A-A (Fig. 3.32) has been calculated and used to separate analytically axial strains from transverse bending strains.

Axial strains calculated in this manner are plotted as abscissas and static loads as ordinates in Figs. 3.33 to 3.38. Each plotted point is marked by its corresponding load number to indicate the corresponding position on the load-deflection curve. Superimposed on these plots are the theoretical elastic load-strain curves calculated using beam theory. These beam theory strains represent the strains due to bending in the plane of the web and are obtained from $\epsilon_b = \frac{M_x y}{EI}$, where $M_x$ is the bending moment at the longitudinal location where strains were measured and y is the location of the stiffener above the neutral axis of the girder cross section.

Axial transverse stiffener strains were obtained by averaging the four strain gage results. These average axial strains have been plotted as abscissas and static loads as ordinates in Figs. 3.39 to 3.43.

The load-versus-axial strain plots for the longitudinal and transverse stiffeners are discussed in Sect. 3.8.

## 3.8 Discussion

### Ultimate Loads

The measured experimental ultimate loads ($P_u^{ex}$) are listed in Table 3.1. In order to compare these with theoretical values, ratios of $P_u^{ex}$ to the reference loads were calculated and are listed in the last three columns of Table 3.1. Since web buckling theory was used in computing $P_{cr}$, it is obvious from the high $P_u^{ex}/P_{cr}$

ratios that this theory underestimates the shear strength of a panel considerably.

The beam theory yield load $P_y$ does not provide an accurate prediction of the shear strength either, judging by the values of $P_u^{ex}/P_y$ in Table 3.1. The distribution of stresses in a panel subjected to high shear is radically different from that assumed in beam theory because of the large lateral web deflections.

Using Basler's theory,[2] $P_o$ was calculated for the test girders ignoring the presence of the longitudinal stiffener. Thus the $P_u^{ex}/P_o$ values listed in Table 3.1 indicate the increase in shear strength due to the longitudinal stiffener for each test. In test LS1-T1 no longitudinal stiffener was present and the $P_u^{ex}/P_o$ ratio shows experimental agreement with Basler's theory within 3%. For the other tests, the static shear strength was increased by the longitudinal stiffeners from 6% to 38% with an average increase of 17%. Thus, the longitudinal stiffeners added considerably to the shear strengths of the test girders.

Lateral Web Movement

The results of the lateral web deflection measurements have been presented for the end panel of each test (Figs. 3.20 to 3.27) because these panels yielded first despite the lower bending moment present. Comparing the deflected web shape in LS1-T1 (no longitudinal stiffener) to the other plots, it is obvious that the longitudinal stiffener considerably controlled the web deflection in all cases.

This was accomplished by the stiffener forcing a nodal point in the deflected shape of the web at the stiffener location. Only in LS3-T1 was there no such nodal point; in this case the longitudinal stiffener buckled before the girder failed (Fig. 3.23). Figure 3.15 shows the extent of the buckling; a string is mounted along the length of the stiffener for a reference.

The web deflection plots show deflection valleys along the tension diagonals of the panels. These valleys are the result of plate buckling along the compression diagonal and thus indicate the existance of tension field action in the panels or subpanels where the valleys were observed. In Fig. 3.20 the valley can be traced from the upper left corner to the lower right corner of the panel. In Fig. 3.23 the valley also crosses the entire panel as it does in the previous case with no longitudinal stiffener; however, this happened because the stiffener buckled. In all of the other tests the longitudinal stiffener forced separate valleys to form in the subpanels. The largest web deflections were always observed in the larger subpanels near the center and along the diagonal valleys.

The longitudinal stiffener usually forced the web to deflect gradually toward the far side of the girder, that is, away from the side with the longitudinal stiffener.

Principal Stresses in Web Subpanels

As shown in Figs. 3.28 and 3.29 principal stresses indicate a tension and a compression diagonal in each subpanel. The tensile stress increased as load increased. However, the compressive stress did not increase beyond the value developed when the web buckled along the compression diagonal. The valleys previously discussed are the observable results of this plate buckling.

For the loads plotted in Figs. 3.28 and 3.29 the upper subpanels had not yet reached their limit in carrying increasingly greater compressive stresses; by virtue of their smaller depth the upper subpanels were considerably stronger than the lower subpanels.

Stiffener Strains

Figures 3.33 to 3.38 shows axial strain in the longitudinal stiffeners as a function of the load applied to the girder at midspan. Figures 3.39 to 3.43 show the same information for the transverse stiffeners.

From the longitudinal stiffener strain plots, it is evident that in all cases with the longitudinal stiffener above the neutral axis, the segment of the stiffener in the end panel carried greater axial force than in the other panels. The force in the longitudinal stiffener is composed of two parts: the horizontal component of the tension field force[6] and a part of the horizontal force resisting the bending moment in the section.

The assumption used in locating the neutral axis of the longitudinal stiffener section (Sect. 3.7) resulted in fair agreement between theoretical elastic strains (calculated using beam theory) and the experimental strains up to 90% of the ultimate load. There was no agreement in the case where the longitudinal stiffener buckled prematurely (Fig. 3.35, LS3-T1). The cause of disagreement in LS3-T2 (Fig. 3.35) has not been definitely established, but it possibly is due to large deflections incurred in the interior panel during test LS3-T1 when the stiffener segment in the exterior panel buckled. It is also possible that the boundary conditions imposed in T2 by the diagonal repair stiffener after T1 caused the deviation.

Figures 3.39 to 3.43 show that in all cases the transverse stiffener carried little or no axial force (indicated by axial strain in the plots) until at least 90% of the ultimate load was attained.

## 3.9 Summary and Conclusions

A significant result of the tests described in Part 3 is that the shear strength of the girders was increased due to the longitudinal stiffeners. This increase varied from 6% to 38%.

The following conclusions can be formulated from the test results:

1. Neither web buckling theory nor beam theory can be used to predict the shear strength of longitudinally stiffened plate girders.
2. The longitudinal stiffeners are very effective in controlling lateral web deflections.
3. Because of the control of web deflections by the longitudinal stiffeners, separate tension fields are developed in the subpanels.
4. The shear strength of longitudinally stiffened panels is attained only after the development of the tension fields.

## NOMENCLATURE

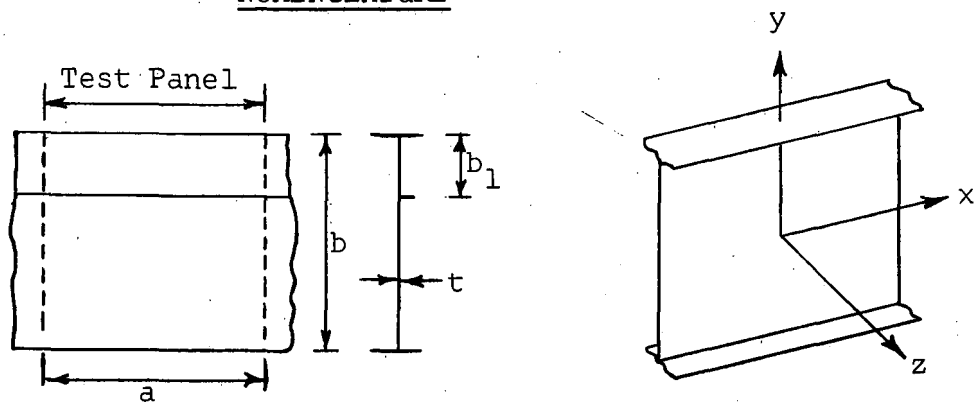


| | |
|---|---|
| a | panel length |
| b | web depth |
| $b_1$ | distance from top flange to center of longitudinal stiffener |
| k | web buckling coefficient |
| t | web thickness |
| $v_{\mathbb{Q}}$ | deflection in the negative y - direction at midspan |
| w | deflection in the positive z - direction |
| x,y,z | cartesian coordinate axes |
| $A_w$ | web area |
| E | modulus of elasticity (29.6 ksi) |
| I | moment of inertia of girder cross section, including longitudinal stiffener |
| $I_s$ | longitudinal stiffener moment of inertia |
| M | moment |
| P | applied load |
| $P_{cr}$ | theoretical web buckling load |
| $P_o$ | theoretical ultimate load for girder without longitudinal stiffener |
| $P_u^{ex}$ | experimentally obtained ultimate load |

| | |
|---|---|
| $P_w$ | working load |
| $P_y$ | load which causes initial yielding |
| $Q$ | static moment of area above the neutral axis about the neutral axis, including longitudinal stiffener |
| $S_a$ | moment of inertia of entire section, including longitudinal stiffener, divided by distance from neutral axis to extreme fiber of compression flange |
| $V$ | shear force |
| $V_{cr}$ | critical shear force |
| $V_w$ | working shear force |
| $\alpha$ | aspect ratio, a/b |
| $\beta$ | slenderness ratio, b/t |
| $\gamma_s$ | stiffener rigidity ratio, $12\ (1-\nu^2)\ I_s/bt^3$ |
| $\epsilon$ | strain, $\sigma/E$ |
| $\epsilon_y$ | yield strain, $\sigma_y/E$ |
| $\eta$ | longitudinal stiffener position, $b_1/b$ |
| $\nu$ | Poisson's Ratio (0.3) |
| $\sigma$ | normal stress |
| $\sigma_{cr}$ | critical normal stress |
| $\sigma_w$ | working normal stress |
| $\sigma_y$ | yield stress |
| $\tau_{cr}$ | critical shear stress |
| $\tau_w$ | working shear stress |
| $\tau_y$ | yield stress in shear, $\sigma_y/\sqrt{3}$ |

# TABLES AND FIGURES

| Test | Loading | $\alpha$ | $\beta$ | $\eta$ | L.S. Size |
|---|---|---|---|---|---|
| LB1 | Pure Bending | 1.0 | 444 | --- | none |
| LB2 | | 1.0 | 447 | 0.20 | 2" x 1/8" |
| LB3 | | 1.0 | 447 | 0.20 | 2½"x 1/8" |
| LB4 | | 1.5 | 447 | 0.20 | 2" x 1/8" |
| LB5 | | 0.75 | 447 | 0.20 | 2" x 1/8" |
| LB6 | | 1.0 | 407 | 0.20 | 2" x ¼" |
| LS1-T1 | High Shear | 1.0 | 256 | --- | none |
| LS1-T2 | | 1.0 | 256 | 0.33 | 4" x 1" |
| LS2-T1 | | 1.0 | 275 | 0.33 | 4" x ½" |
| LS3-T1 | | 1.5 | 276 | 0.33 | 2" x ½" |
| LS3-T2 | | 1.5 | 276 | 0.33 | 3½"x ½" |
| LS3-T3 | | 0.75 | 276 | 0.33 | 3½"x ½" |
| LS4-T1 | | 1.0 | 260 | 0.20 | 3½"x ½" |
| LS4-T2 | | 1.0 | 260 | 0.50 | 3½"x ½" |

Table 1.1 Test Parameters

| Test | Comp. Flg. | | Tension Flg. | | Web | | Long. Stiff. | | Trans. Stiff. | |
|---|---|---|---|---|---|---|---|---|---|---|
| | Thick-ness | Width | Thick-ness | Width | Thick-ness | Depth * | Thick-ness | Width | Thick-ness | Width * |
| LB1 | 0.754 | 12.01 | 0.756 | 12.00 | 0.124 | 55.0 | -- | -- | 0.25 | 3.0 |
| LB2 | 0.753 | 11.99 | 0.755 | 12.03 | 0.123 | 55.0 | 0.123 | 2.0* | 0.25 | 3.0 |
| LB3 | 0.752 | 12.00 | 0.752 | 12.00 | 0.123 | 55.0 | 0.123 | 2.5* | 0.25 | 3.0 |
| LB4 | 0.753 | 11.98 | 0.754 | 12.00 | 0.123 | 55.0 | 0.123 | 2.0* | 0.25 | 3.0 |
| LB5 | 0.758 | 12.00 | 0.757 | 12.02 | 0.123 | 55.0 | 0.123 | 2.0* | 0.25 | 3.0 |
| LB6 | 0.633 | 10.18 | 0.636 | 10.20 | 0.135 | 55.0 | 0.256 | 2.00 | 0.25 | 3.0 |
| LS1-T1 | 1.498 | 14.12 | 1.497 | 14.10 | 0.195 | 50.0 | -- | -- | 0.75 | 3.0 |
| LS1-T2 | 1.498 | 14.12 | 1.497 | 14.10 | 0.195 | 50.0 | 1.016 | 4.04 | 0.75 | 3.0 |
| LS2-T1 | 1.494 | 14.12 | 1.503 | 14.12 | 0.182 | 50.0 | 0.500<br>1.006 | 3.97<br>5.52 | 0.75 | 3.0 |
| LS3-T1 | 1.516 | 14.24 | 1.516 | 14.20 | 0.181 | 50.0 | 0.502 | 1.97 | 0.375 | 5.0 |
| LS3-T2 | 1.516 | 14.24 | 1.516 | 14.20 | 0.181 | 50.0 | 0.511 | 3.44 | 0.375 | 5.0 |
| LS3-T3 | 1.516 | 14.24 | 1.516 | 14.20 | 0.181 | 50.0 | 0.510 | 3.44 | 0.50 | 5.0 |
| LS4-T1 | 1.511 | 14.12 | 1.508 | 14.22 | 0.192 | 50.0 | 0.511 | 3.47 | 0.50 | 3.0 |
| LS4-T2 | 1.511 | 14.12 | 1.508 | 14.22 | 0.192 | 50.0 | 0.511 | 3.50 | 0.50 | 4.5 |

* Nominal Sizes

Table 1.2 Plate Dimensions

| Test | Component | $\sigma_y$ (ksi) | % Elong. (in 8 inches) | Ladle Comp. % C | $M_n$ | P | S |
|---|---|---|---|---|---|---|---|
| LB1 | Comp. Flg. | 37.6 | 29.0 | .25 | .67 | .018 | .023 |
| | Web* | 33.3 | 28.2 | .16 | .62 | .010 | .025 |
| | Tens. Flg. | 37.4 | 29.6 | .25 | .67 | .018 | .023 |
| LB2 | Comp. Flg. | 37.0 | 27.6 | .25 | .67 | .018 | .023 |
| | Web & L.S.* | 34.1 | 28.7 | .16 | .62 | .010 | .025 |
| | Tens. Flg. | 37.1 | 28.2 | .25 | .67 | .018 | .023 |
| LB3 | Comp. Flg. | 36.0 | 30.0 | .25 | .67 | .018 | .023 |
| | Web & L.S.* | 34.5 | 27.4 | .16 | .62 | .010 | .025 |
| | Tens. Flg. | 36.1 | 25.6 | .25 | .67 | .018 | .023 |
| LB4 | Comp. Flg. | 34.9 | 30.8 | .25 | .67 | .018 | .023 |
| | Web & L.S.* | 35.8 | 29.6 | .16 | .62 | .010 | .025 |
| | Tens. Flg. | 35.9 | 29.8 | .25 | .67 | .018 | .023 |
| LB5 | Comp. Flg. | 35.3 | 27.0 | .25 | .67 | .018 | .023 |
| | Web & L.S.* | 35.6 | 30.2 | .16 | .62 | .010 | .025 |
| | Tens. Flg. | 35.5 | 29.9 | .25 | .67 | .018 | .023 |
| LB6 | Comp. Flg. | 33.1 | 32.2 | .21 | .59 | .014 | .019 |
| | Long. Stiff. | 37.2 | 29.6 | .23 | .58 | .009 | .021 |
| | Web* | 34.0 | 24.8 | | | | |
| | Tens. Flg. | 34.1 | 31.0 | .21 | .59 | .014 | .019 |
| LS1-T1 | Comp. Flg. | 30.5 | 33.8 | .20 | 1.11 | .009 | .022 |
| | Web* | 46.8 | 23.8 | .19 | .53 | .010 | .021 |
| | Tens. Flg. | 30.2 | 34.7 | .20 | 1.11 | .009 | .022 |
| LS1-T2 | Long. Stiff. | 30.6 | 30.3 | | | | |
| LS2-T1 | Comp. Flg. | 29.4 | 33.4 | .20 | 1.11 | .009 | .022 |
| | Long. Stiff. | 39.8 | 28.9 | | | | |
| | Web* | 39.4 | 29.0 | .16 | .58 | .010 | .024 |
| | Tens. Flg. | 30.0 | 35.0 | .20 | 1.11 | .009 | .022 |
| LS3-T1 | Comp. Flg. | 29.8 | 33.0 | .20 | 1.11 | .009 | .022 |
| | Long. Stiff. | 39.2 | 26.9 | | | | |
| | Web* | 38.2 | 28.6 | .19 | .53 | .010 | .021 |
| | Tens. Flg. | 29.5 | 35.5 | .20 | 1.11 | .009 | .022 |
| LS3-T2 | Long. Stiff. | 35.8 | 29.7 | | | | |
| LS3-T3 | Long. Stiff. | 35.8 | 29.7 | | | | |
| LS4-T1 | Comp. Flg. | 30.5 | 34.5 | .20 | 1.11 | .009 | .022 |
| | Long. Stiff. | 36.0 | 28.6 | | | | |
| | Web* | 48.6 | 23.0 | .19 | .53 | .010 | .021 |
| | Tens. Flg. | 30.0 | 31.5 | .20 | 1.11 | .009 | .022 |
| LS4-T2 | Long. Stiff. | 36.3 | 29.3 | | | | |

* Web values are average values from the two tensile specimens (Maximum difference between the two yield stresses was 2.8 ksi)

Table 1.3 Material Properties

| Test | k | $P_{cr}$ (kips) | $P_w$ (kips) | $P_y$ (kips) | $P_o$ (kips) |
|---|---|---|---|---|---|
| LB1 | 23.9 | 15.1 | 91.2 | 175.7 | 155.0 |
| LB2 | 129.4 | 81.3 | 91.2 | 172.2 | 153.6 |
| LB3 | 129.4 | 81.4 | 91.2 | 169.1 | 149.9 |
| LB4 | 129.4 | 81.1 | 91.2 | 163.8 | 143.6 |
| LB5 | 129.4 | 81.7 | 91.2 | 166.8 | 148.3 |
| LB6 | 129.4 | 75.2 | 62.9 | 119.3 | 101.6 |
| LS1-T1 | 9.34 | 74.3 | 158.4 | 523.6 | 351.5 |
| LS1-T2 | 15.9 | 126.6 | 158.4 | 514.6 | 351.5 |
| LS2-T1 | 15.9 | 102.4 | 158.4 | 408.7 | 276.9 |
| LS3-T1 | 13.7 | 87.1 | 127.7 | 396.0 | 215.1 |
| LS3-T2 | 13.7 | 87.1 | 127.7 | 394.7 | 215.1 |
| LS3-T3 | 19.0 | 120.8 | 179.4 | 394.7 | 302.7 |
| LS4-T1 | 12.3 | 93.4 | 158.4 | 531.8 | 357.7 |
| LS4-T2 | 25.4 | 193.0 | 158.4 | 536.2 | 357.7 |

Table 1.4 Reference Loads

| Test | Variables | | Reference Loads | | | | Test Results | | |
|---|---|---|---|---|---|---|---|---|---|
| | $\alpha$ | $\gamma_s$ | $P_{cr}$ | $P_w$ | $P_y$ | $P_o$ | $P_u^{ex}$ | $P_u^{ex}/P_y$ | $P_u^{ex}/P_o$ |
| LB1 | 1.0 | 0 | 15.1 | 91.2 | 175.7 | 155.0 | 156.5 | .891 | 1.01 |
| LB2 | 1.0 | 38.4 | 81.3 | 91.2 | 172.2 | 153.6 | 152.0 | .883 | 0.99 |
| LB3 | 1.0 | 75.1 | 81.4 | 91.2 | 169.1 | 149.9 | 150.0 | .887 | 1.00 |
| LB4 | 1.5 | 38.4 | 81.1 | 91.2 | 163.8 | 143.6 | 147.0 | .897 | 1.02 |
| LB5 | 0.75 | 38.4 | 81.7 | 91.2 | 166.8 | 148.3 | 150.8 | .904 | 1.02 |
| LB6 | 1.0 | 60.5 | 75.2 | 62.9 | 119.3 | 101.6 | 112.8 | .946 | 1.11 |

Table 2.1 Test Results

| Specimen | $\alpha$ | $\gamma_s$ | $(w_w)_{max}$ (in.) | $w_o$ (in.) | $\Delta w$ % |
|---|---|---|---|---|---|
| LB1 | 1.0 | 0 | 0.221 | 0.092 | 140 |
| LB2 | 1.0 | 38.4 | 0.215 | 0.186 | 16 |
| LB3 | 1.0 | 75.1 | 0.256 | 0.225 | 14 |
| LB4 | 1.5 | 38.4 | 0.231 | 0.166 | 39 |
| LB5 | 0.75 | 38.4 | 0.076 | 0.065 | 17 |
| LB6 | 1.0 | 60.5 | 0.153 | 0.142 | 8 |

Table 2.2 Web Deflection Comparison

| Test | $P_u^{ex}$ (kips) | $P_u^{ex}/P_{cr}$ | $P_u^{ex}/P_y$ | $P_u^{ex}/P_o$ |
|---|---|---|---|---|
| LS1-T1 | 363.5 | 4.89 | 0.69 | 1.03 |
| LS1-T2 | 414.0 | 3.27 | 0.80 | 1.18 |
| LS2-T1 | 315.5 | 3.08 | 0.77 | 1.14 |
| LS3-T1 | 278.5 | 3.20 | 0.70 | 1.29 |
| LS3-T2 | 296.0 | 3.40 | 0.75 | 1.38 |
| LS3-T3 | 338.0 | 2.80 | 0.86 | 1.12 |
| LS4-T1 | 380.5 | 4.07 | 0.72 | 1.06 |
| LS4-T2 | 405.5 | 2.10 | 0.76 | 1.13 |

Table 3.1 Test Results

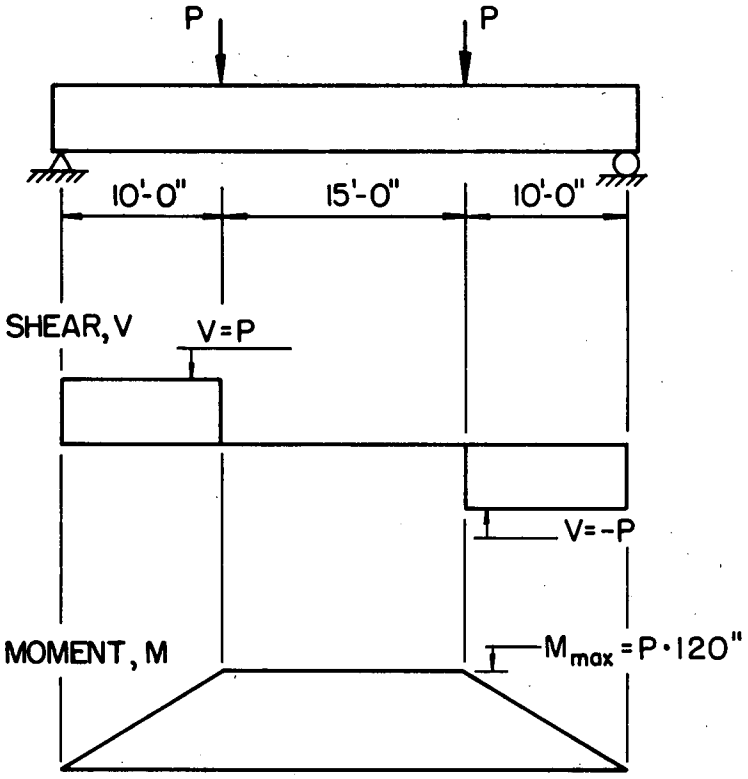


Fig. 1.1 Setup for Bending Tests

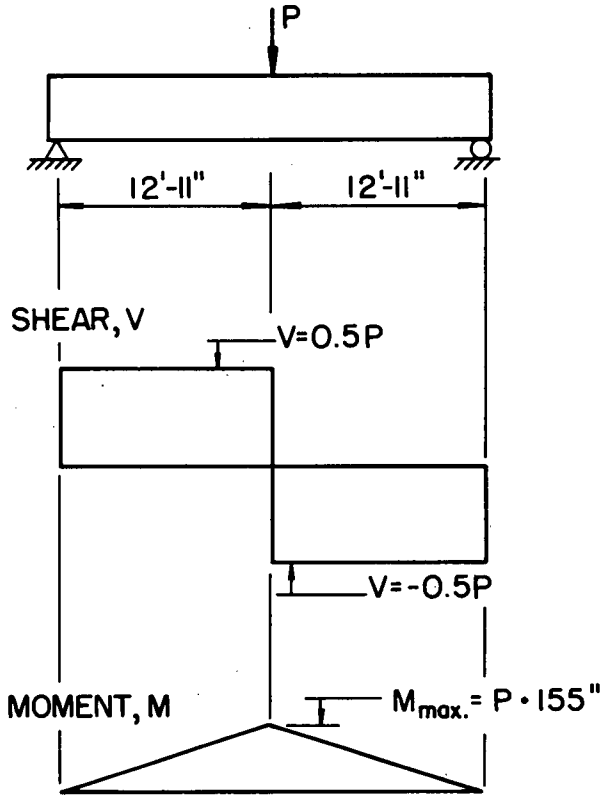


Fig. 1.2 Setup for Shear Tests

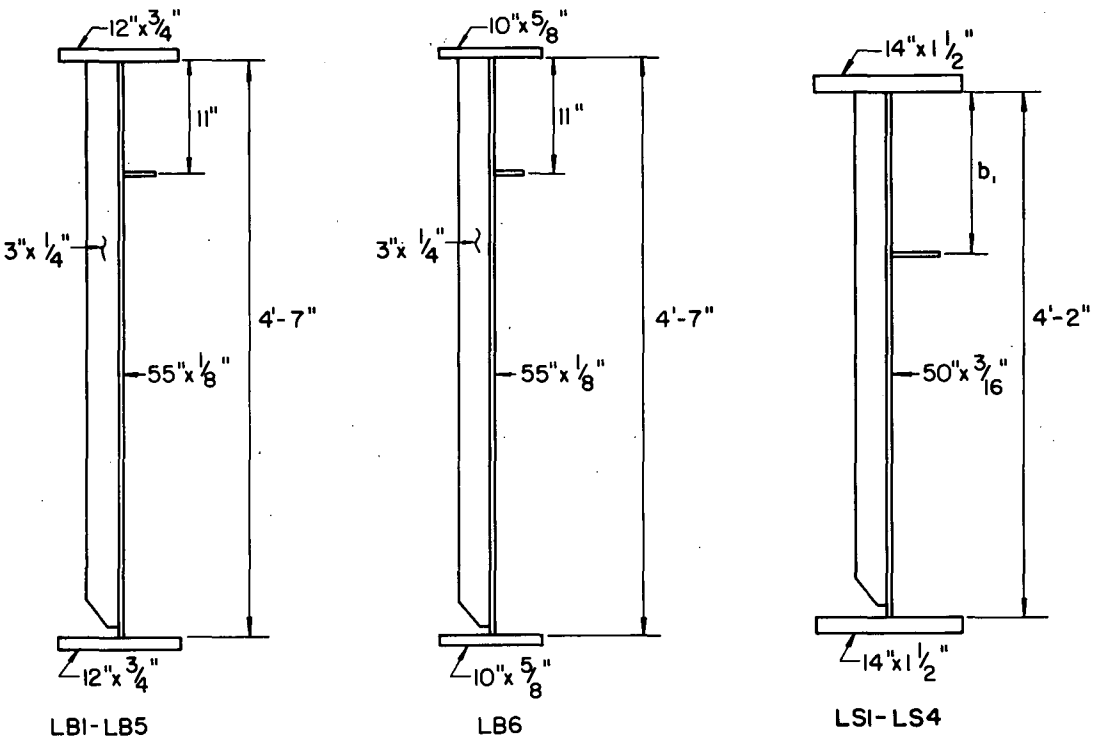


Fig. 1.3 Test Specimen Cross Sections

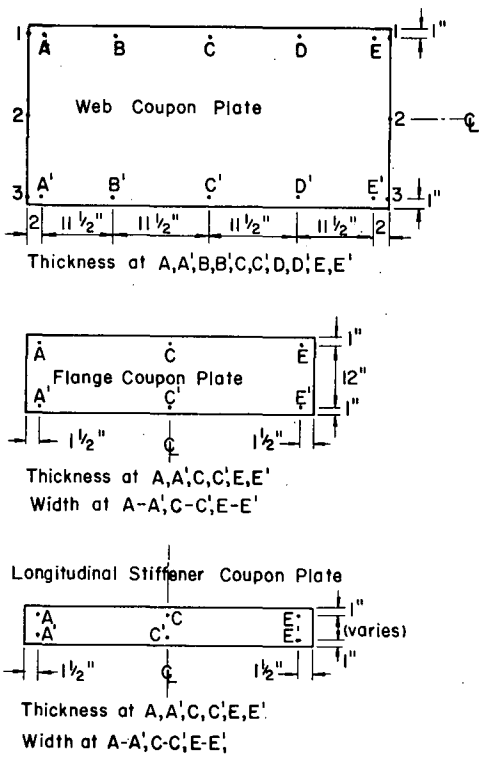


Fig. 1.4 Typical Locations of Coupons and Tensile Specimens

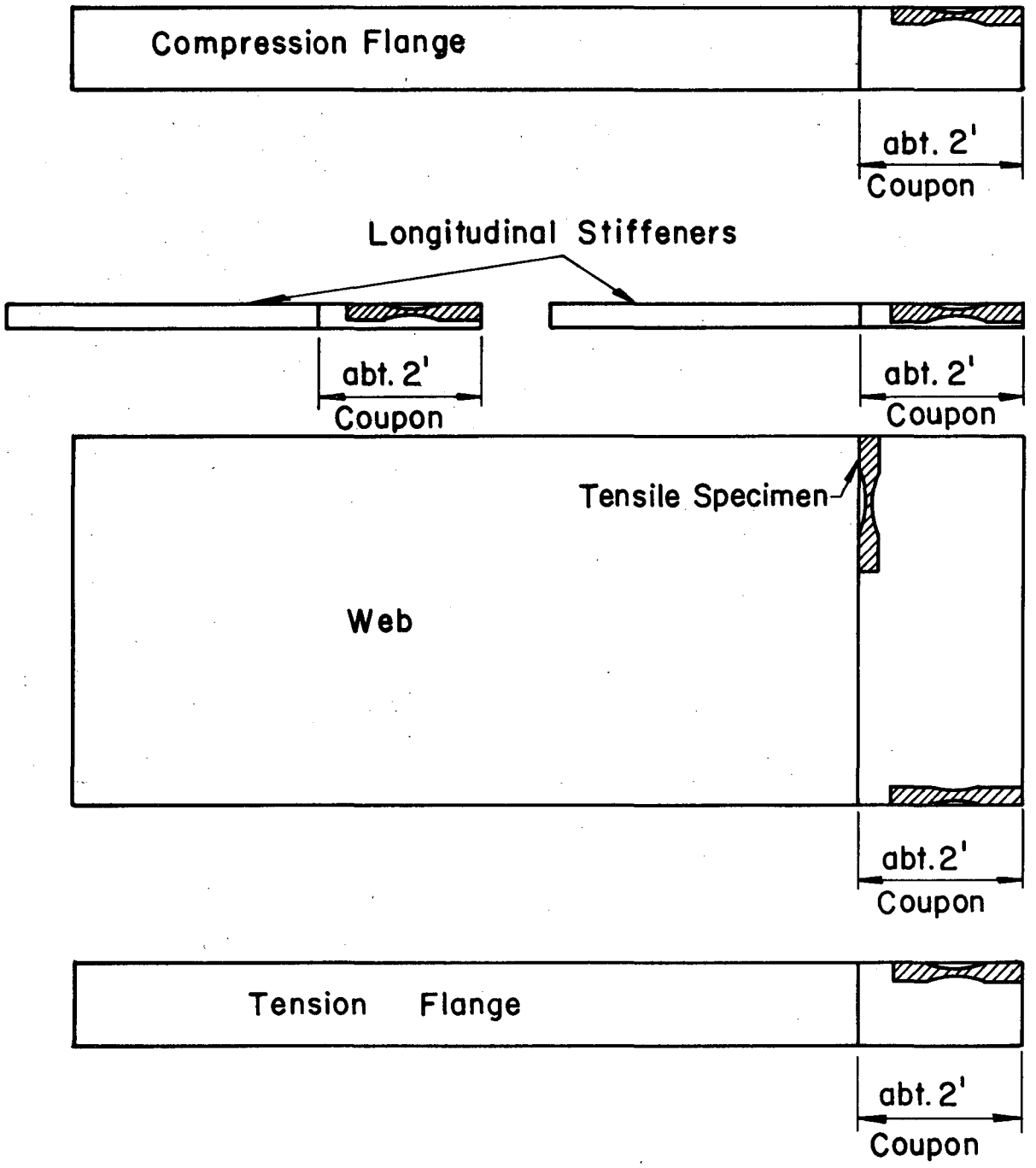


Fig. 1.5 Location of Coupon Measurements

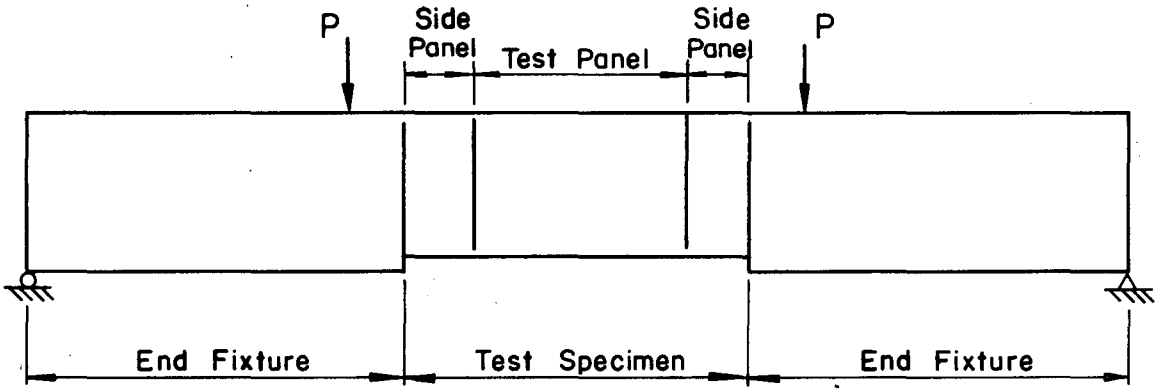


Fig. 2.1 Schematic Test Setup

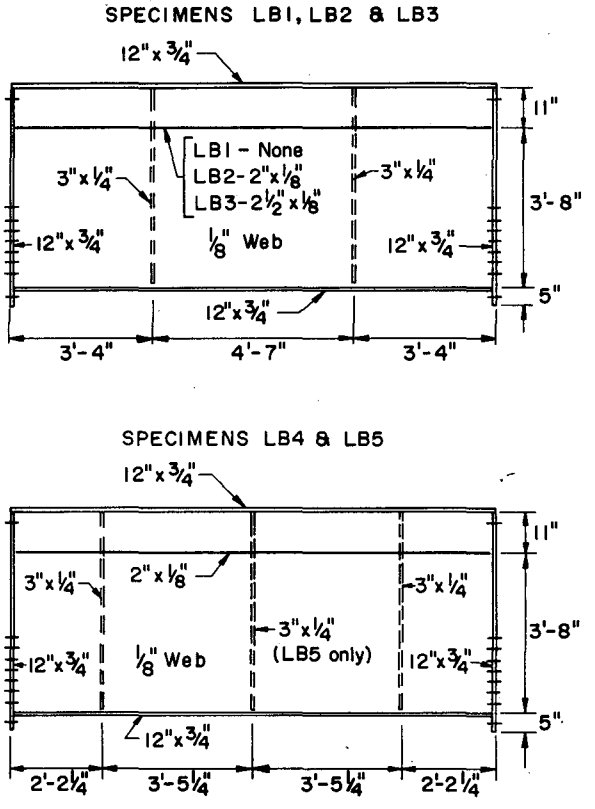


Fig. 2.2 Test Specimens LB1 to LB5

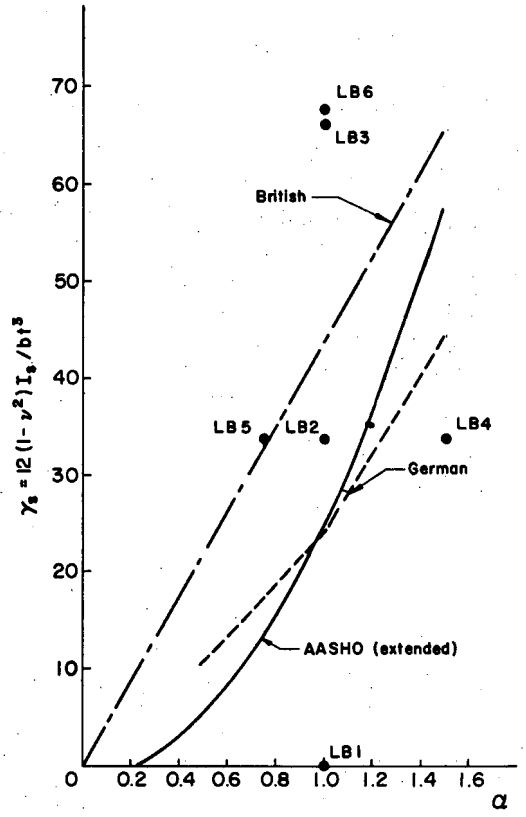


Fig. 2.3 Test Specimen Parameters

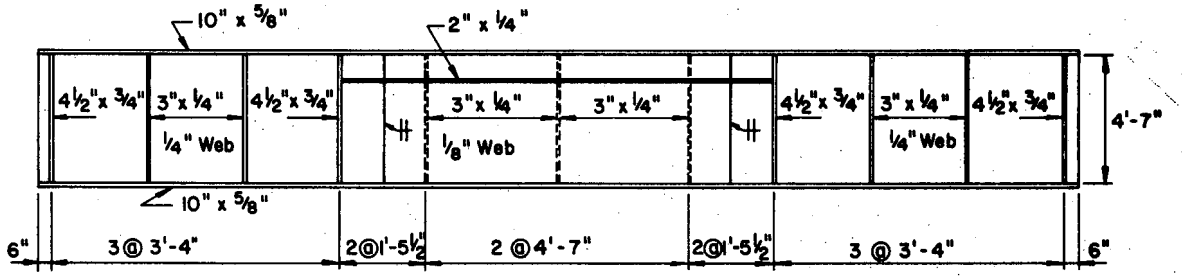


Fig. 2.4 Test Specimen LB6

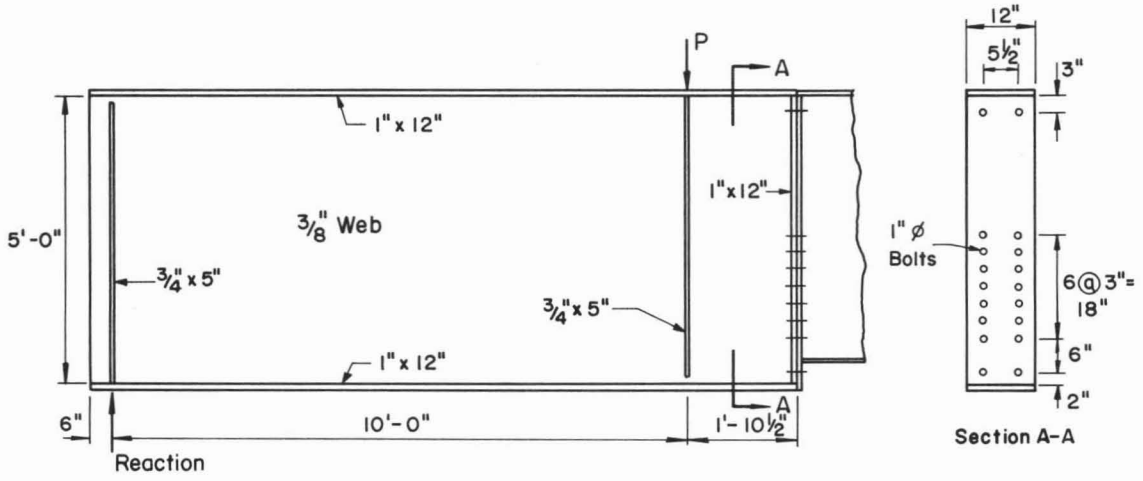


Fig. 2.5 End Fixture and Bolted Joint

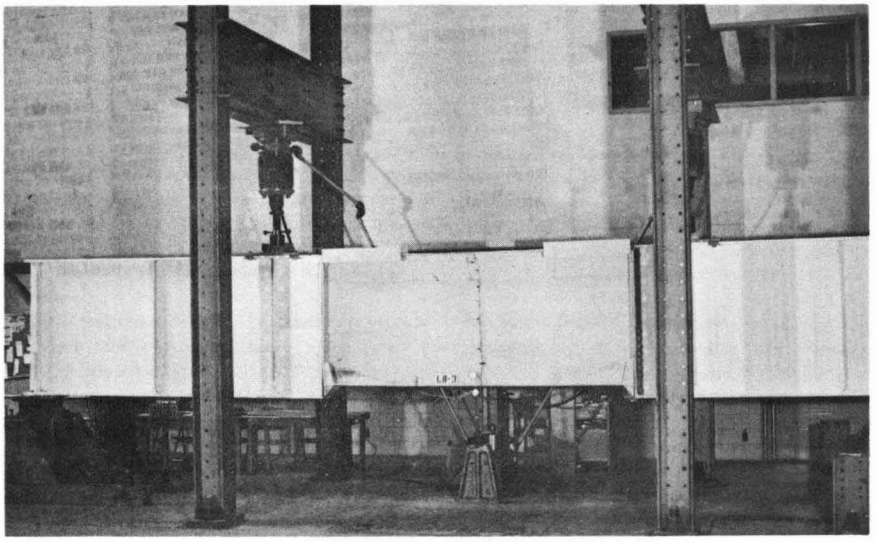

Fig. 2.6 Test Setup

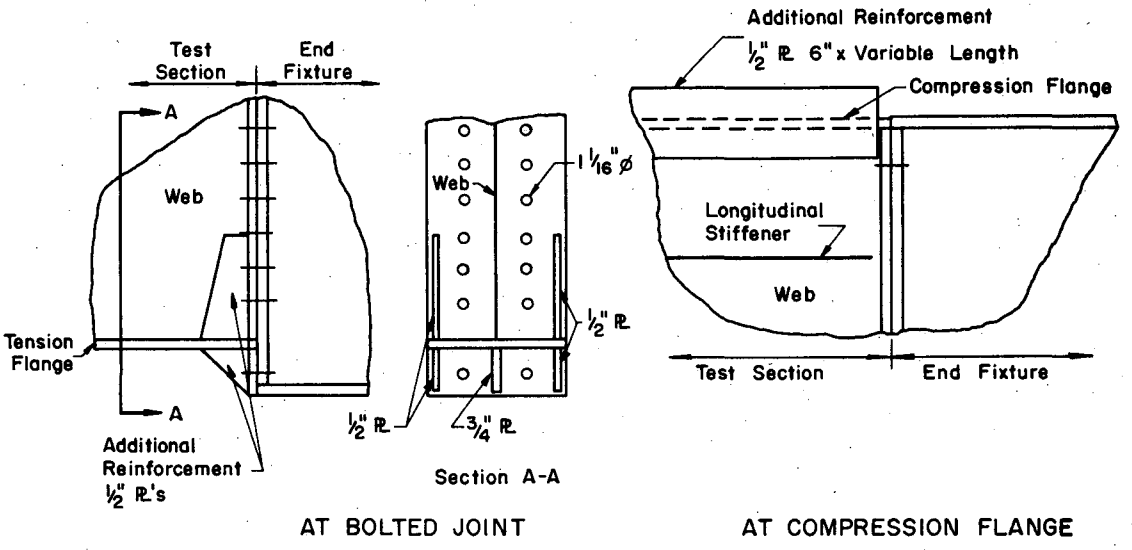


Fig. 2.7 Reinforcement of Side Panels

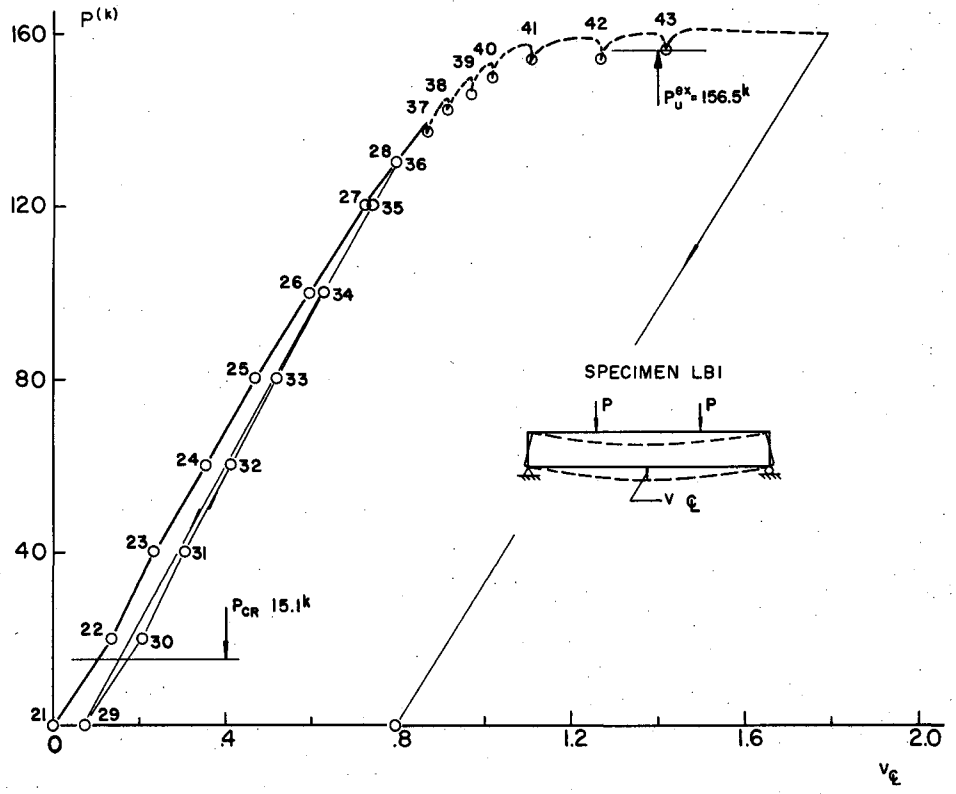


Fig. 2.8 Load-Vs-Centerline Deflection Curve

(Specimen LB1)

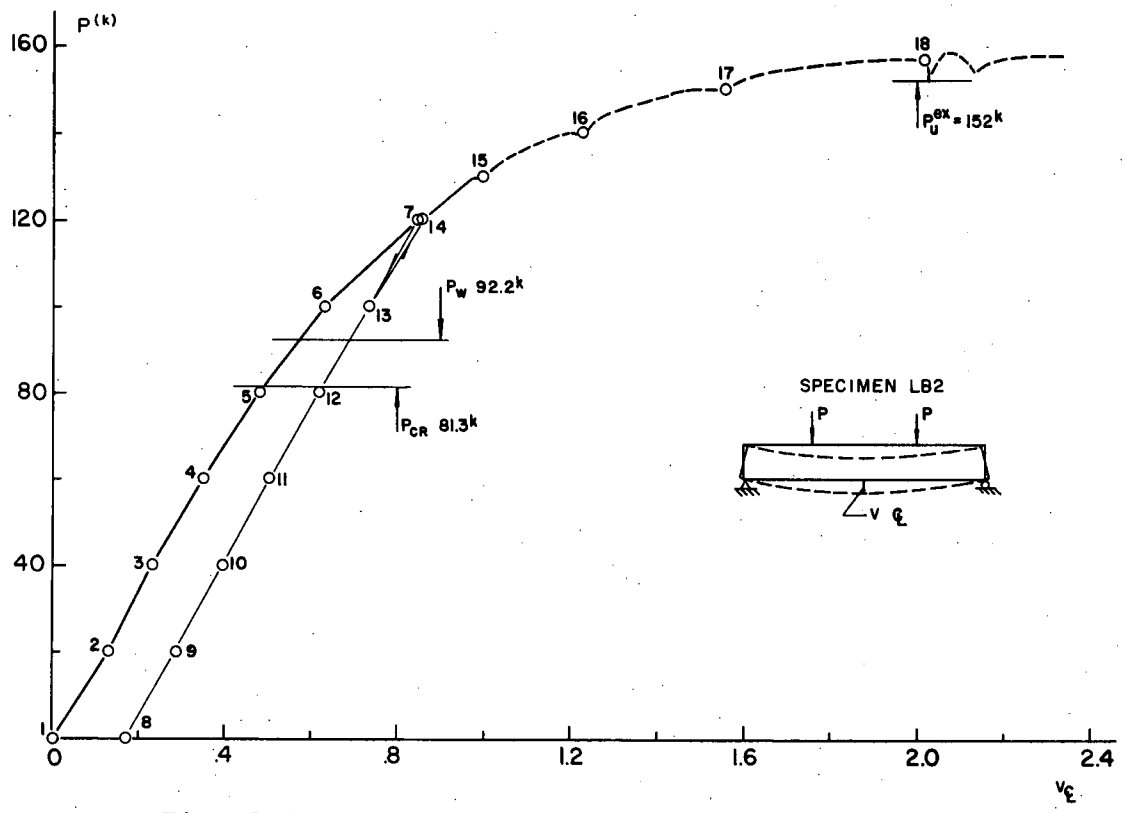


Fig. 2.9 Load-Vs-Centerline Deflection Curve

(Specimen LB2)

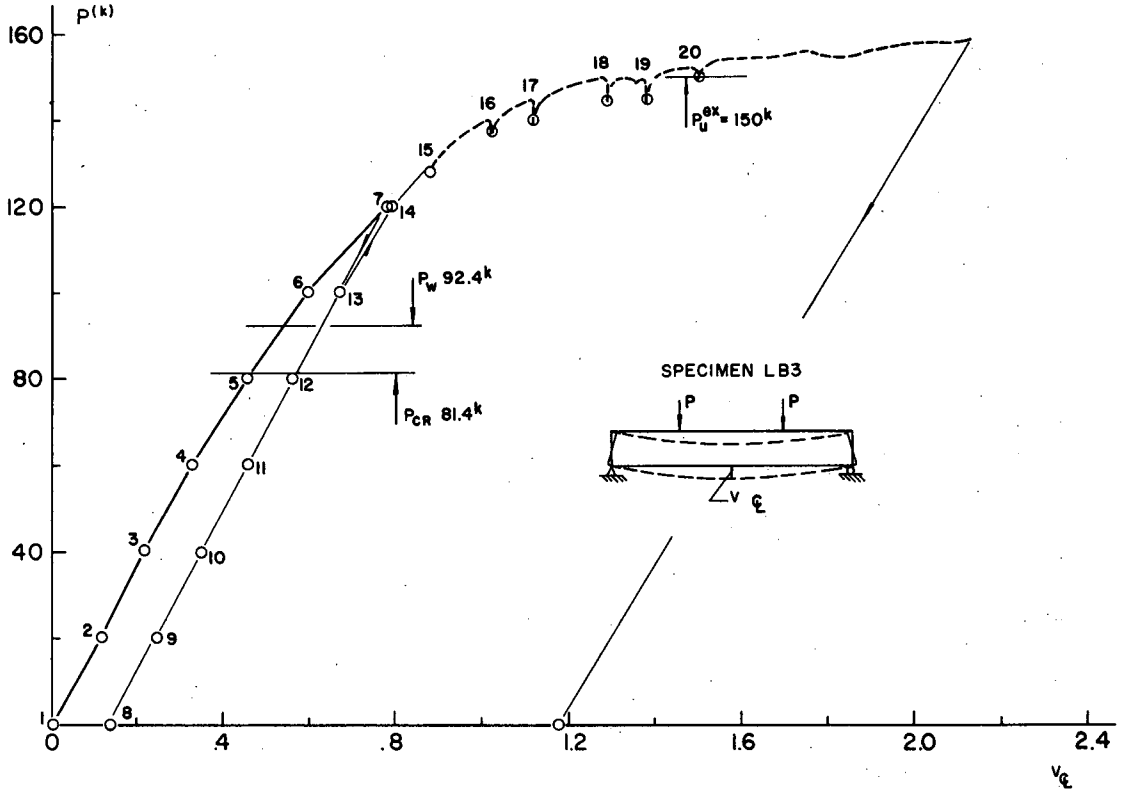


Fig. 2.10 Load-Vs-Centerline Deflection Curve

(Specimen LB3)

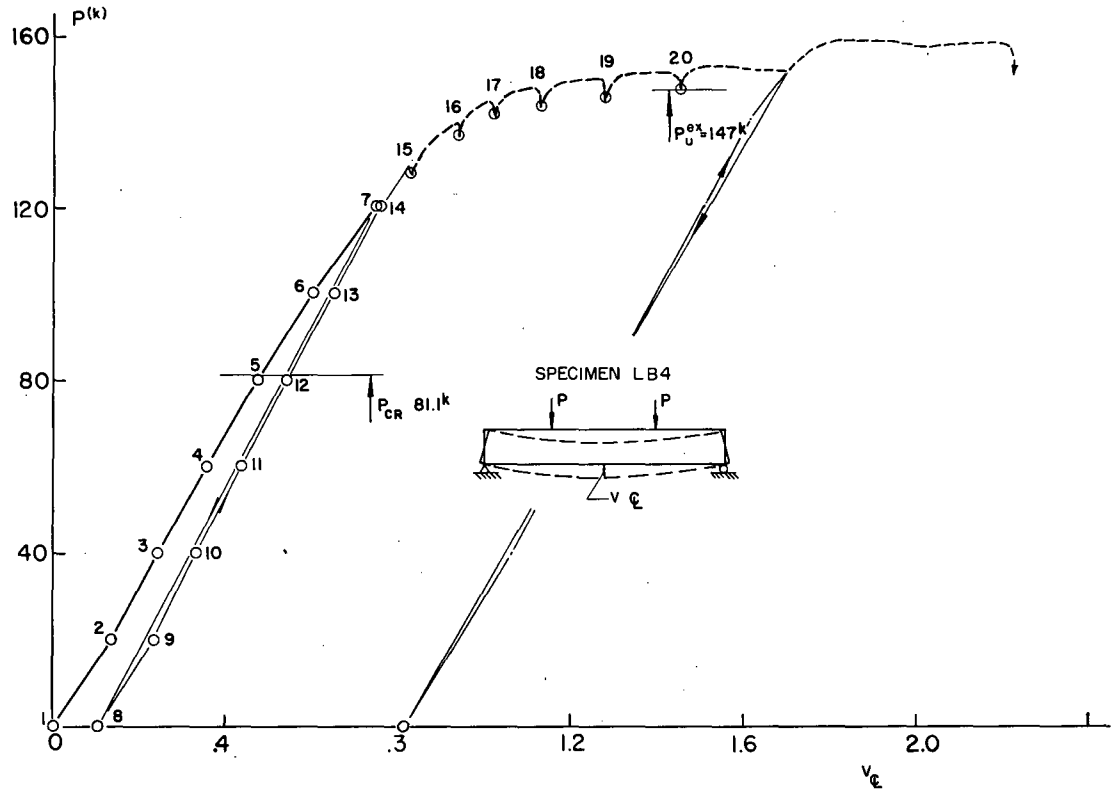


Fig. 2.11 Load-Vs-Centerline Deflection Curve (Specimen LB4)

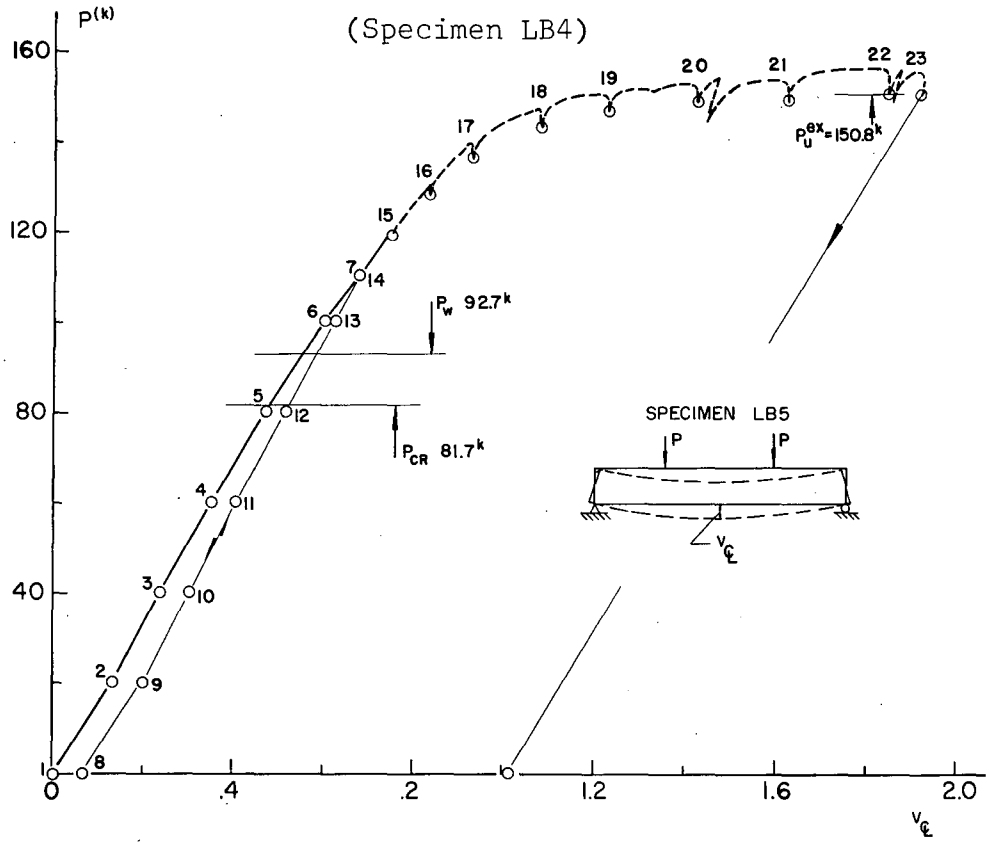


Fig. 2.12 Load-Vs-Centerline Deflection Curve (Specimen LB5)

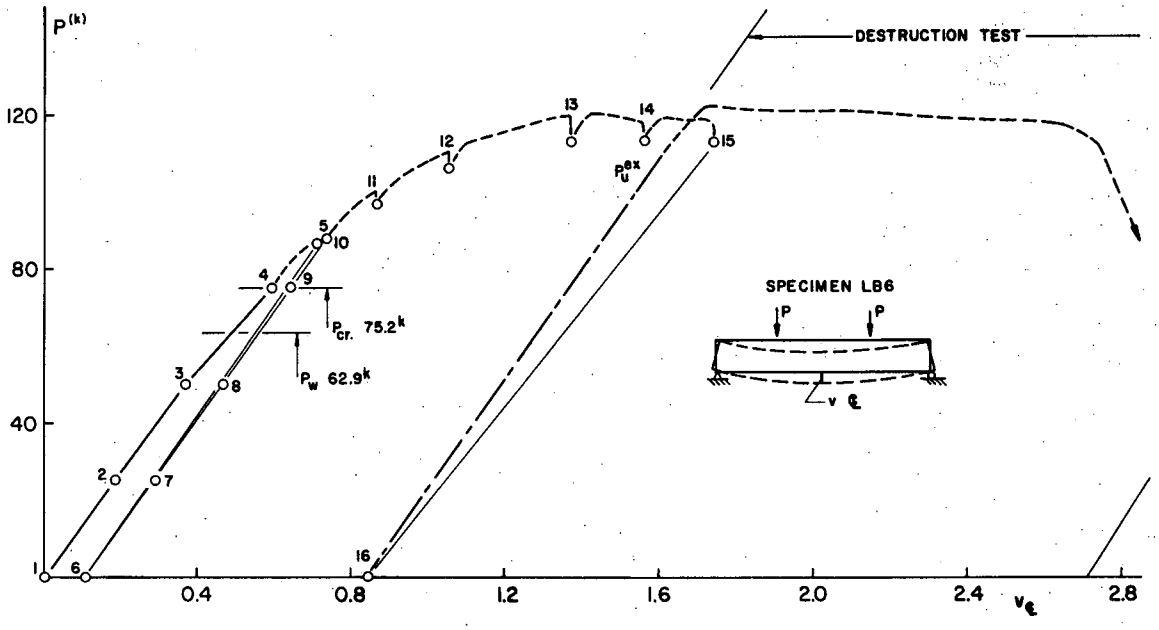


Fig. 2.13 Load-Vs-Centerline Deflection Curve

(Specimen LB6)

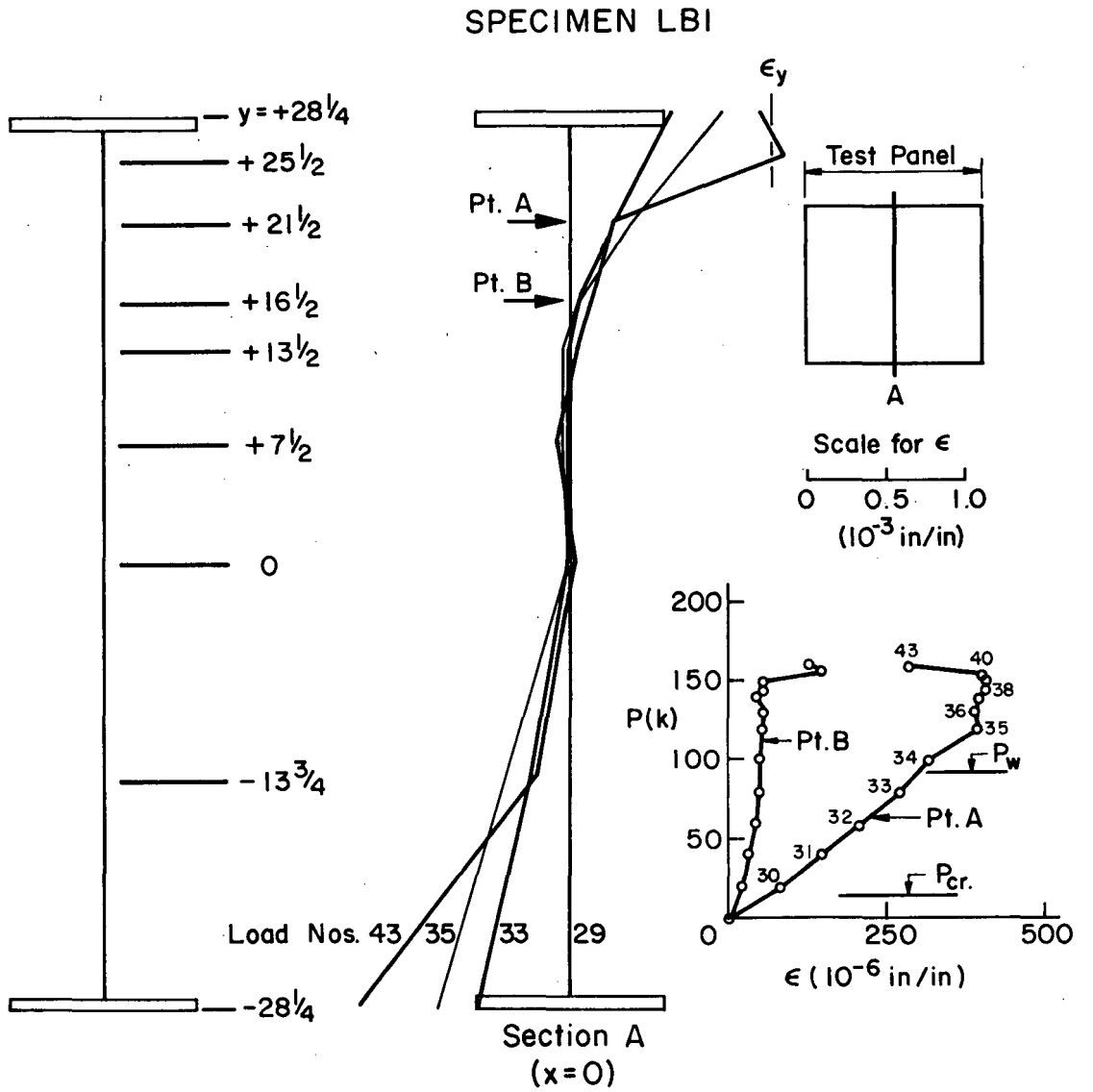


Fig. 2.14 Strain Distribution (Specimen LB1)

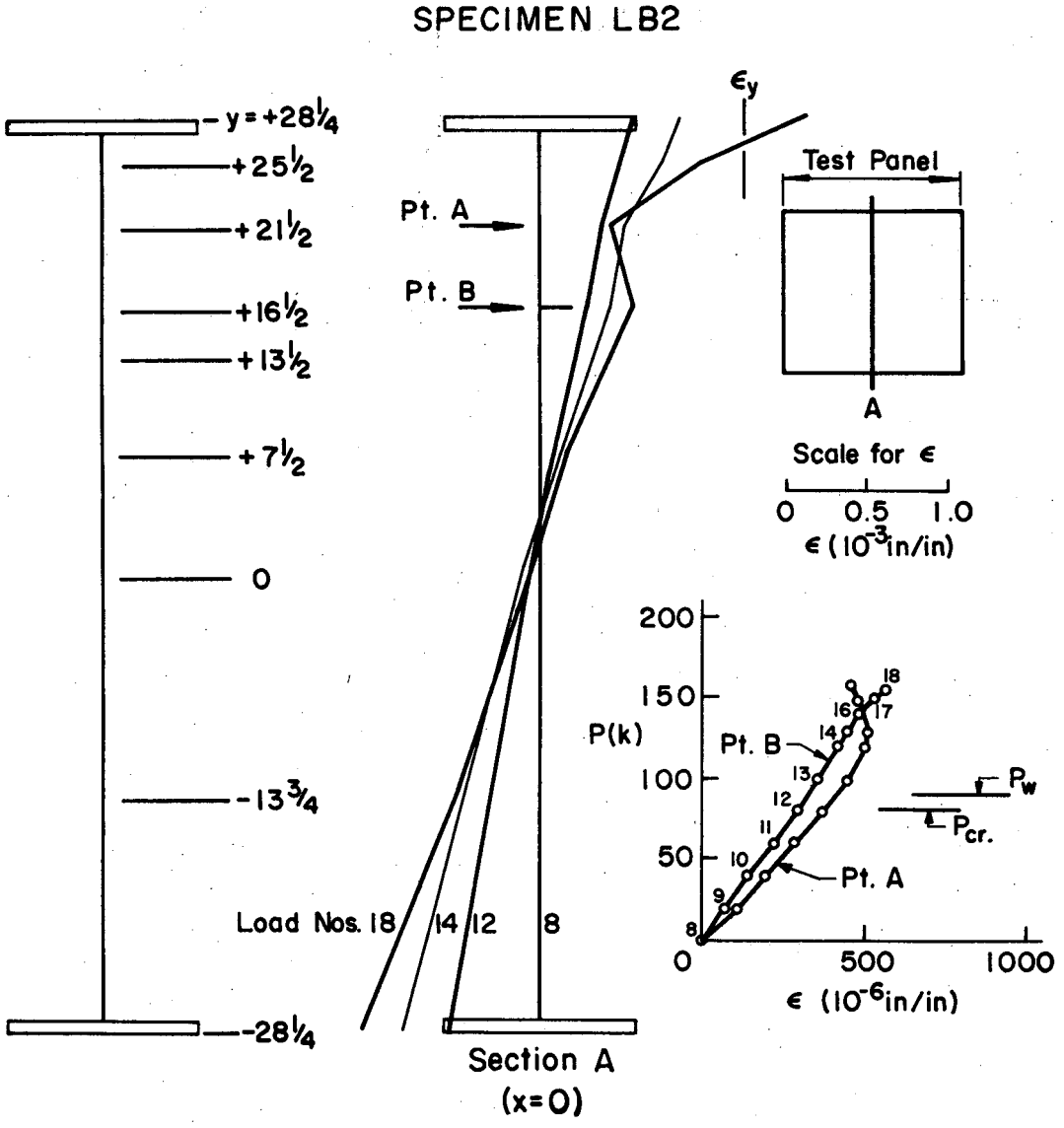


Fig. 2.15 Strain Distribution (Specimen LB2)

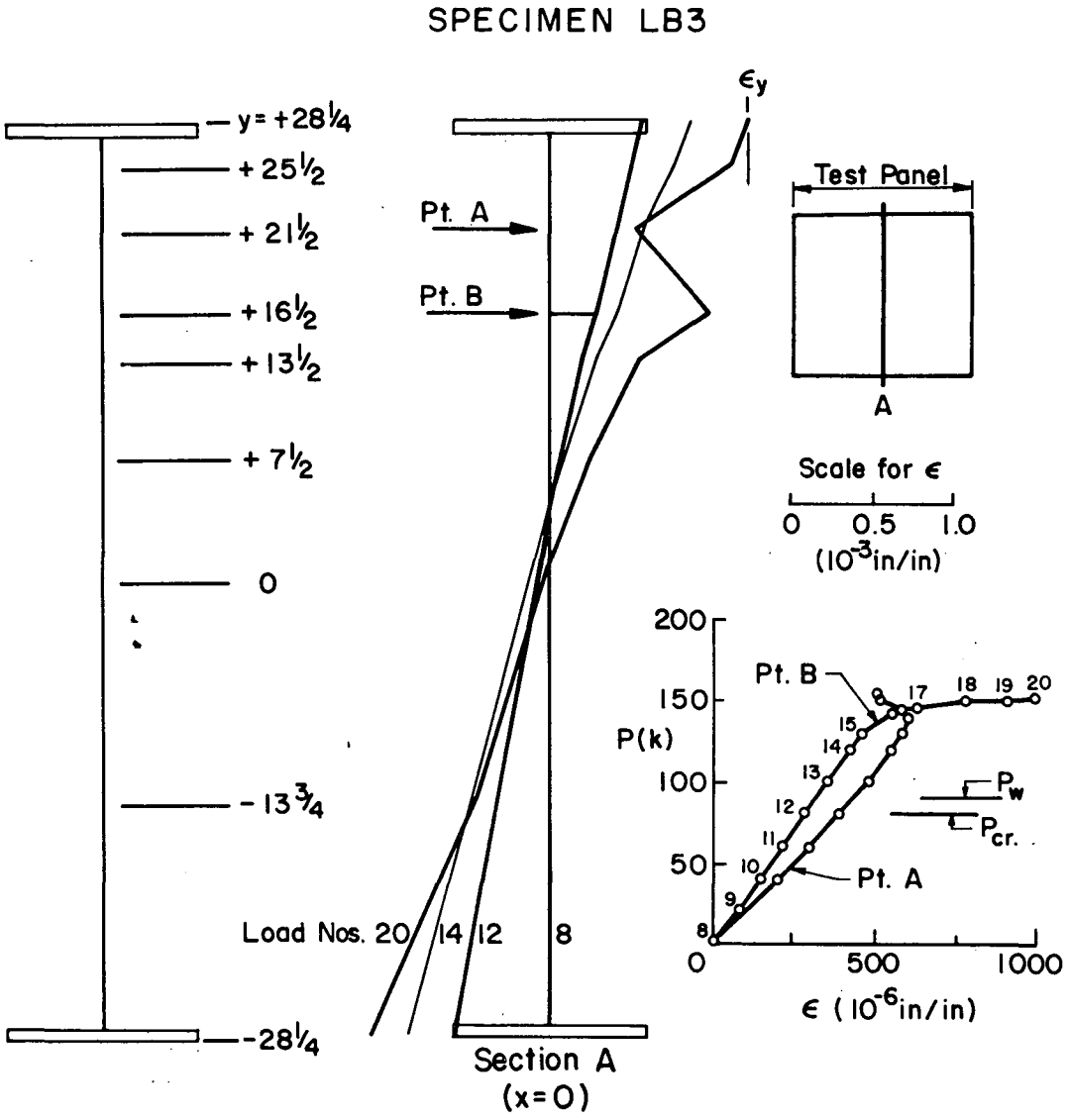


Fig. 2.16 Strain Distribution (Specimen LB3)

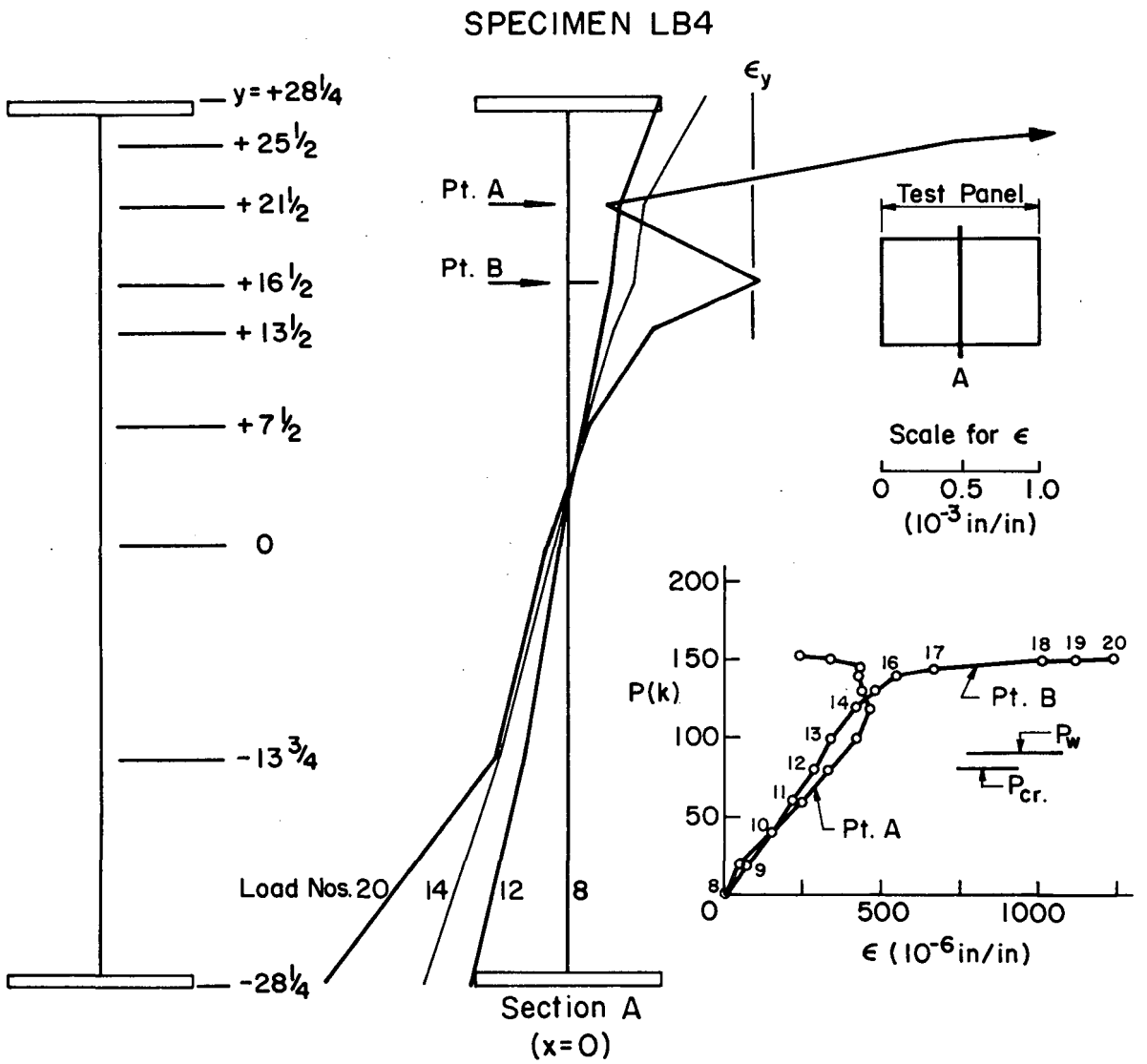


Fig. 2.17 Strain Distribution (Specimen LB4)

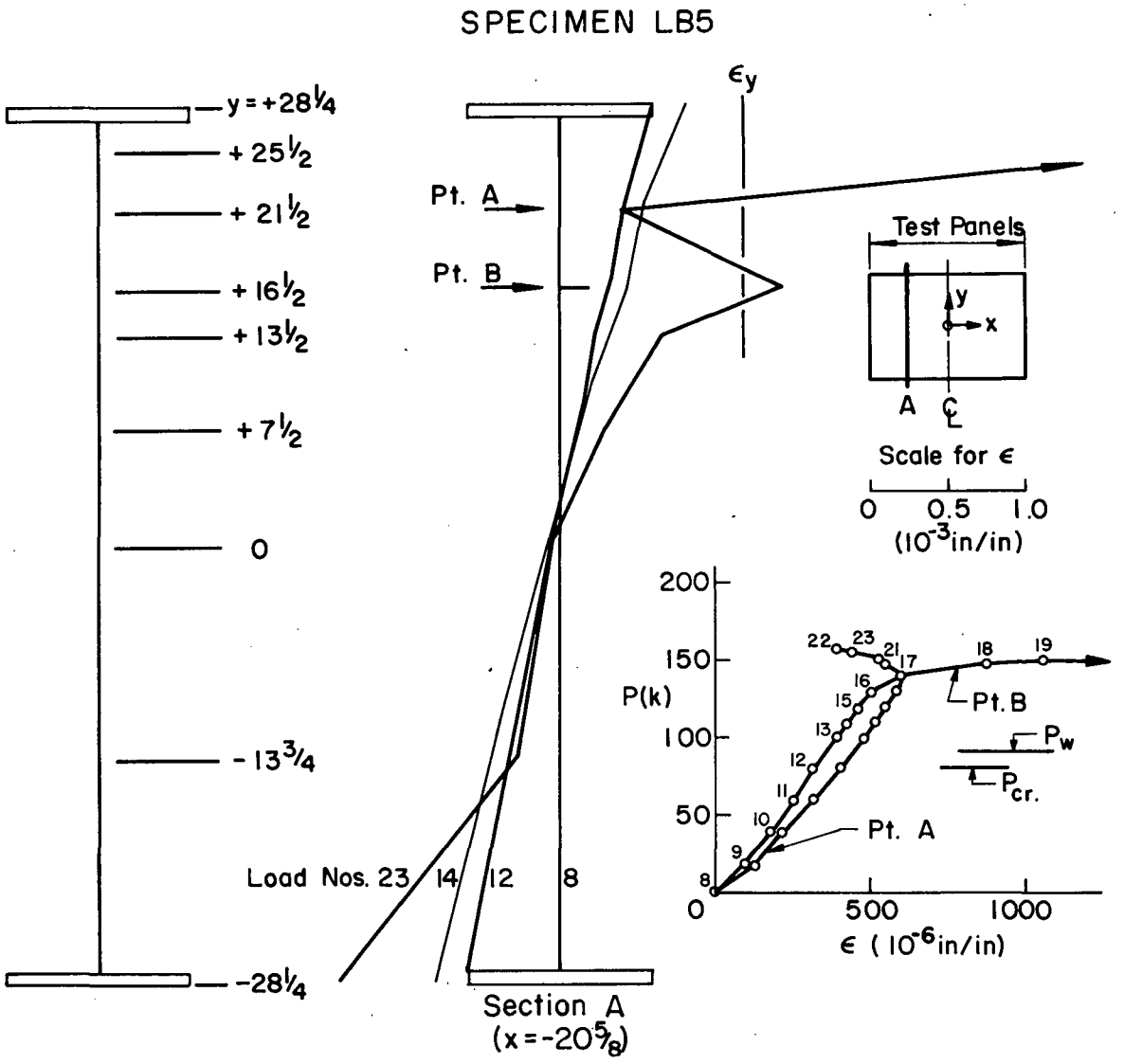


Fig. 2.18 Strain Distribution (Specimen LB5)

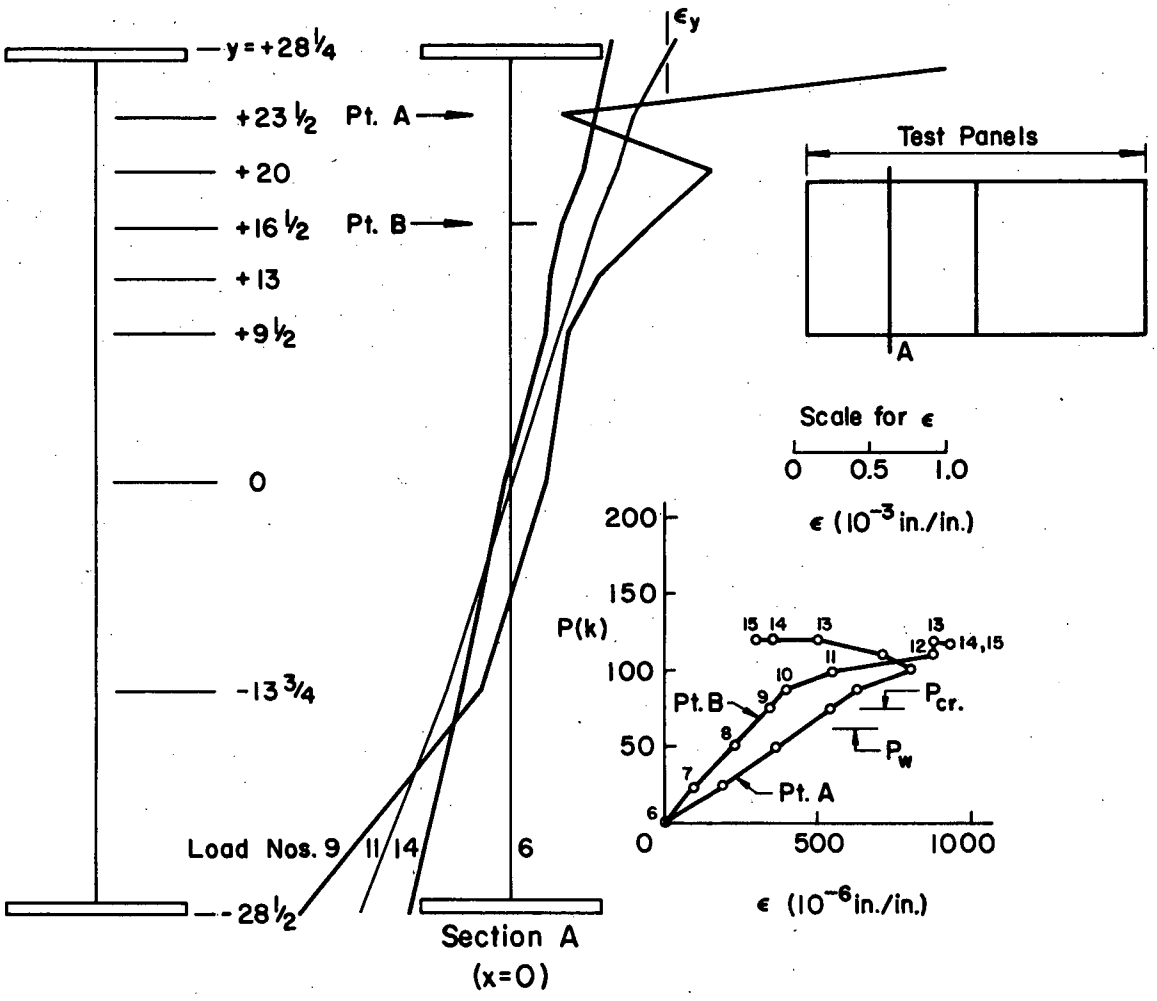


GIRDER LB6

Fig. 2.19 Strain Distribution (Specimen LB6)

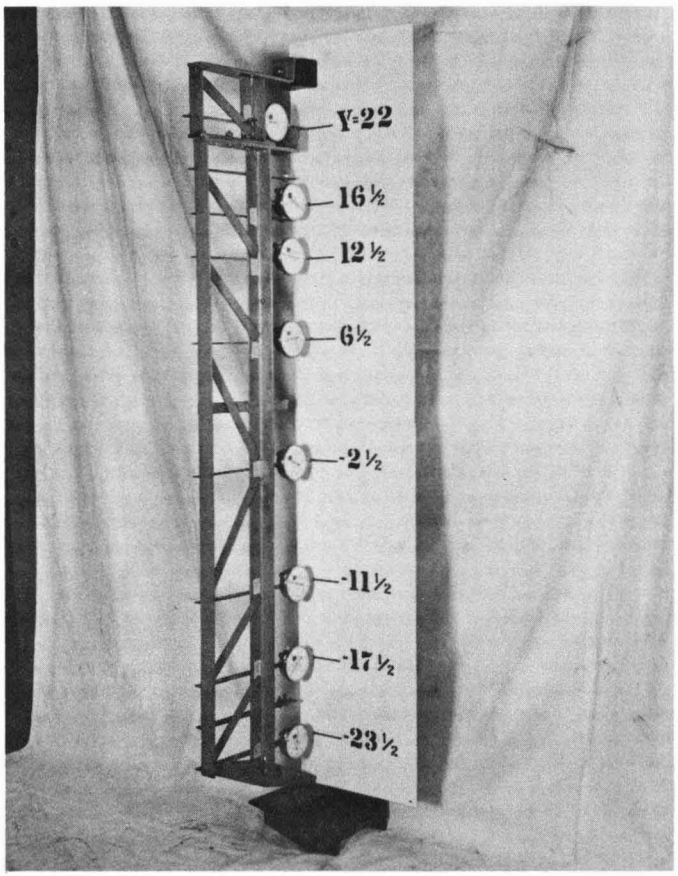


Fig. 2.20 Web Deflection Measuring Device

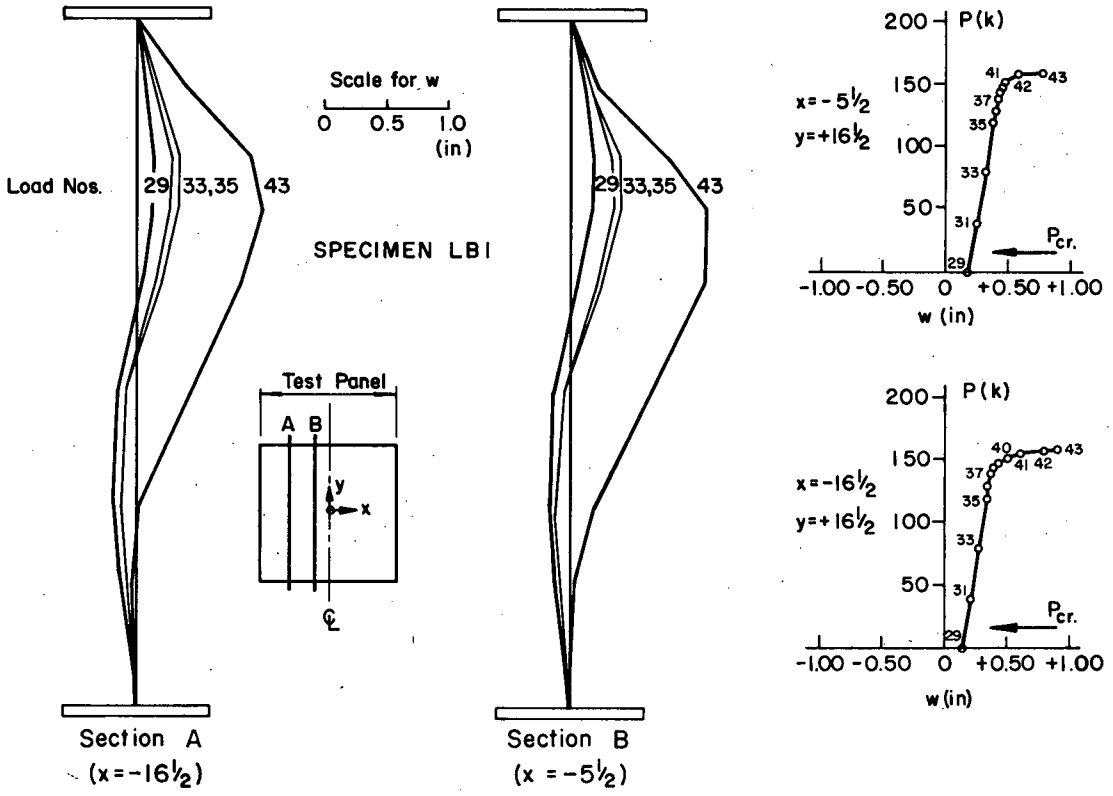


Fig. 2.21 Web Deflections (Specimen LB1)

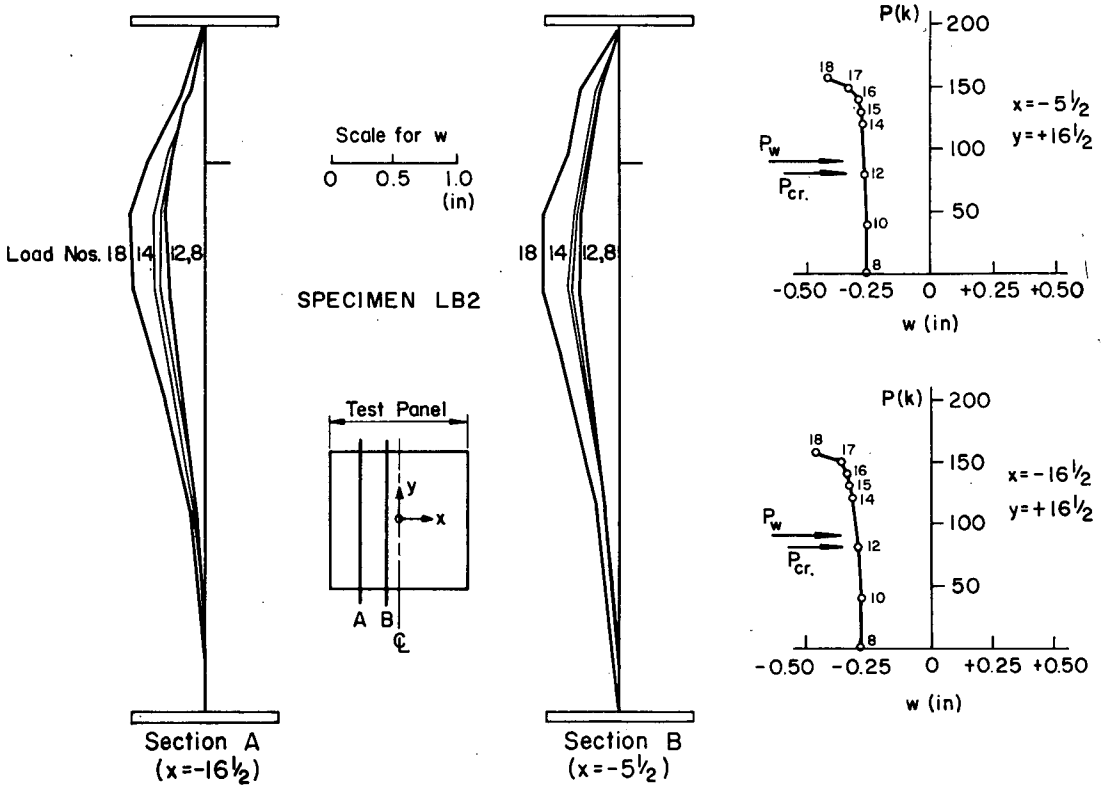


Fig. 2.22 Web Deflections (Specimen LB2)

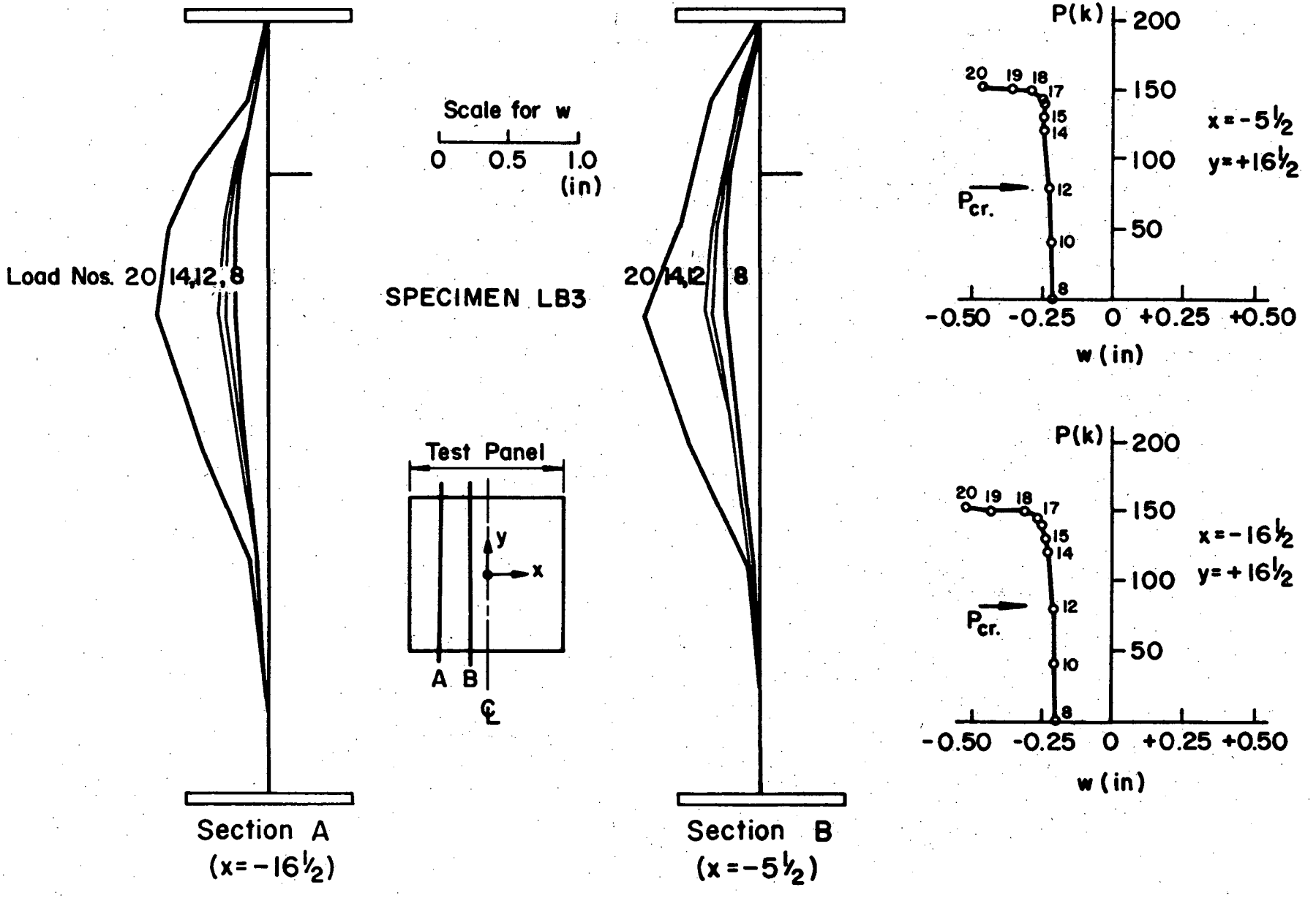


Fig. 2.23 Web Deflections (Specimen LB3)

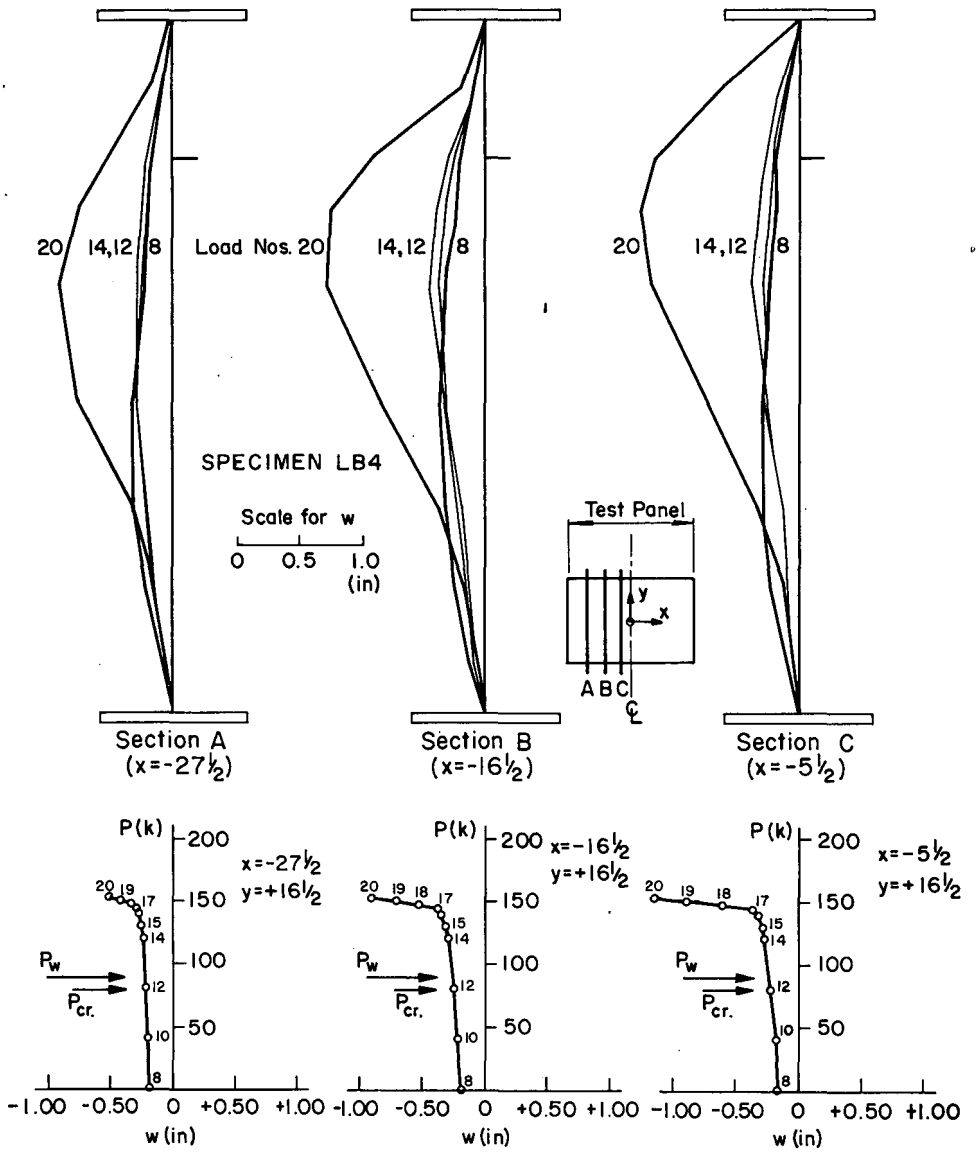


Fig. 2.24 Web Deflections (Specimen LB4)

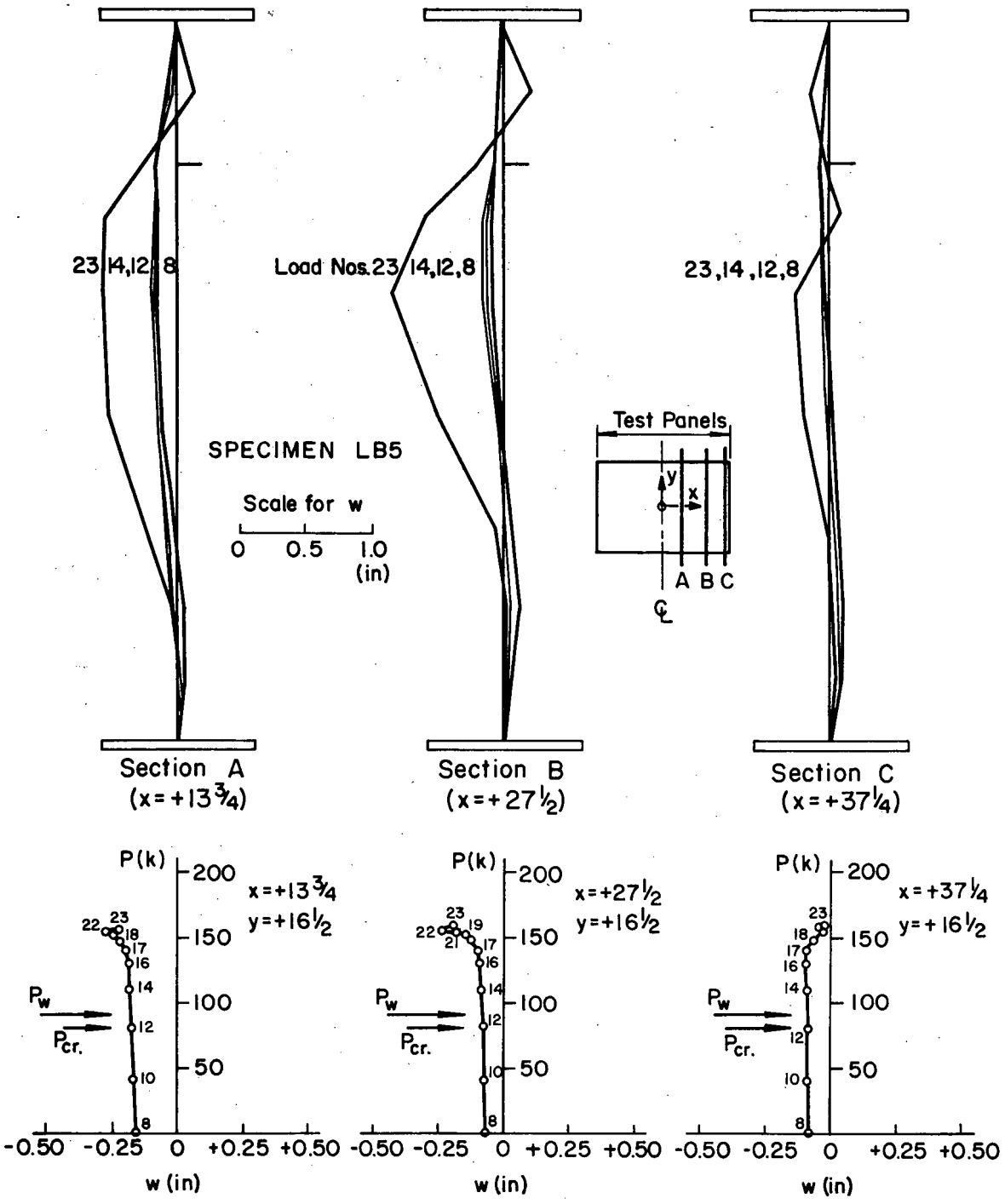


Fig. 2.25 Web Deflections (Specimen LB5)

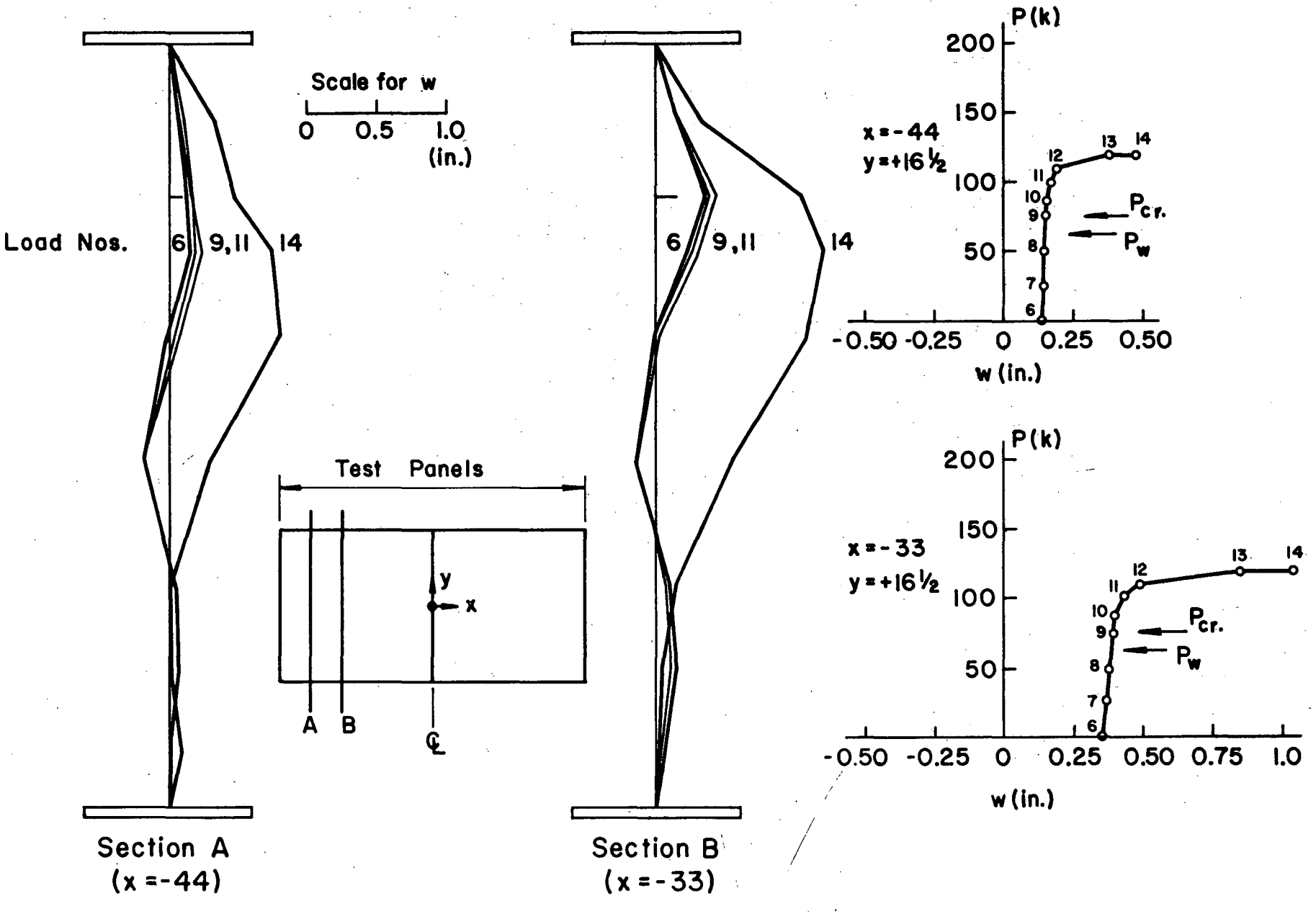


Fig. 2.26 Web Deflections (Specimen LB6)

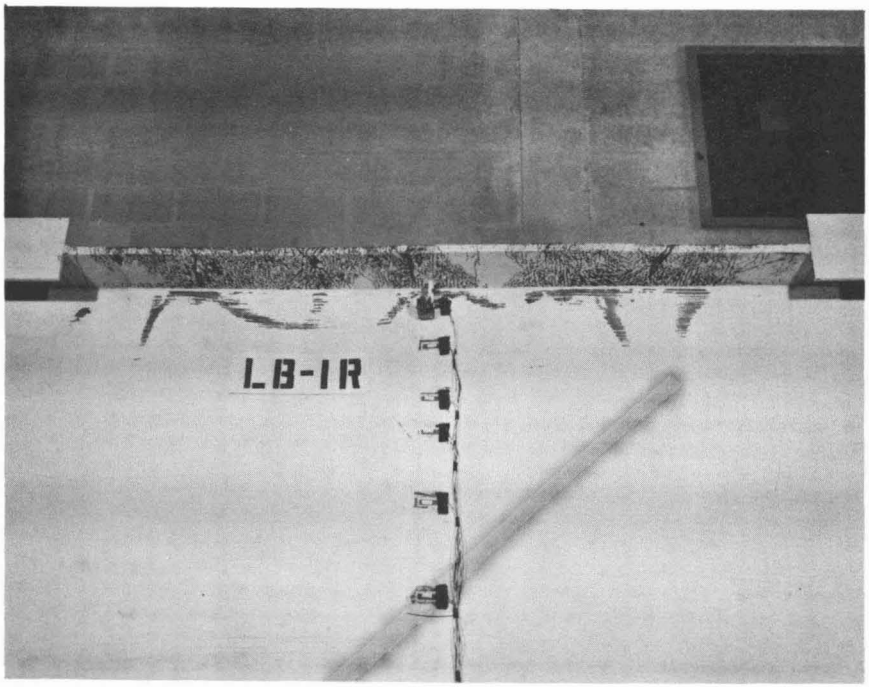


Fig. 2.27 Yield Pattern in Compression Flange and Web, Near Side (Specimen LB1)

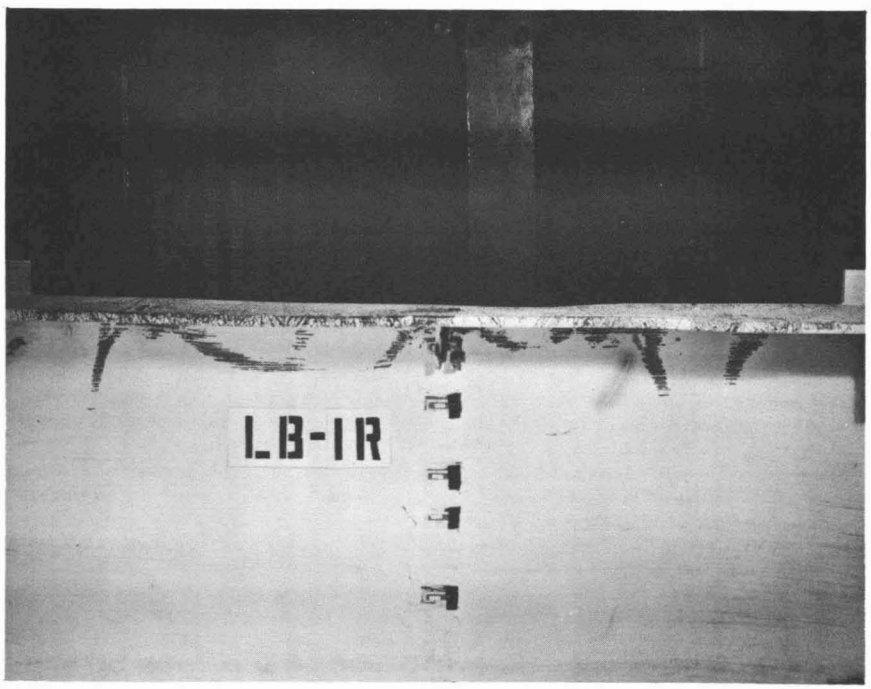


Fig. 2.28 Edge View of Compression Flange, Near Side (Specimen LB1)

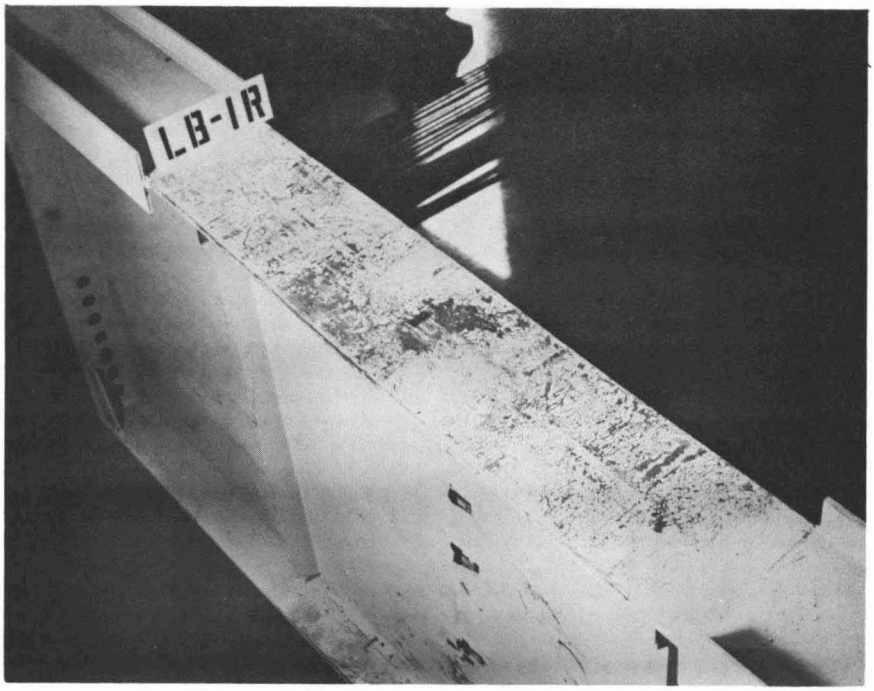


Fig. 2.29 Yield Pattern on Top Surface of Compression Flange (Specimen LB1)

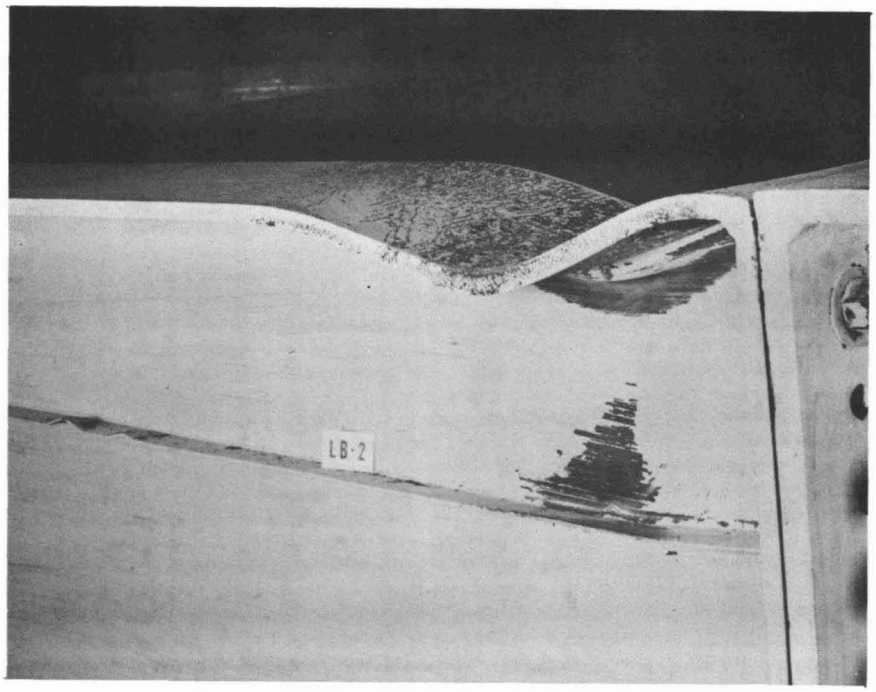


Fig. 2.30 Vertical Buckle, Near Side (Specimen LB2)

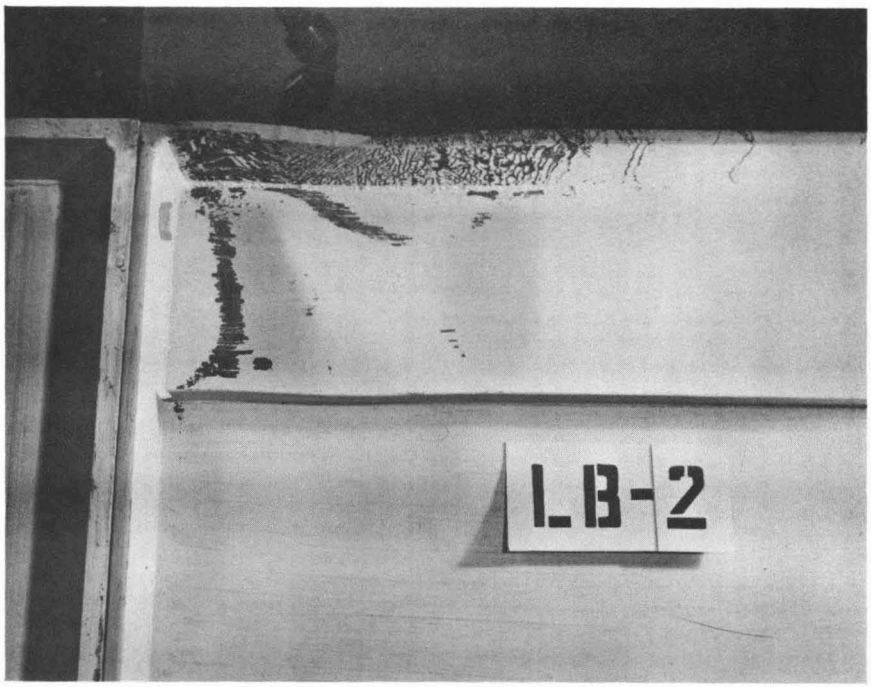


Fig. 2.31 Yielding in Side Panel, Near Side

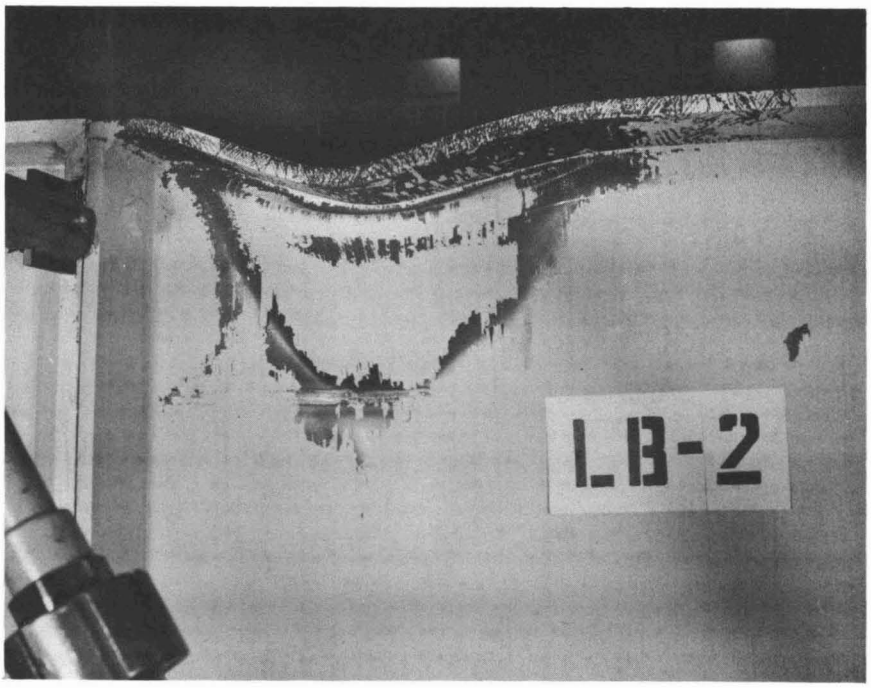


Fig. 2.32 Vertical Buckle, Far Side (Specimen LB2)

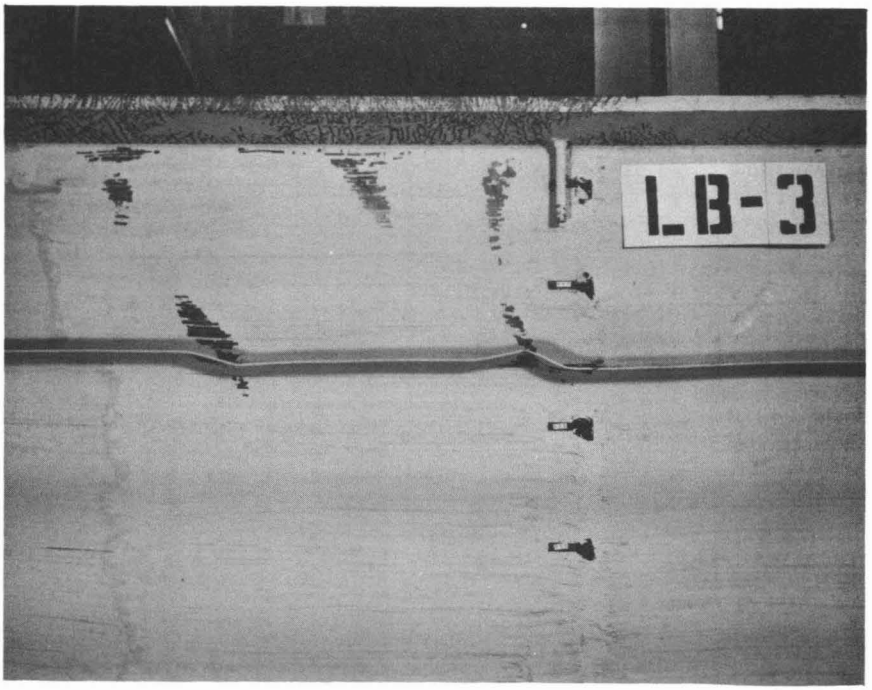


Fig. 2.33 Yield Pattern and Longitudinal Stiffener Buckles, Near Side (Specimen LB3)

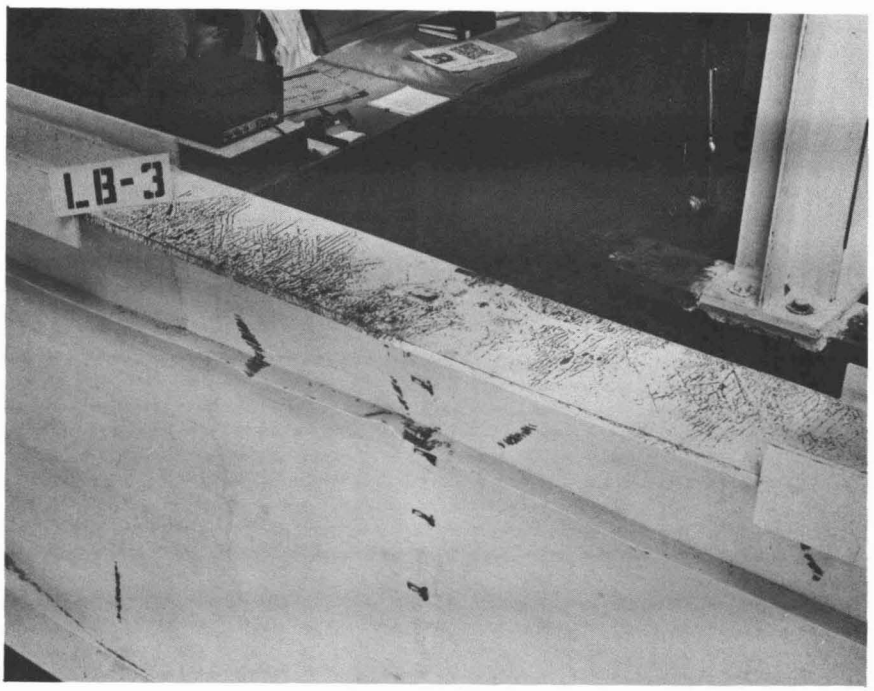


Fig. 2.34 Compression Flange Yield Pattern (Specimen LB3)

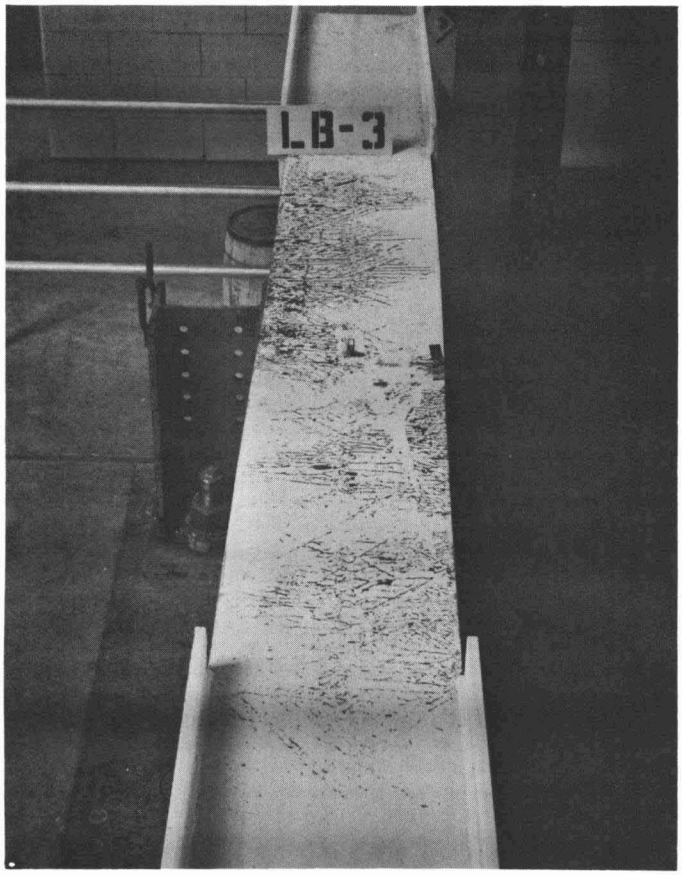


Fig. 2.35 Yield Pattern on Top Surface of Compression Flange (Specimen LB3)

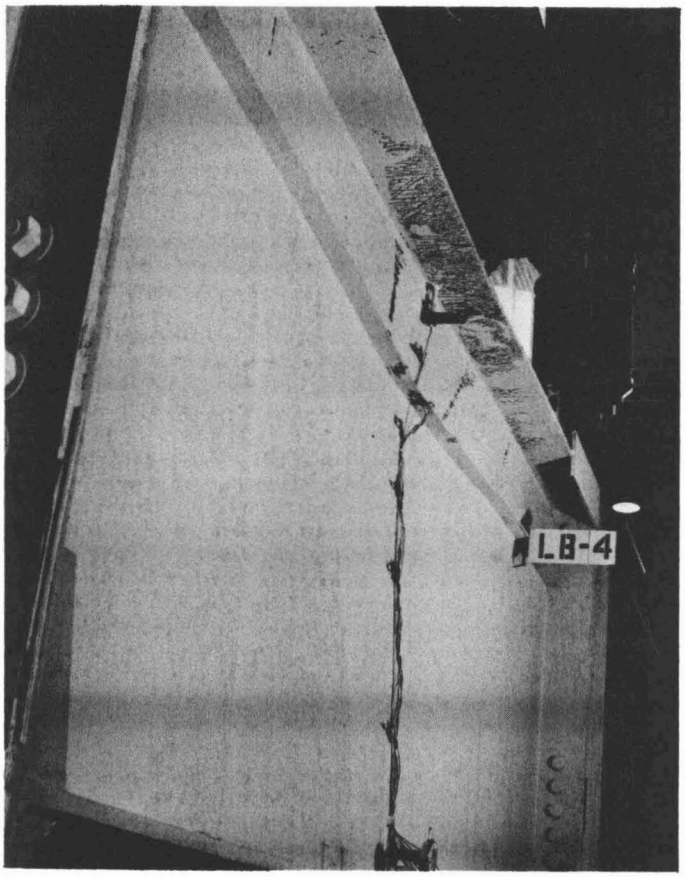


Fig. 2.36 Test Panel After Ultimate Load, Near Side (Specimen LB4)

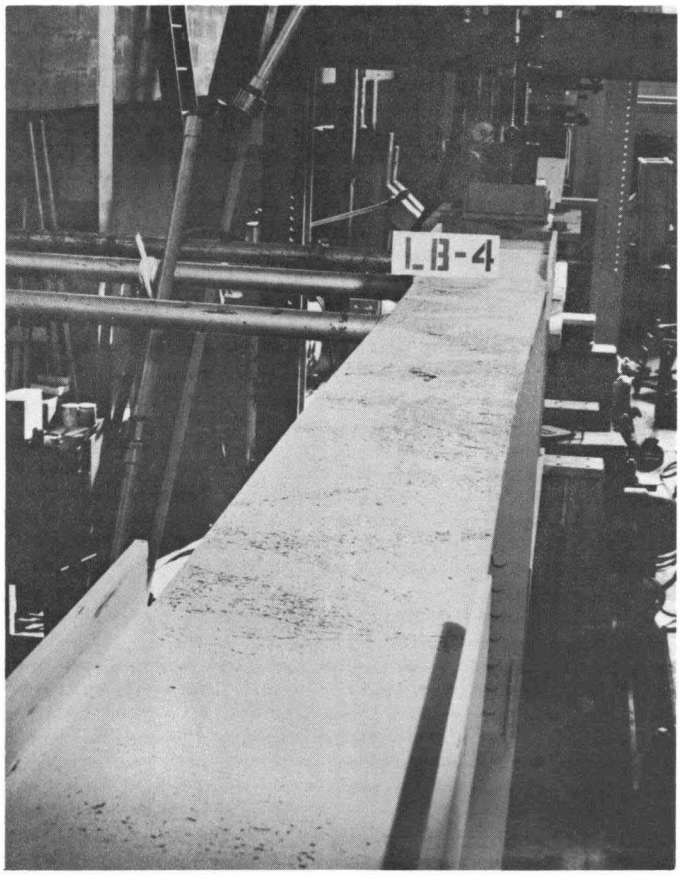


Fig. 2.37 Compression Flange Yield Pattern After Ultimate Load (Specimen LB4)

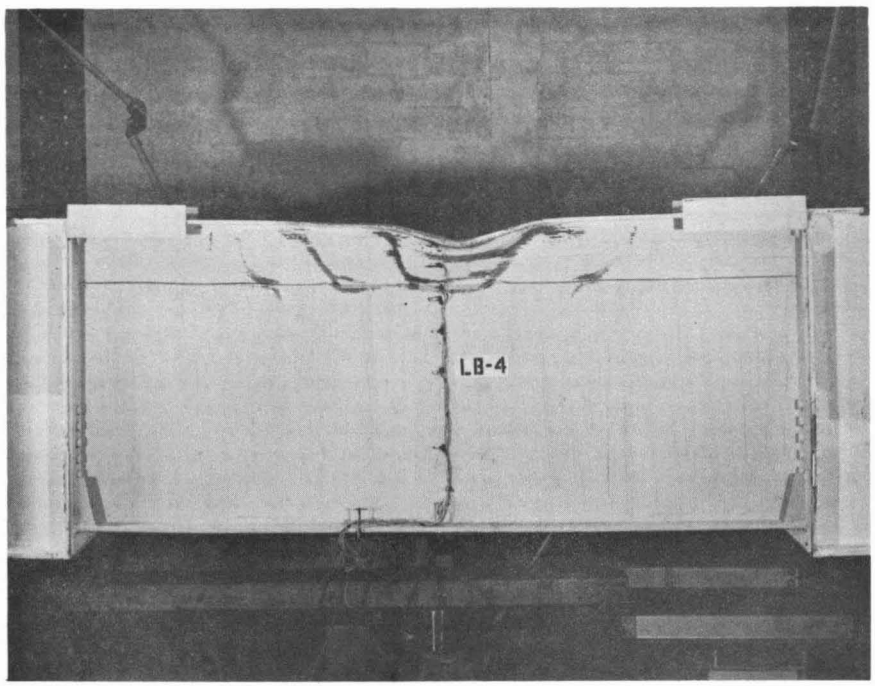


Fig. 2.38 Failure Due to Vertical Buckling, Near Side (Specimen LB4)

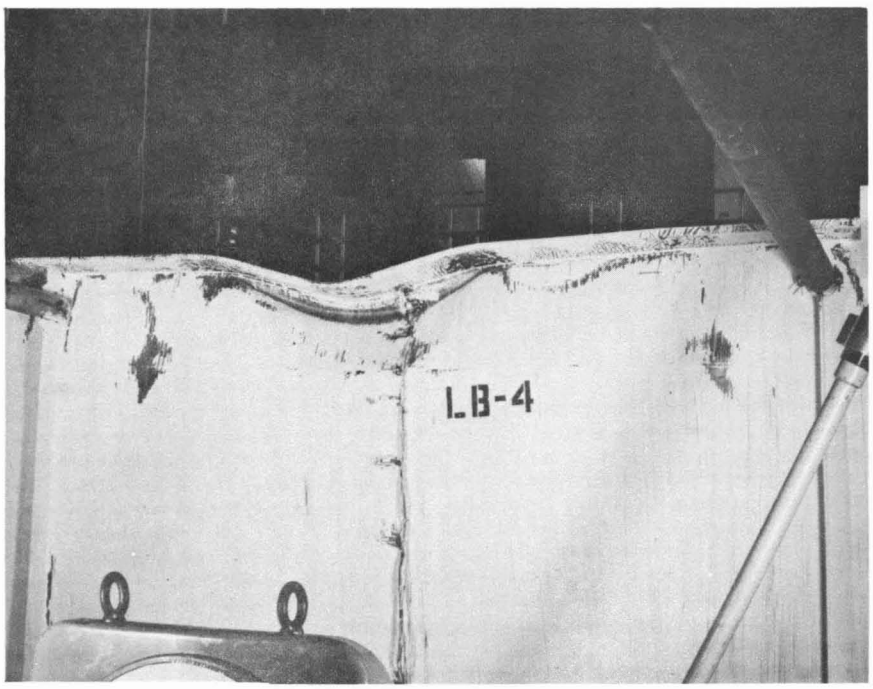


Fig. 2.39 Failure Due to Vertical Buckling, Far Side (Specimen LB4)

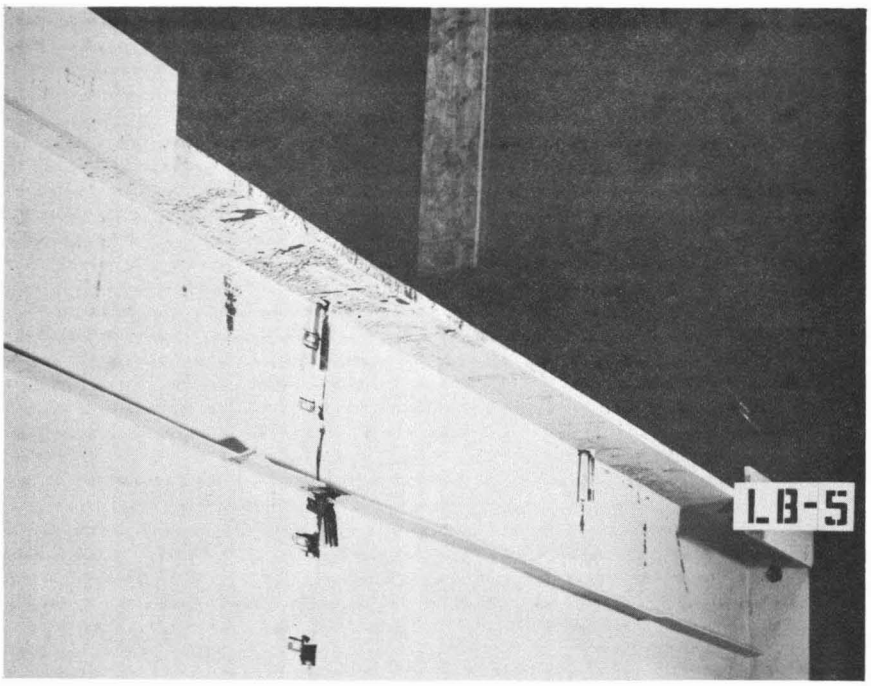


Fig. 2.40 Yield Pattern and Horizontal Stiffener Buckles, Near Side (Specimen LB5)

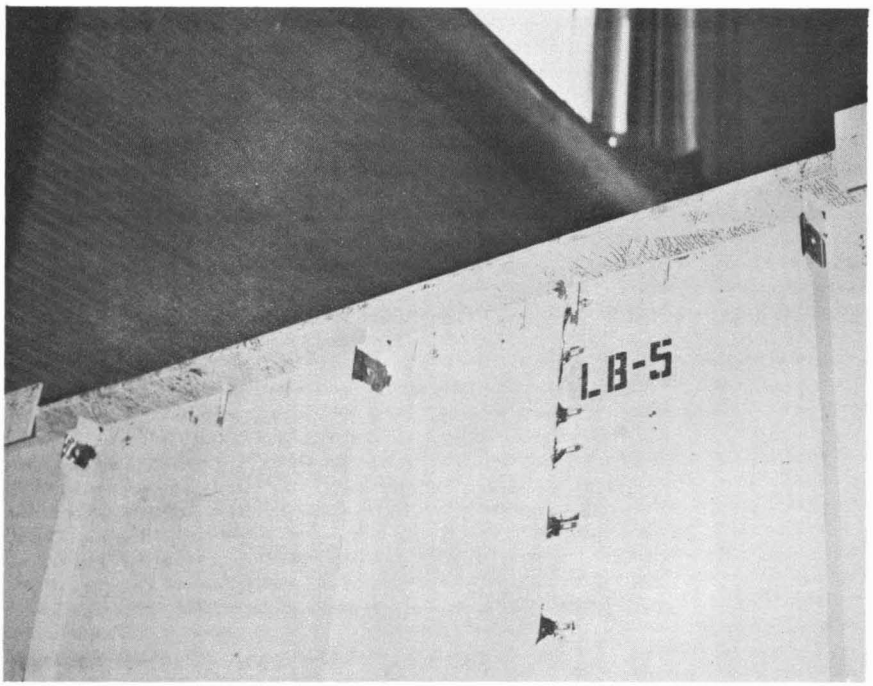


Fig. 2.41 Yield Pattern, Far Side (Specimen LB5)

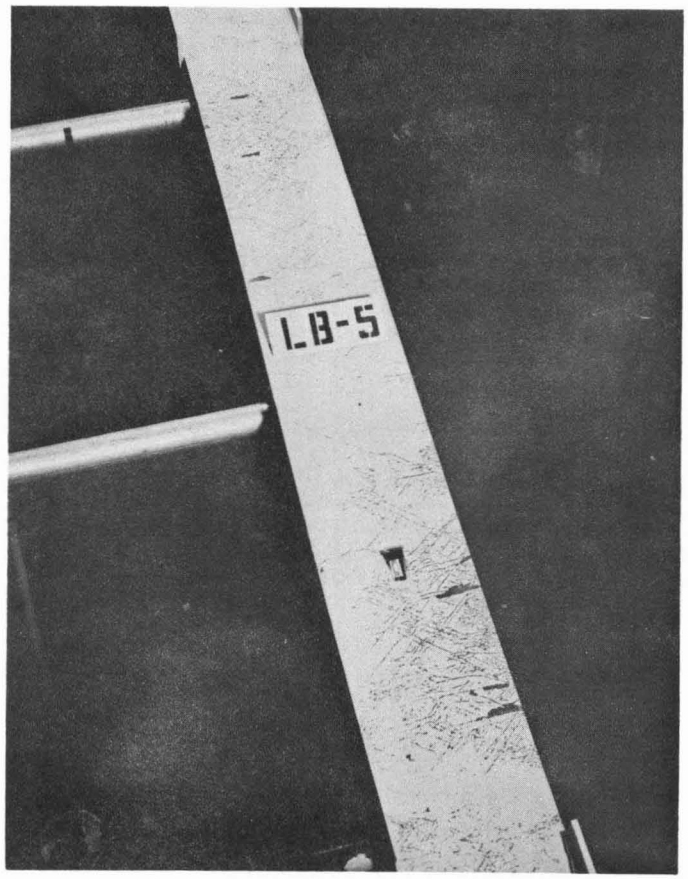


Fig. 2.42 Compression Flange Yield Pattern
(Specimen LB5)

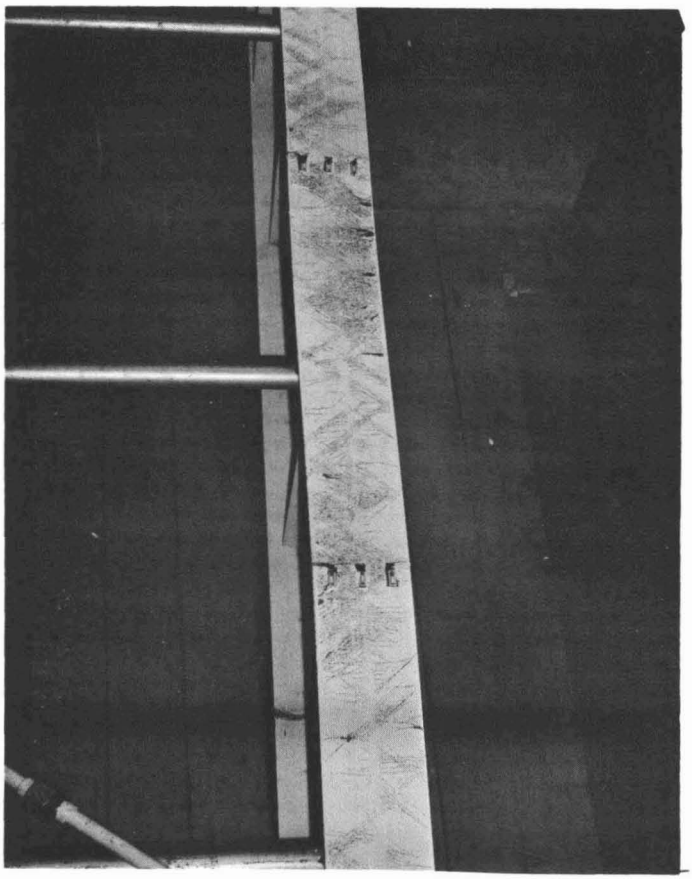

Fig. 2.43 Compression Flange Yield Pattern After Ultimate Load (Specimen LB6)

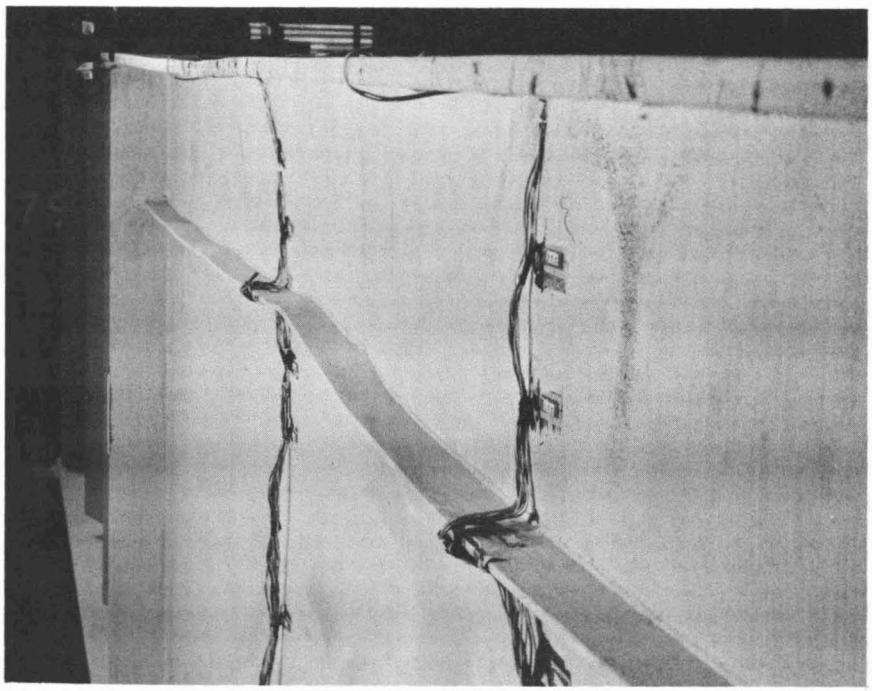

Fig. 2.44 Longitudinal Stiffener Deformations After Ultimate Load (Specimen LB6)

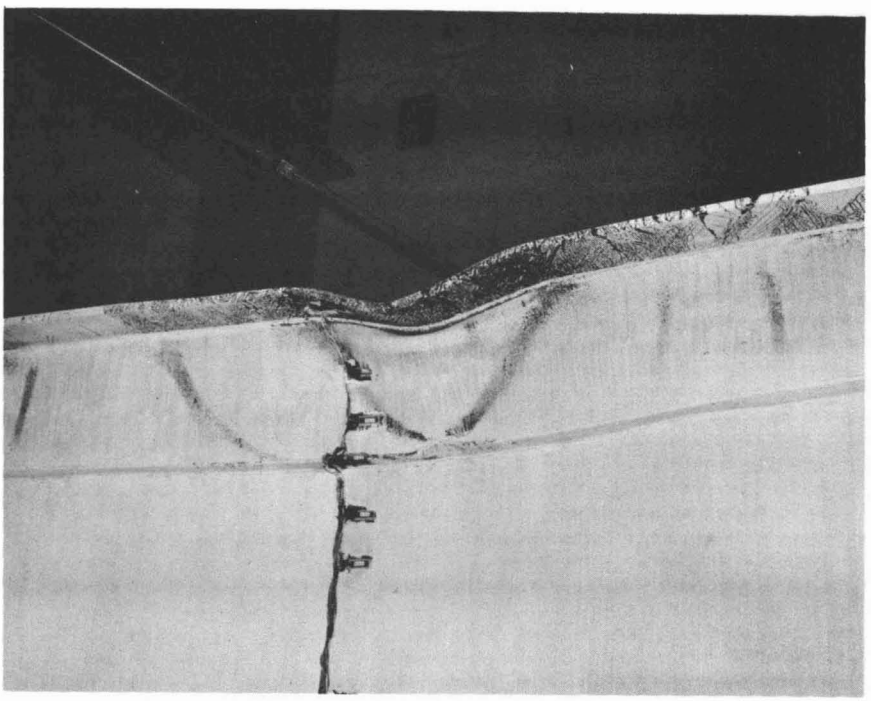

Fig. 2.45 Vertical Buckling Failure, Near Side (Specimen LB6)

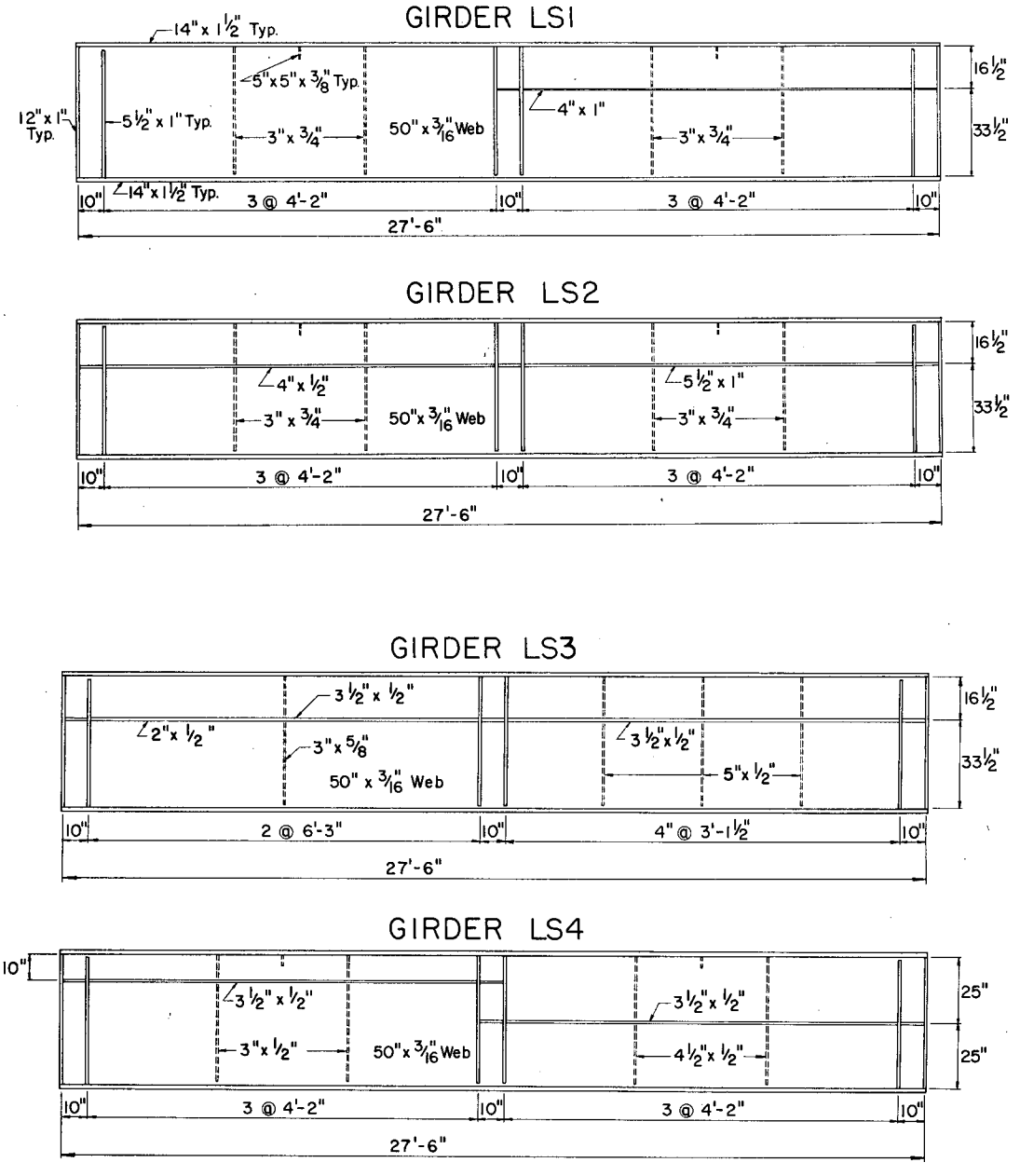


Fig. 3.1 Test Girders

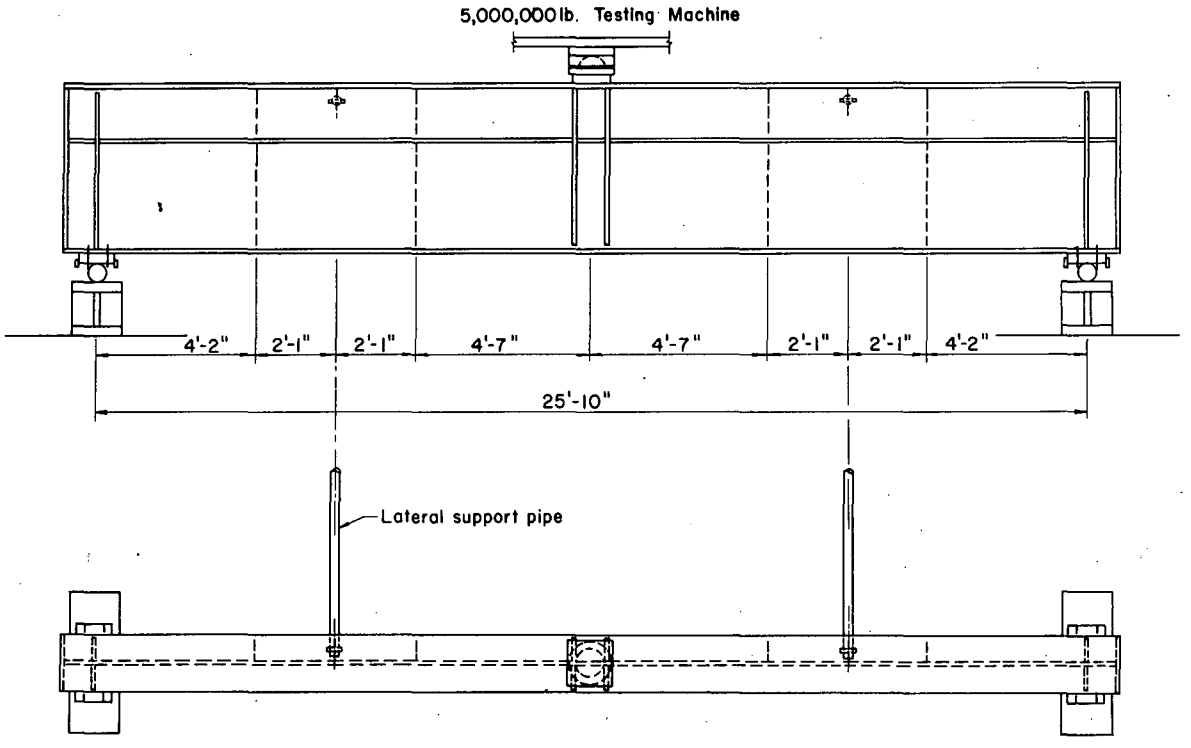


Fig. 3.2 Test Setup

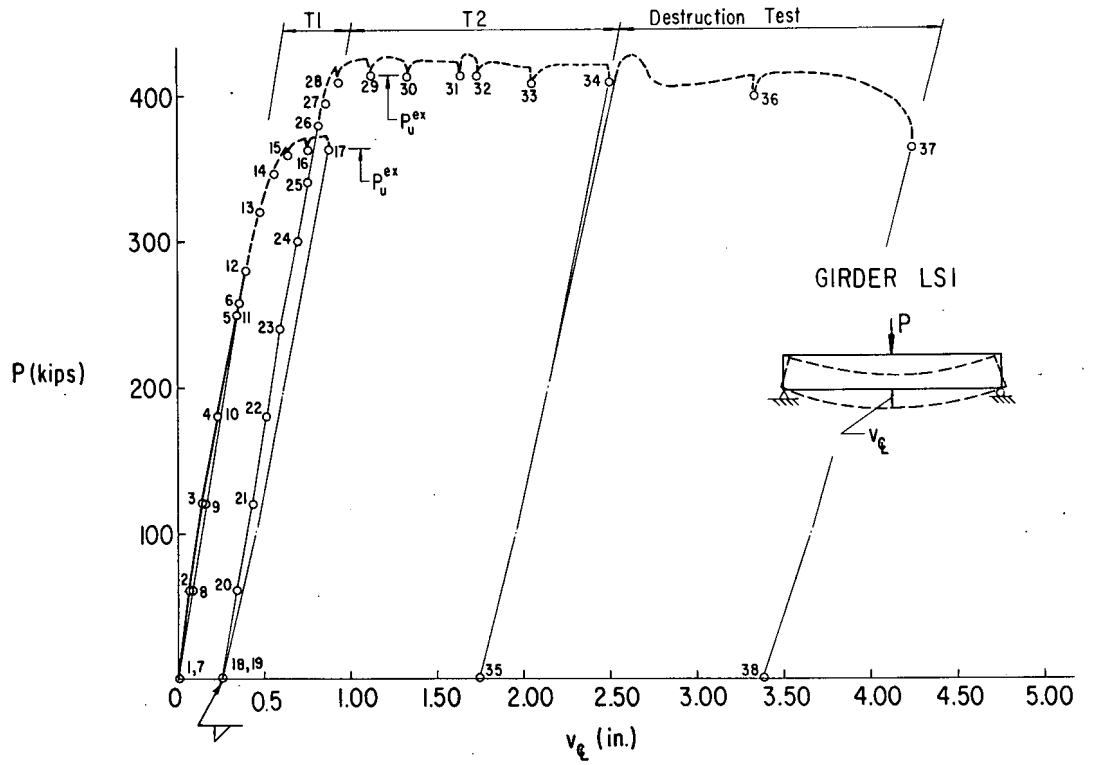


Fig. 3.3 Load-Vs-Centerline Deflection Curve for Girder LS1

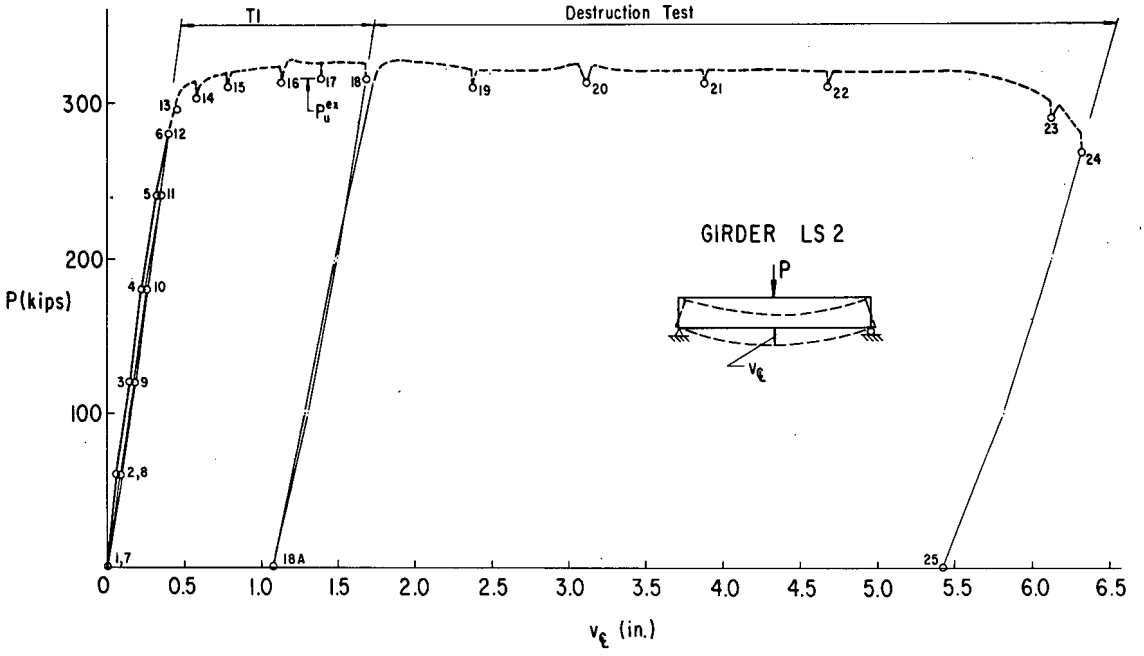


Fig. 3.4 Load-Vs-Centerline Deflection Curve for Girder LS2

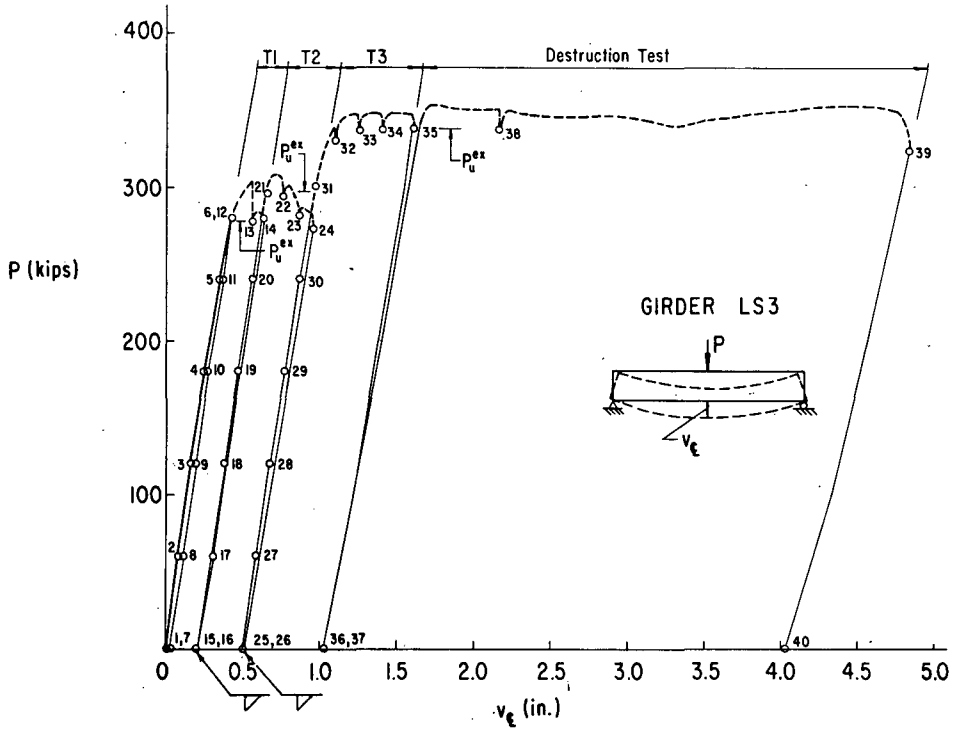


Fig. 3.5 Load-Vs-Centerline Deflection Curve for Girder LS3

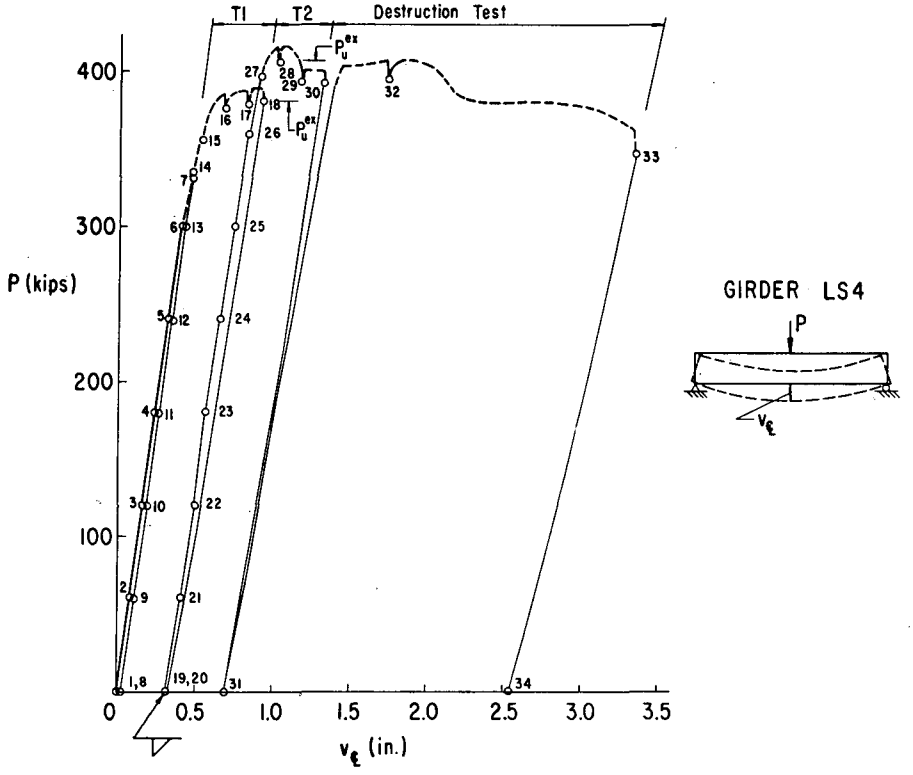


Fig. 3.6 Load-Vs-Centerline Deflection Curve for Girder LS4

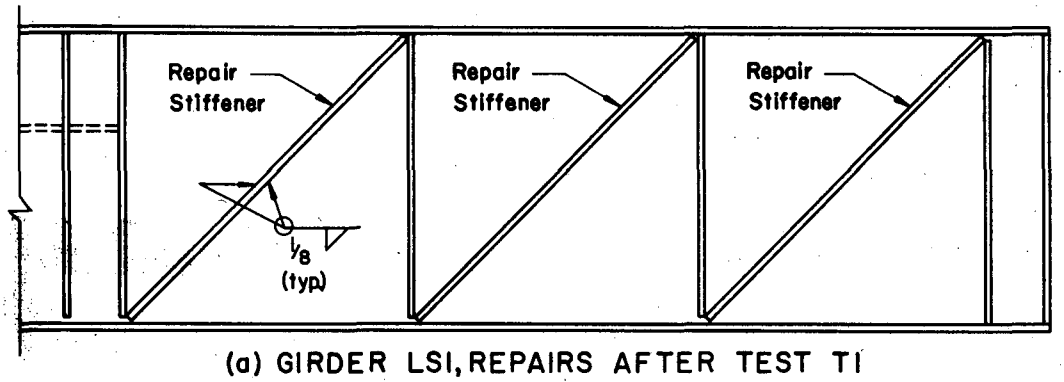


(a) GIRDER LSI, REPAIRS AFTER TEST TI

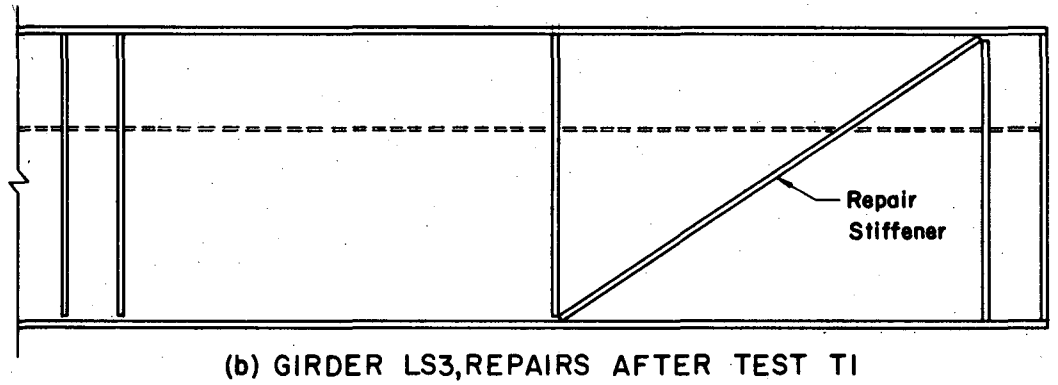


(b) GIRDER LS3, REPAIRS AFTER TEST TI

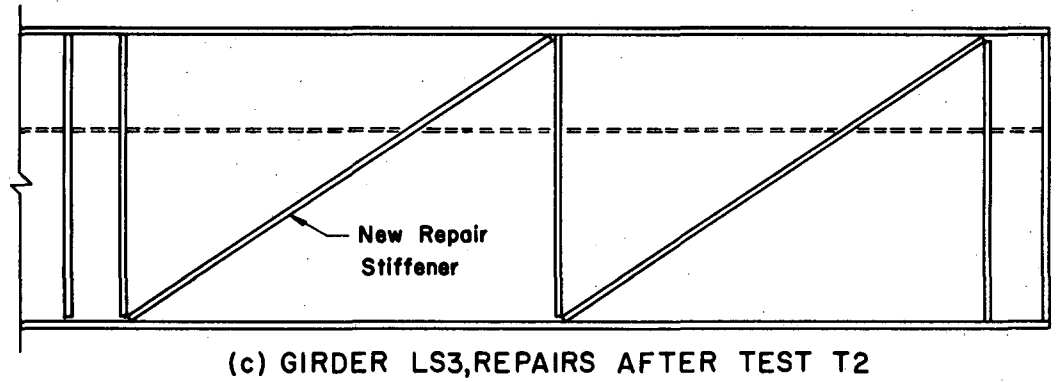


(c) GIRDER LS3, REPAIRS AFTER TEST T2

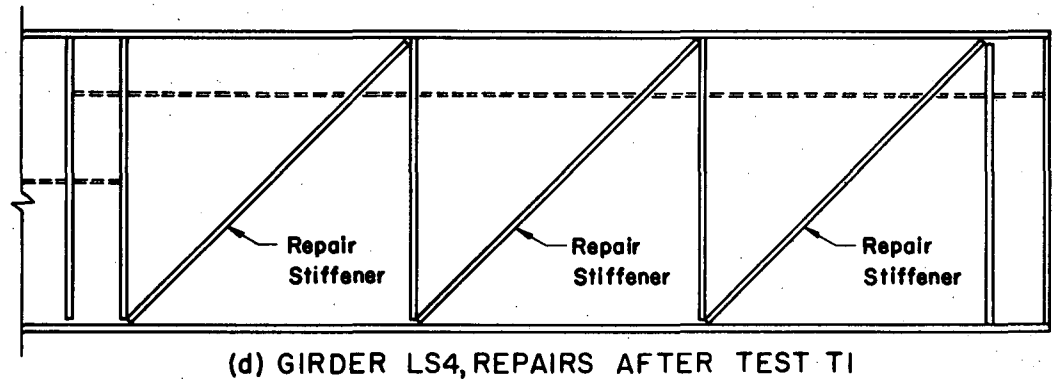


(d) GIRDER LS4, REPAIRS AFTER TEST TI

NOTE: ALL REPAIR STIFFENERS WERE CUT FROM 6" x ½" MILD STEEL BARS AND FITTED TO THE DEFORMED SHAPE OF THE WEB BEFORE BEING WELDED INTO PLACE.

Fig. 3.7 Repairs of Failed Panels

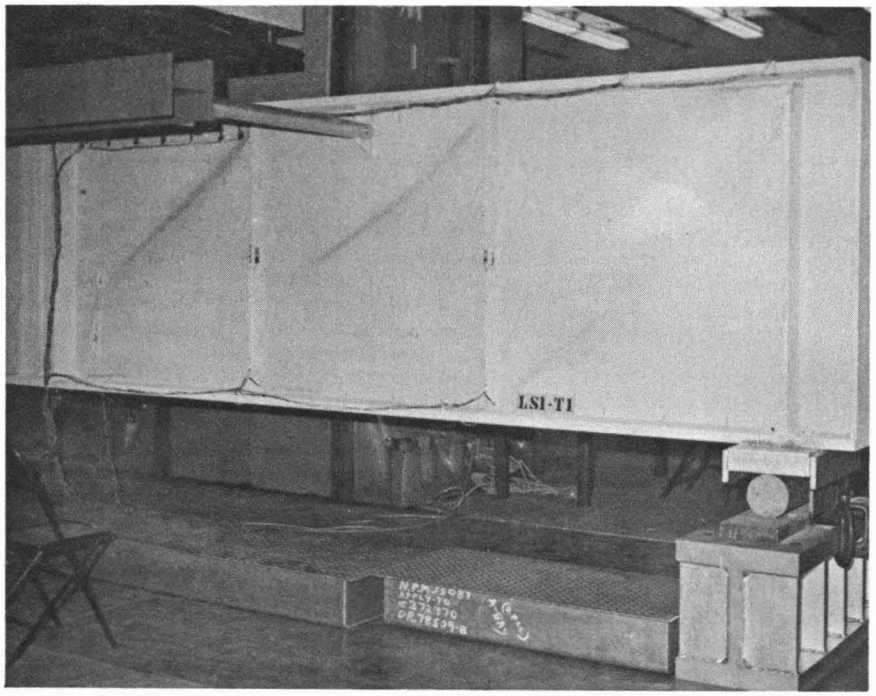


Fig. 3.8 Yield Patterns in Girder LS1 at Load No. 14

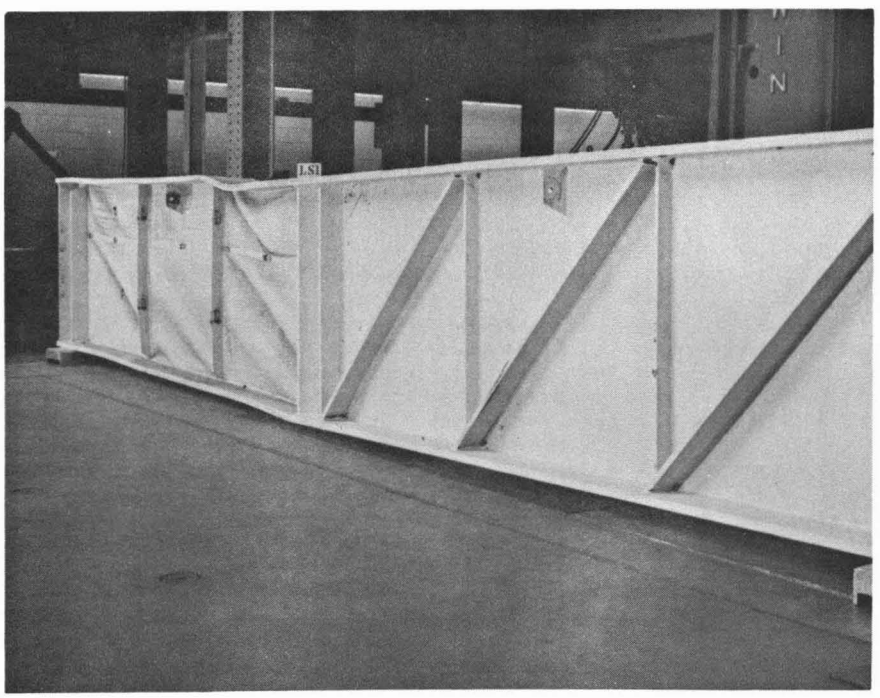


Fig. 3.9 Girder LS1 After Destruction Test (far side)

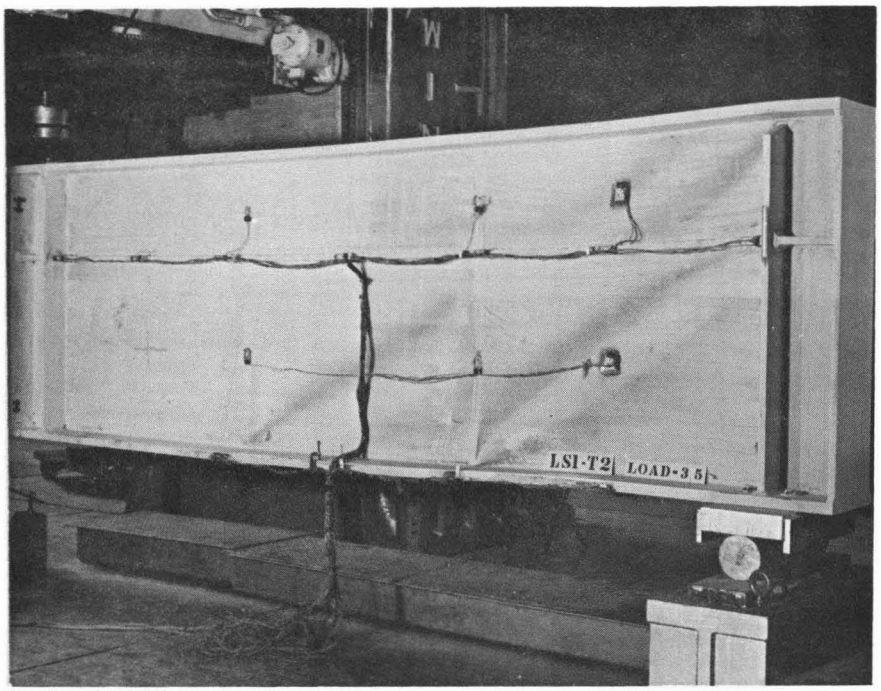


Fig. 3.10 Appearance of Girder LS1 at Load No. 35

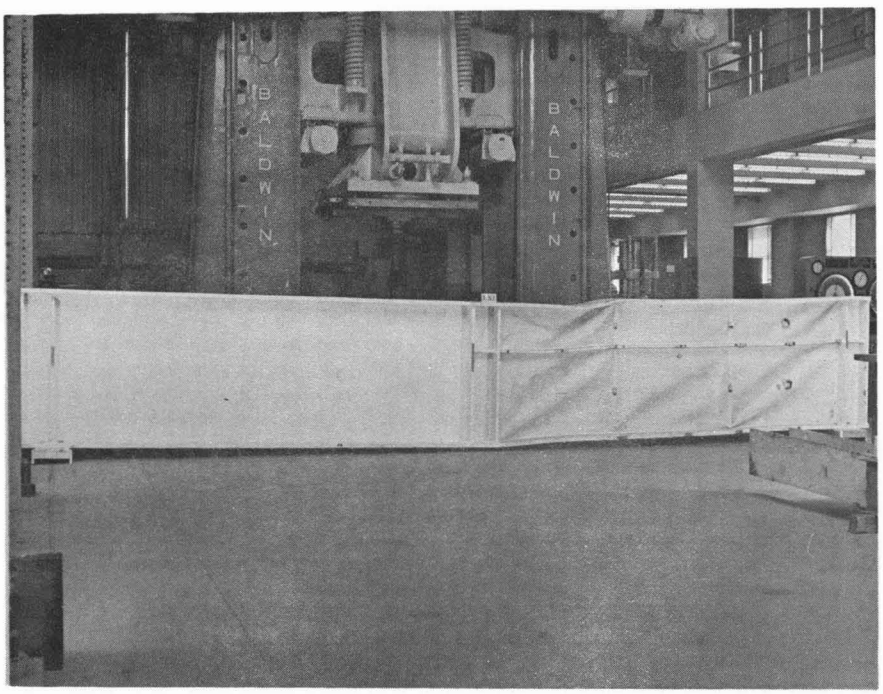


Fig. 3.11 Girder LS1 after Destruction Test (near side)

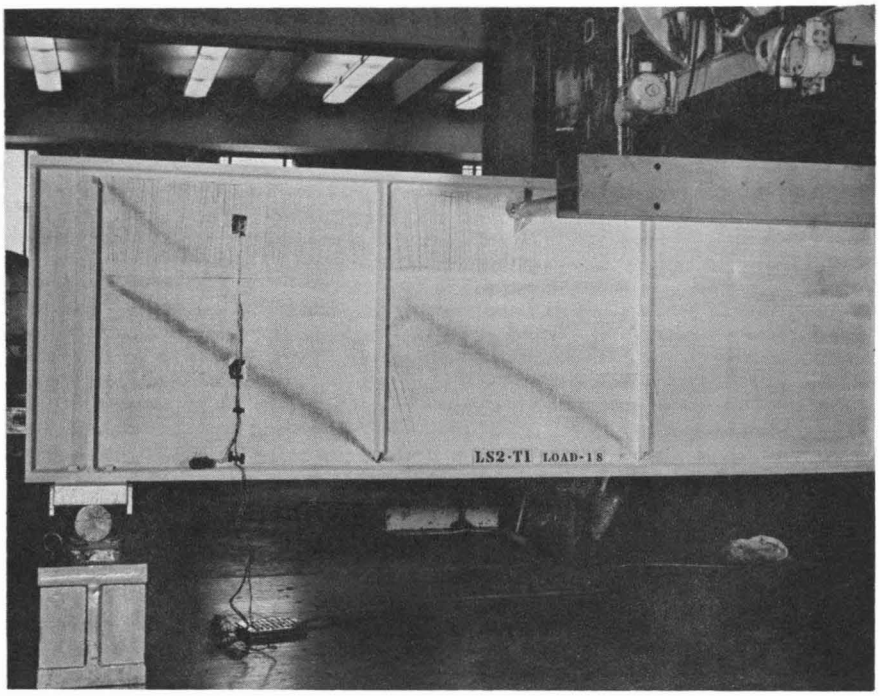


Fig. 3.12 Girder LS2 at Load No. 18 (+ x end)

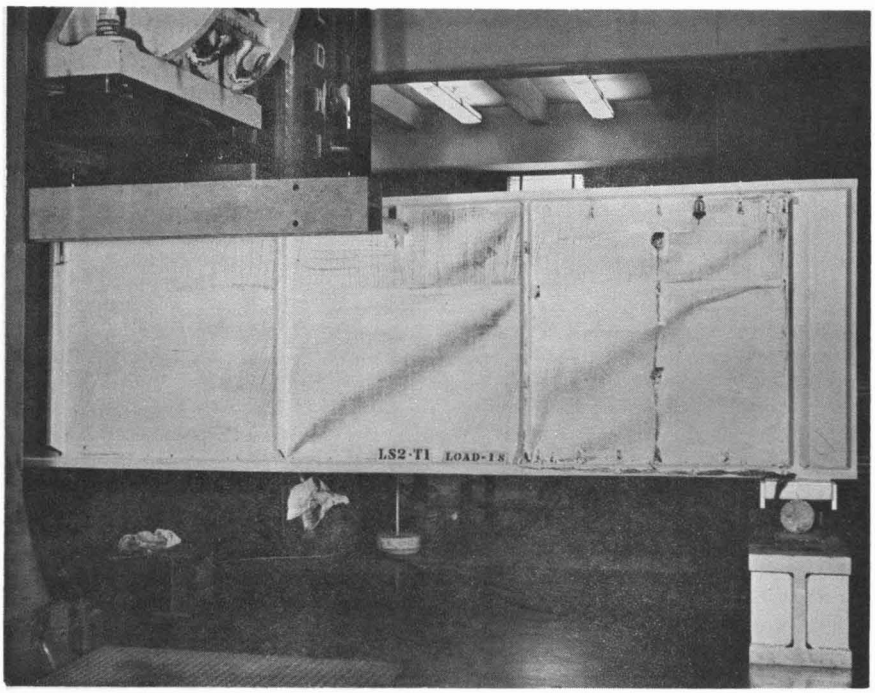


Fig. 3.13 Girder LS2 at Load No. 18 (- x end)

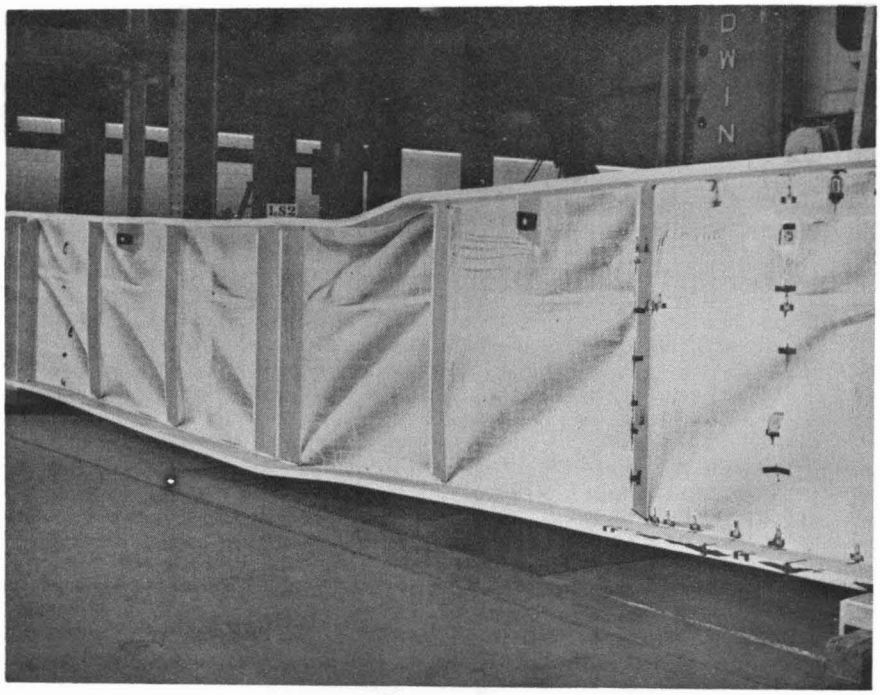


Fig. 3.14 Girder LS2 after Destruction Test

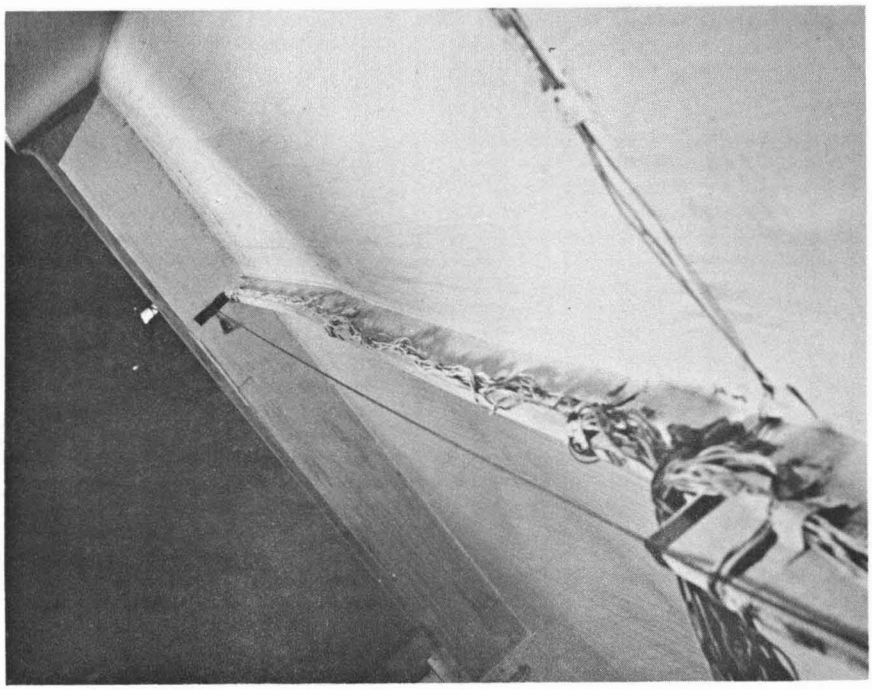

Fig. 3.15 Buckled Longitudinal Stiffener in Girder LS3 After Test T1

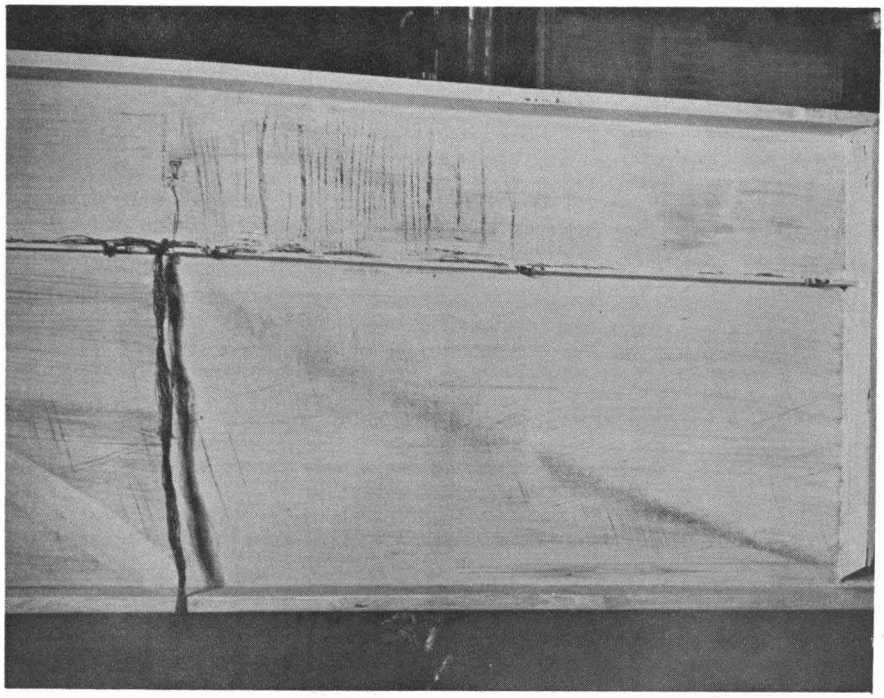

Fig. 3.16 Test Panel of Girder LS3 after Test

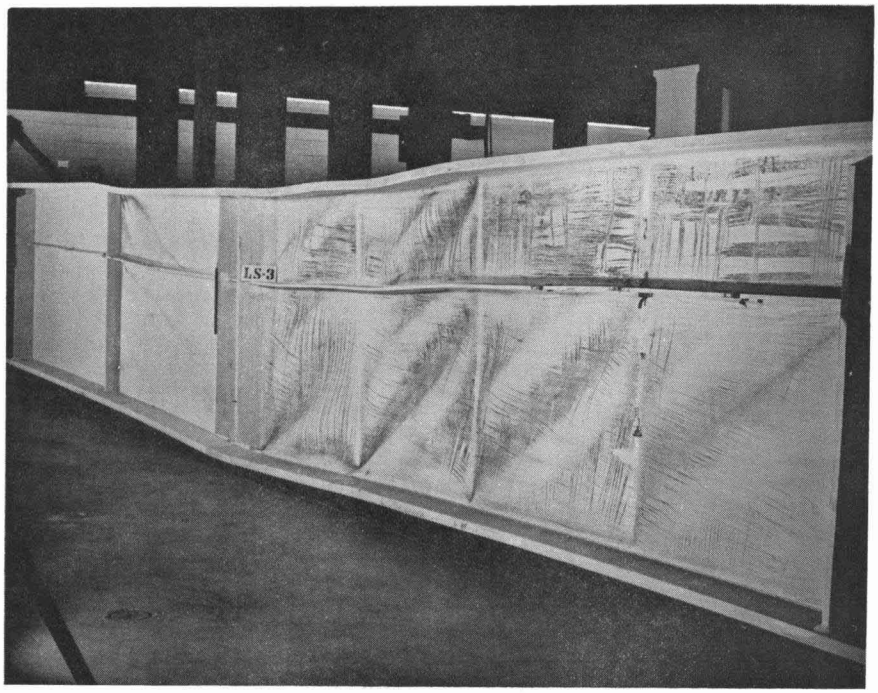


Fig. 3.17 Girder LS3 after Destruction Test

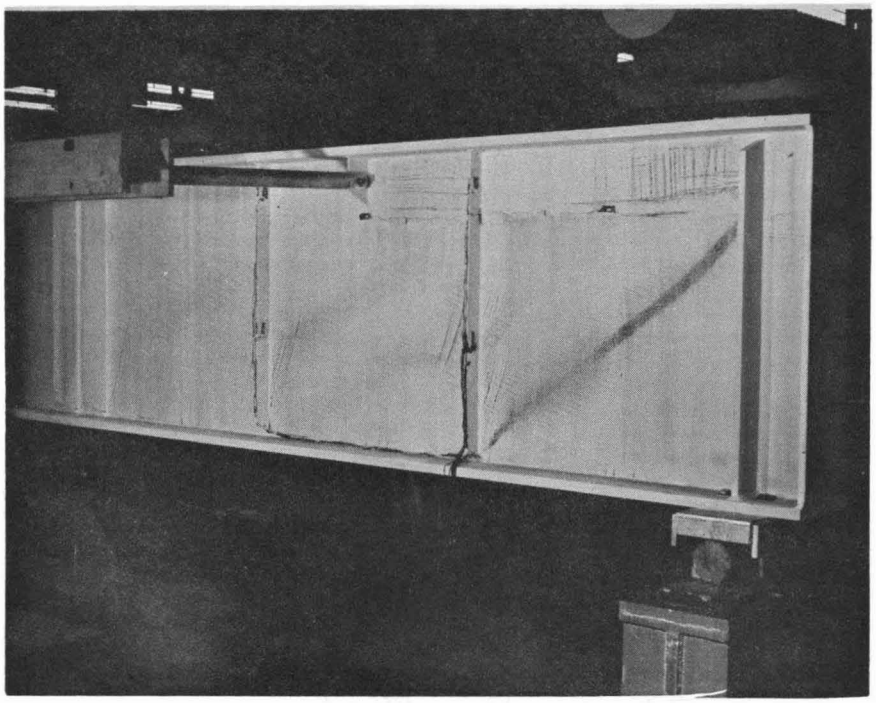

Fig. 3.18 Yield Patterns in Girder LS4 at Load No. 18

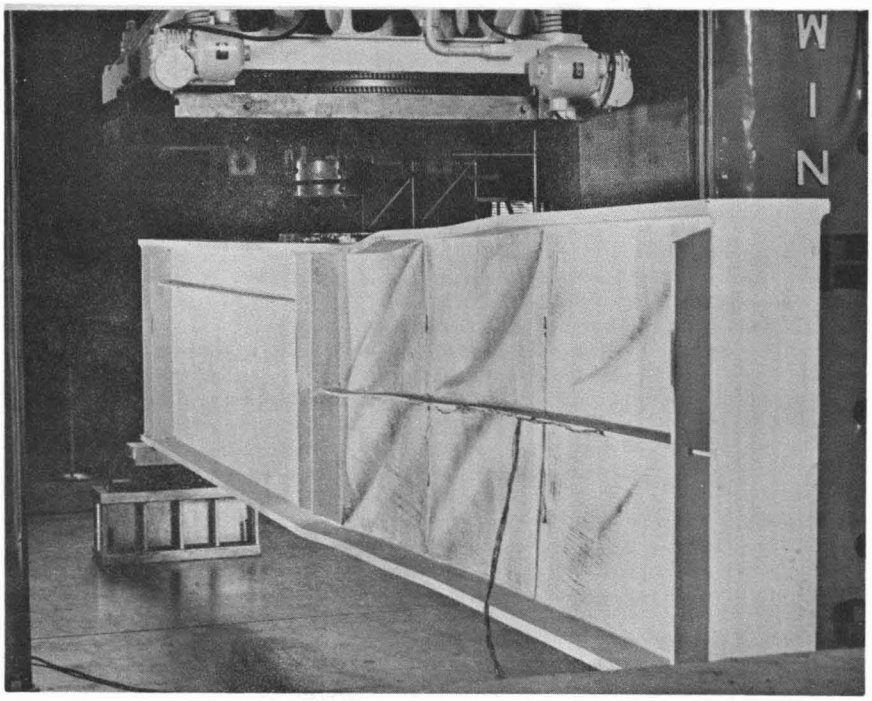


Fig. 3.19 Girder LS4 after Destruction Test

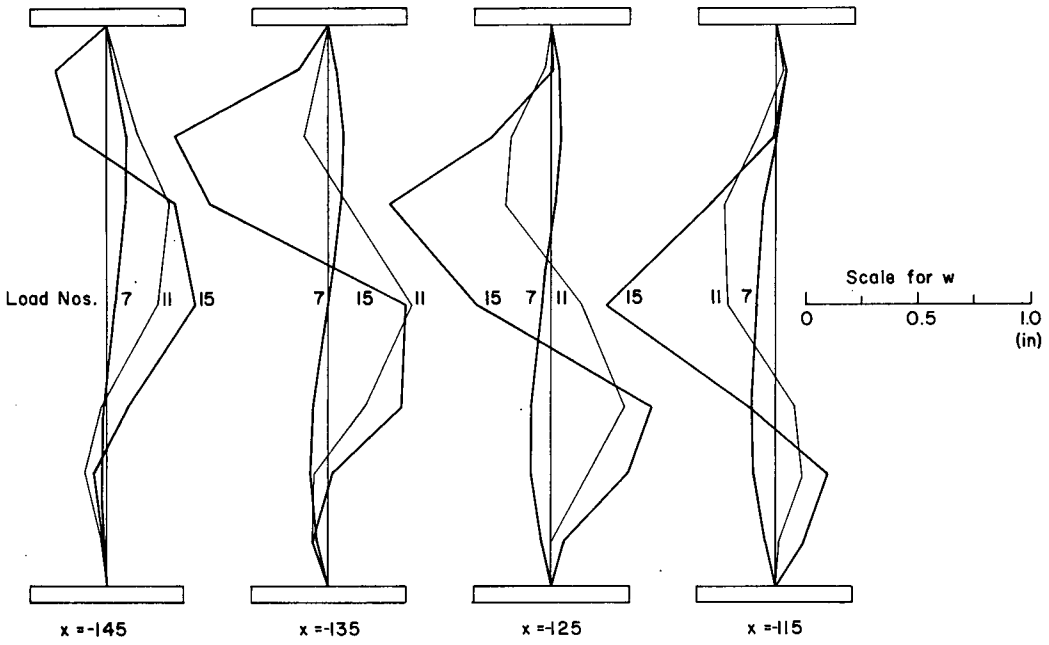


Fig. 3.20 Web Deflections (Test LS1-T1)

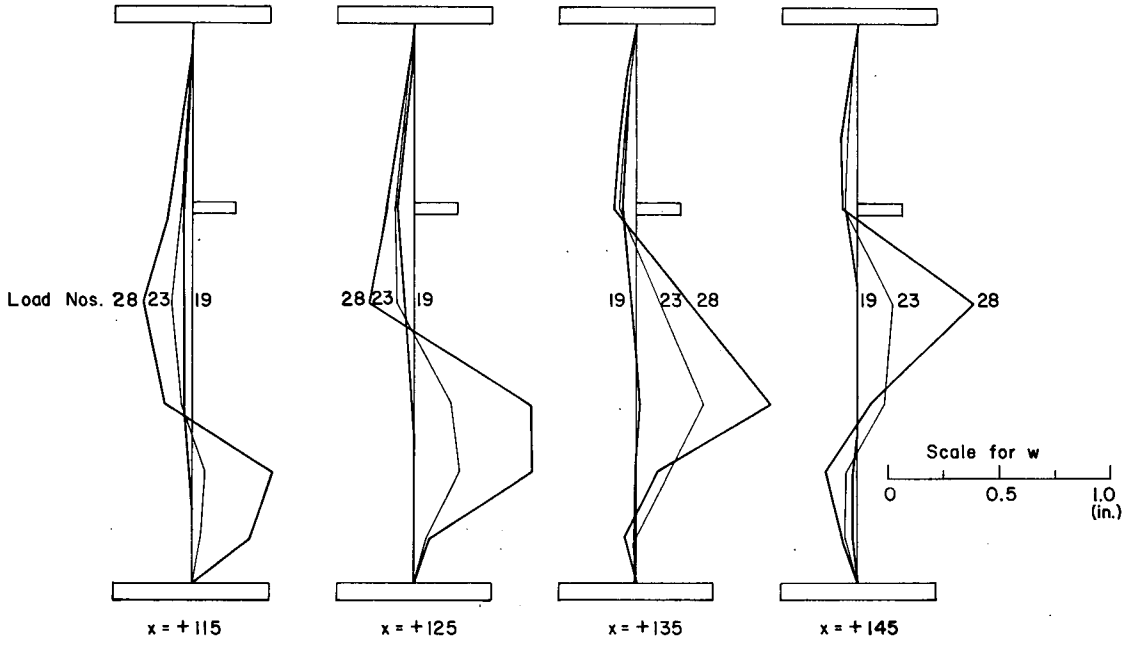


Fig. 3.21 Web Deflections (Test LS1-T2)

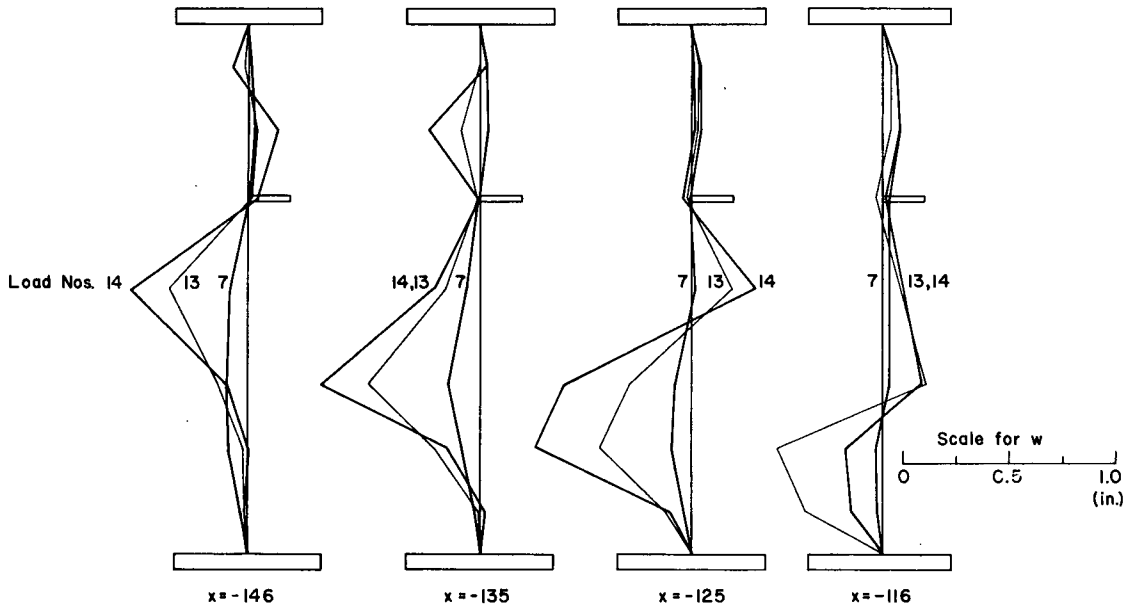


Fig. 3.22 Web Deflections (Test LS2-T1)

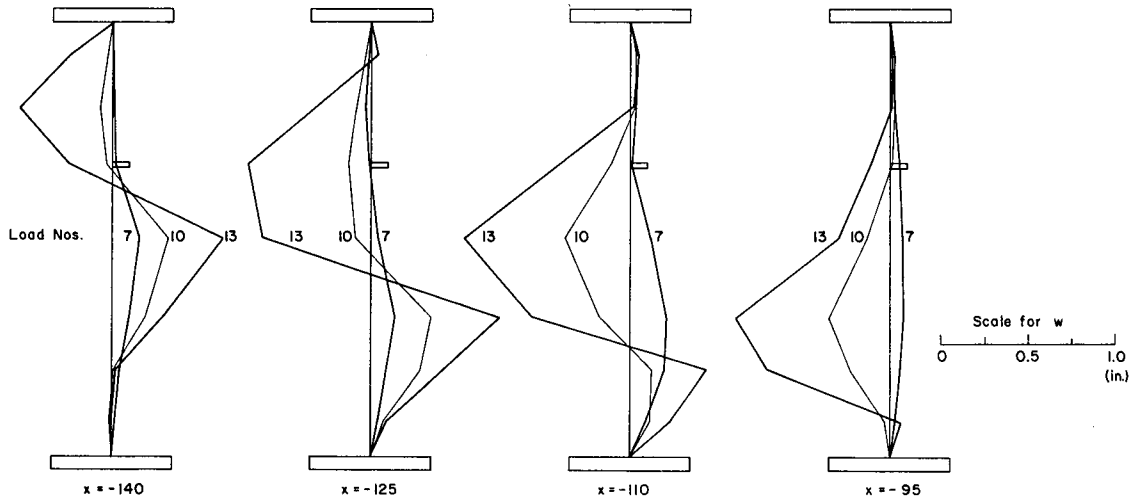


Fig. 3.23 Web Deflections (Test LS3-T1)

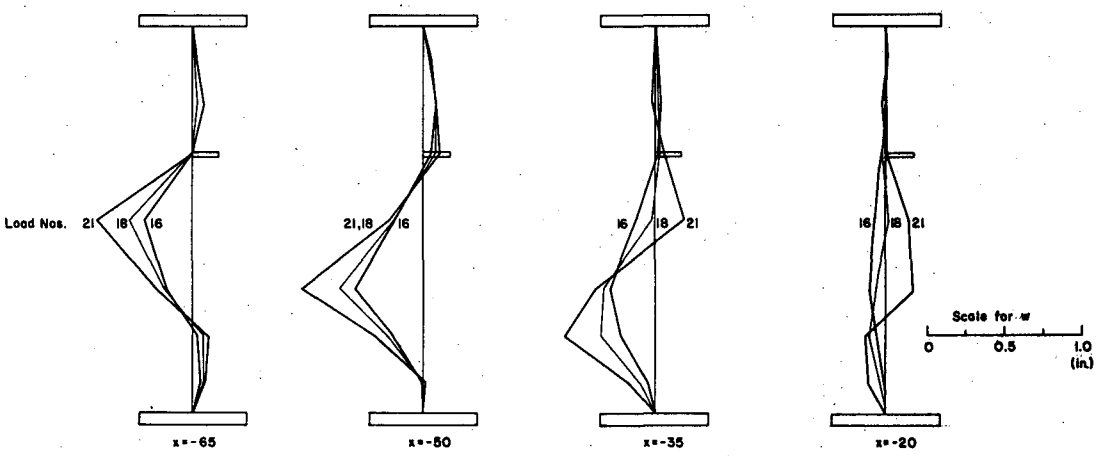


Fig. 3.24 Web Deflections (Test LS3-T2)

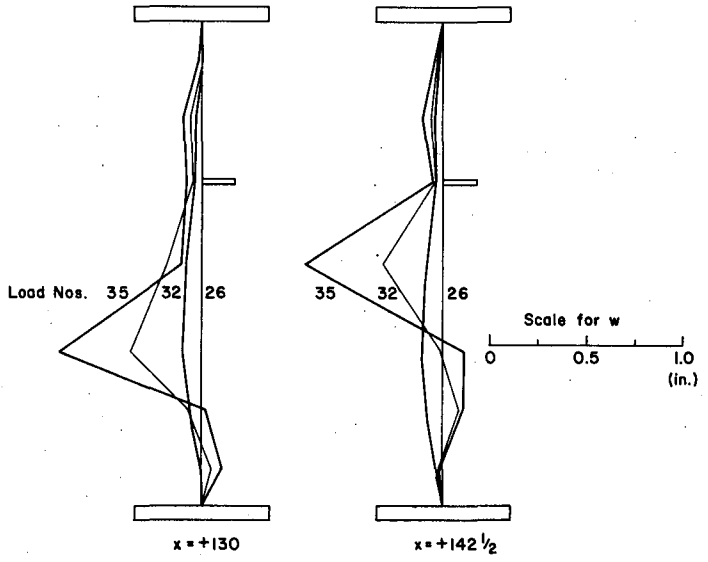


Fig. 3.25 Web Deflections (Test LS3-T3)

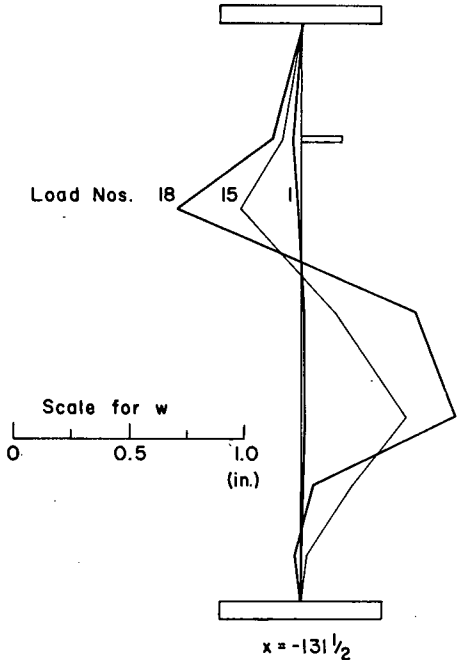


Fig. 3.26 Web Deflections (Test LS4-T1)

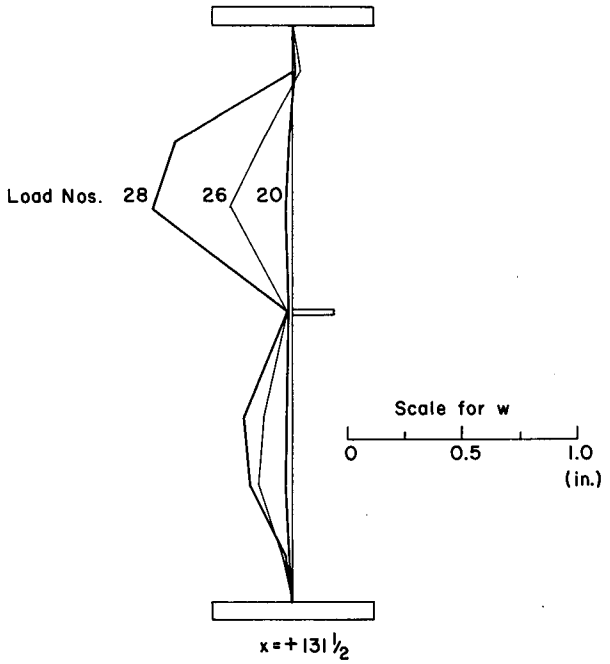


Fig. 3.27 Web Deflections (Test LS4-T2)

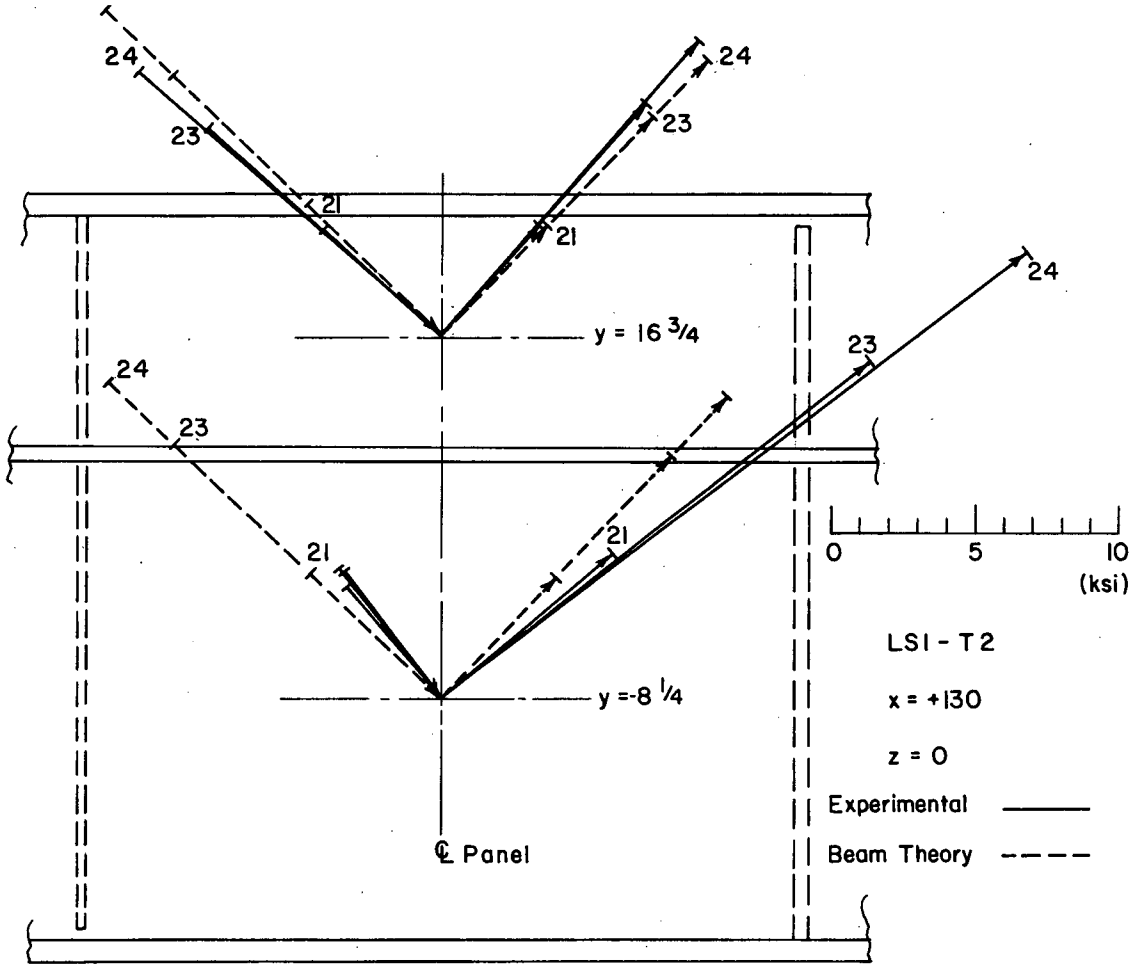


Fig. 3.28 Principal Stresses in Web of Girder LS1, Test T2

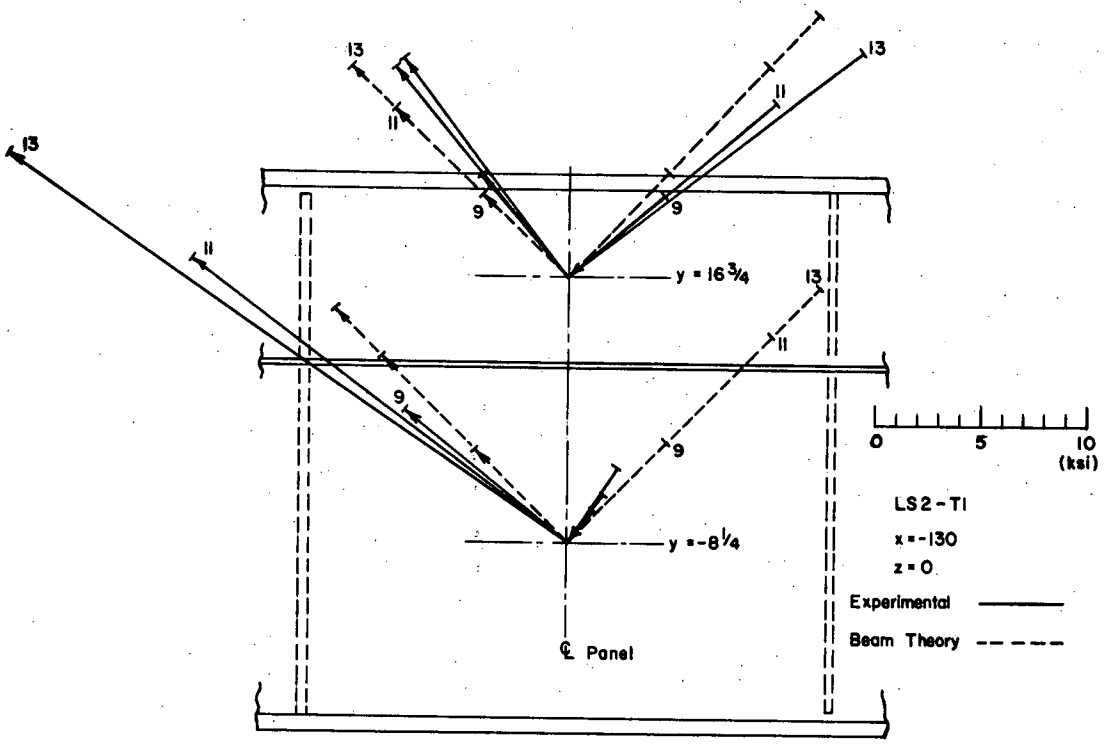


Fig. 3.29 Principal Stresses in Web of Girder LS2, Test T1

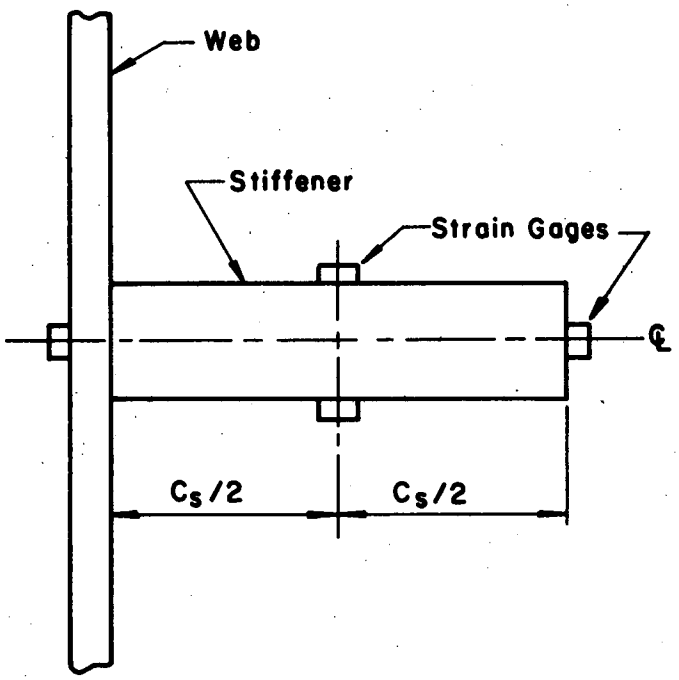


Fig. 3.30 Locations of Strain Gages on Stiffeners

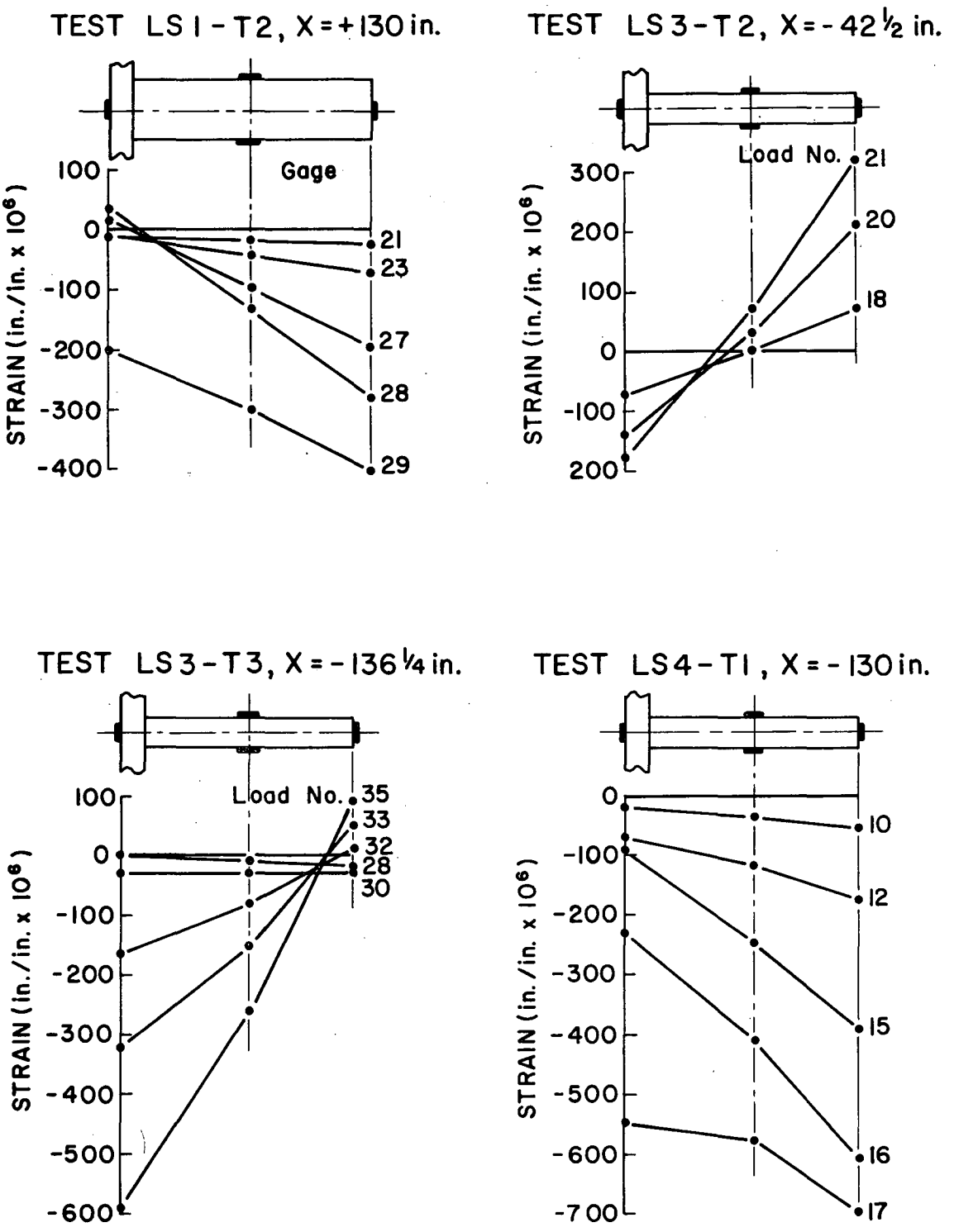


Fig. 3.31 Typical Longitudinal Stiffener Strain Data

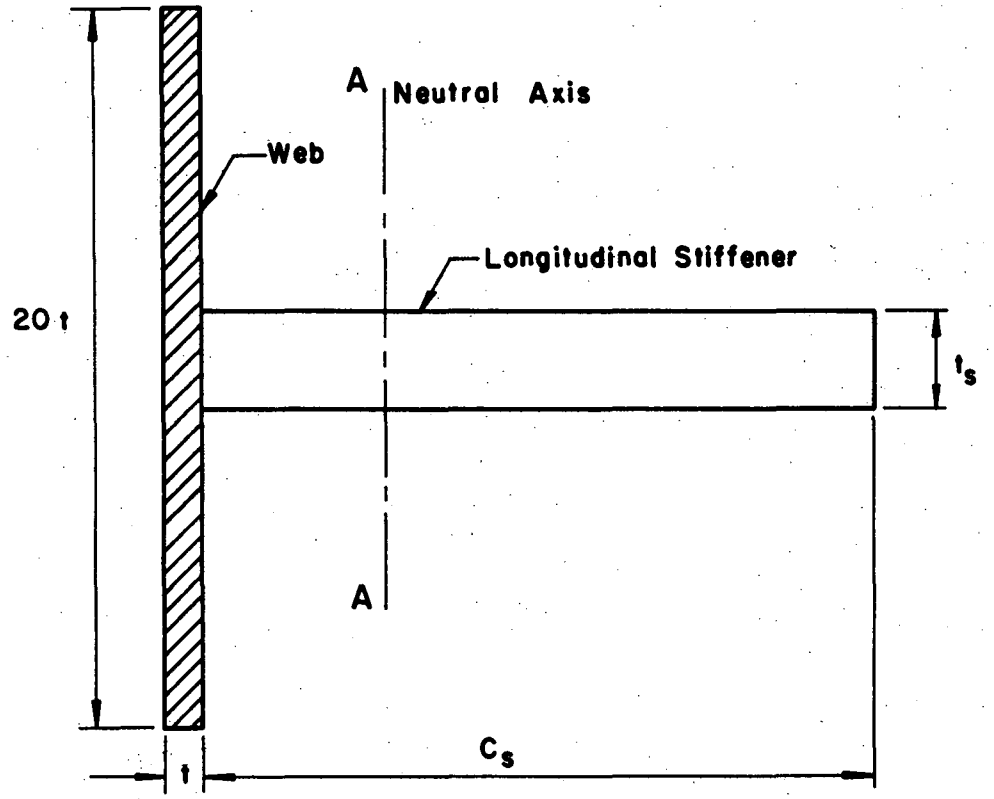


Fig. 3.32 Assumed Stiffener Section

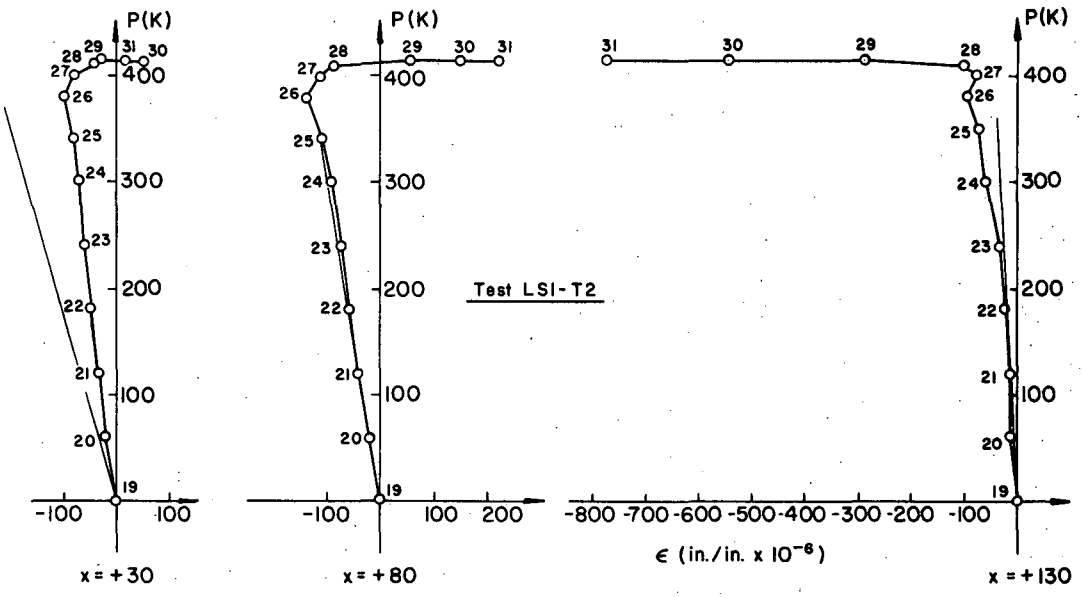


Fig. 3.33 Longitudinal Stiffener Axial Strains, Test LS1-T2

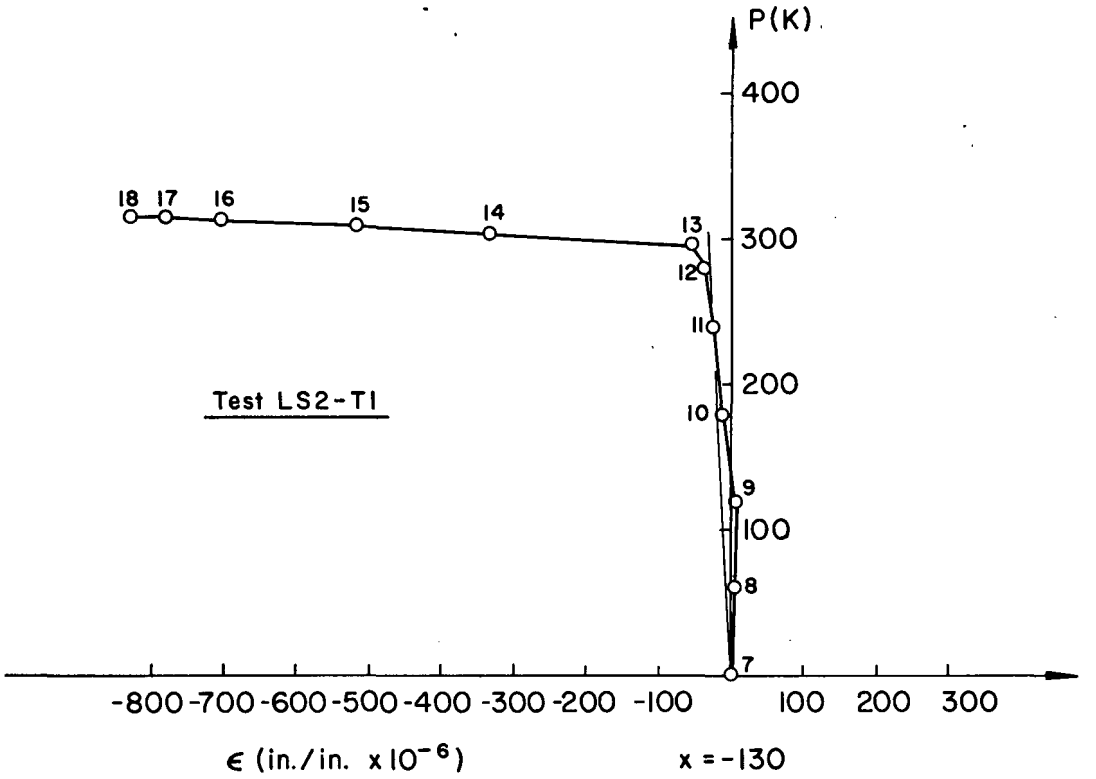


Fig. 3.34 Longitudinal Stiffener Axial Strains, Test LS2-T1

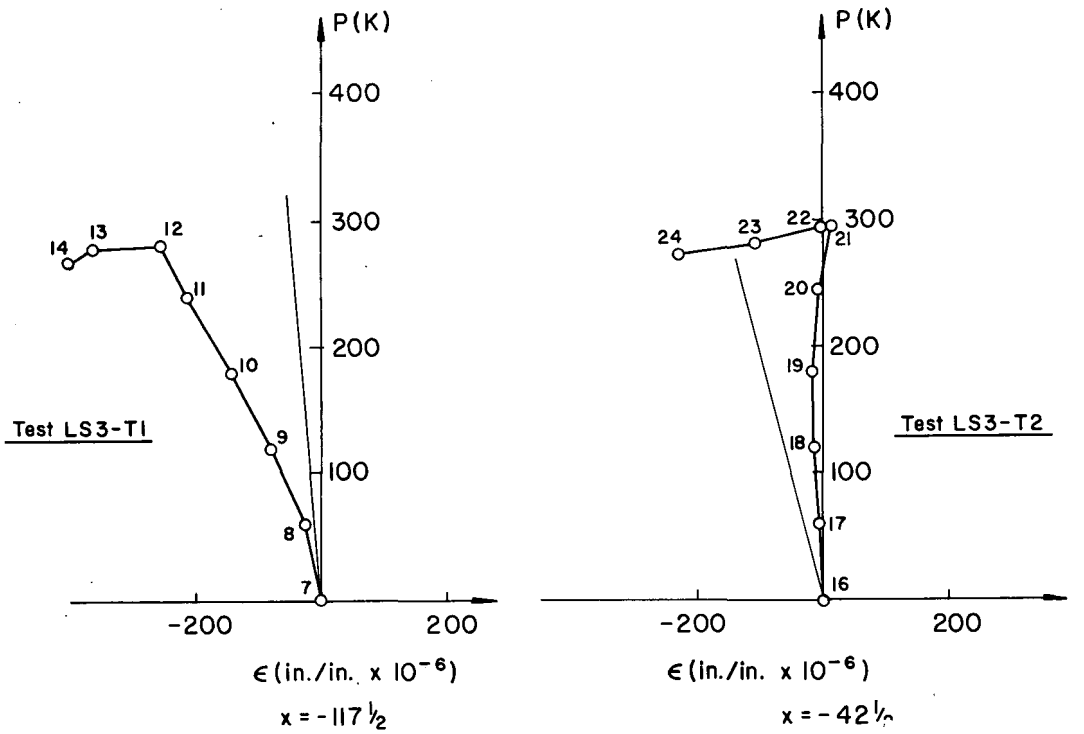


Fig. 3.35 Longitudinal Stiffener Axial Strains, Tests LS3-T1 & T2

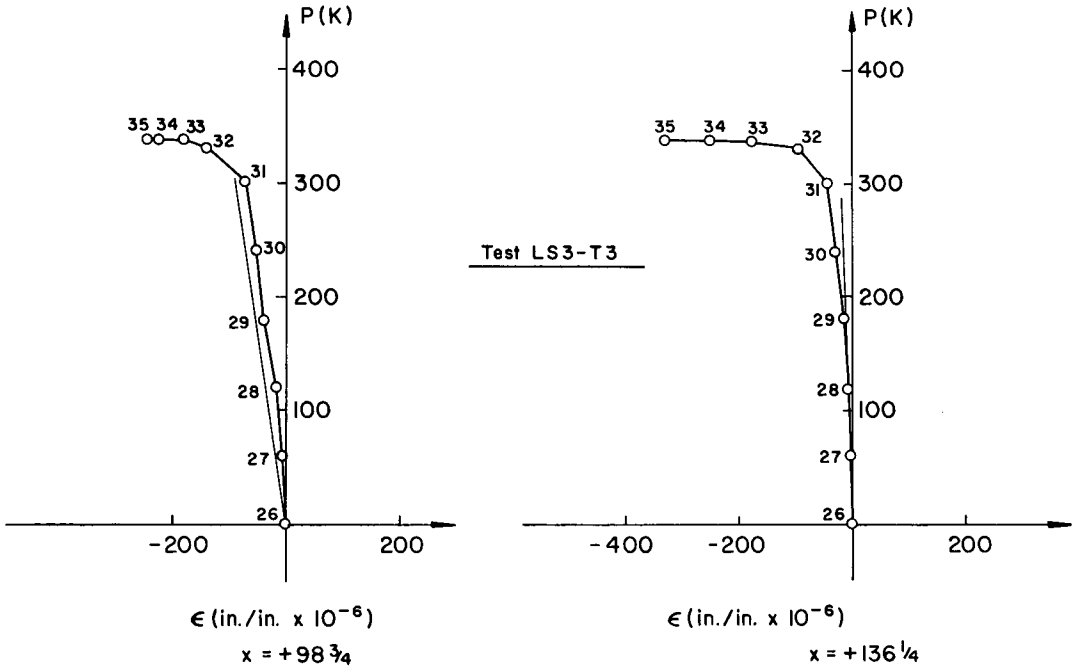


Fig. 3.36 Longitudinal Stiffener Axial Strains, Test LS3-T3

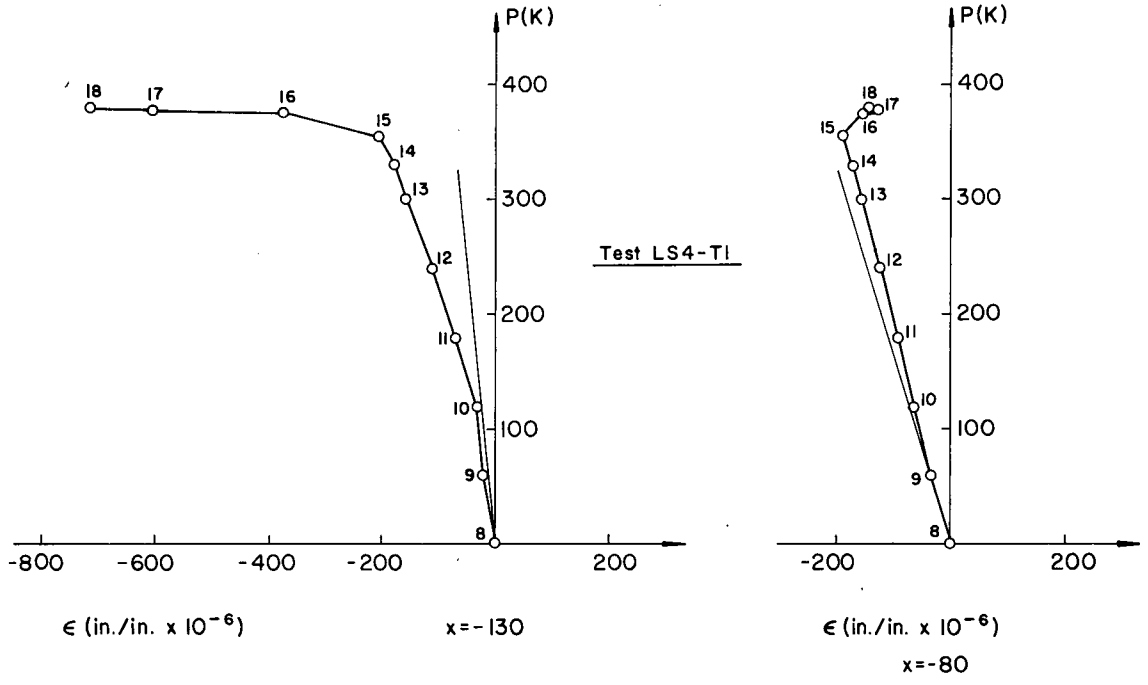


Fig. 3.37 Longitudinal Stiffener Axial Strains, Test LS4-T1

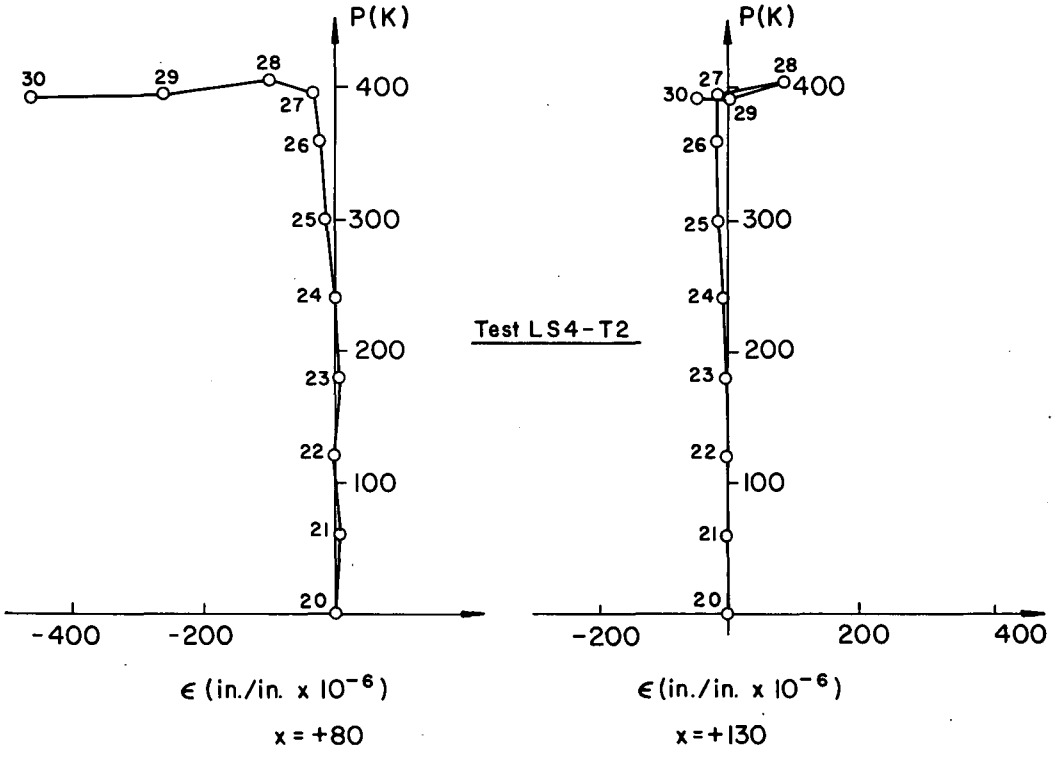


Fig. 3.38 Longitudinal Stiffener Axial Strains, Test LS4-T2

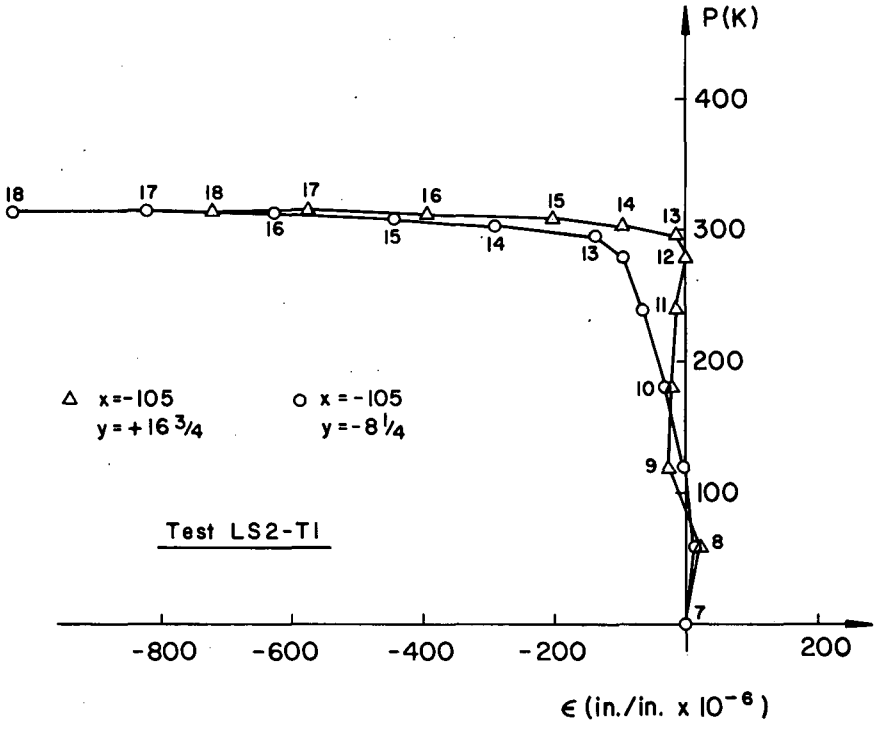


Fig. 3.39 Transverse Stiffener Axial Strains, Test LS2-T1

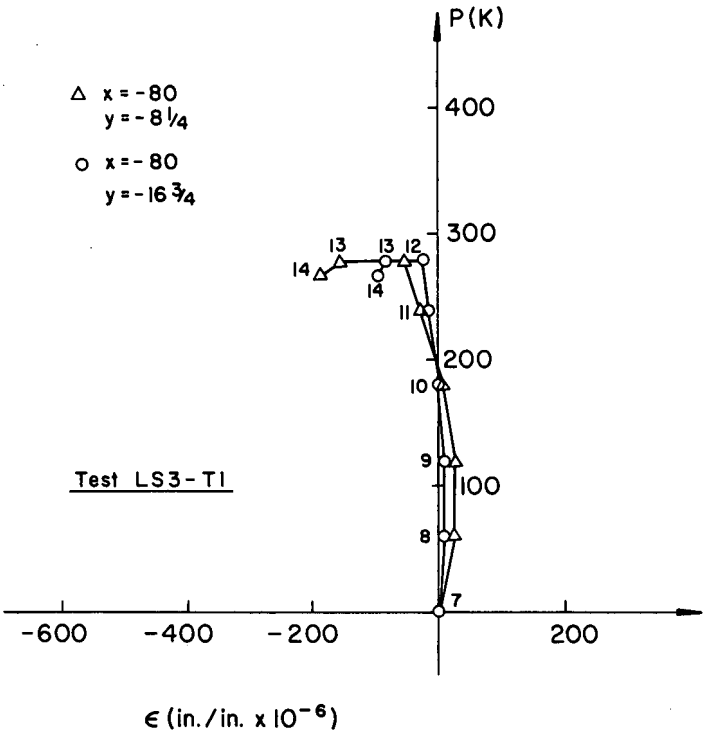


3.40 Transverse Stiffener Axial Strains, Test LS3-T1

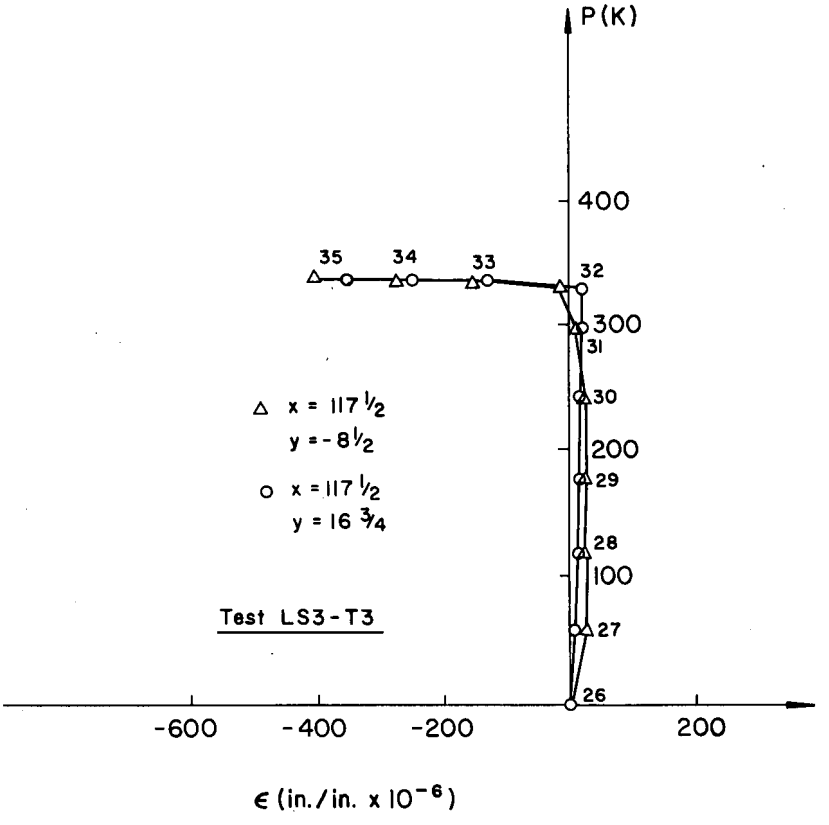


Fig. 3.41 Transverse Stiffener Axial Strains, Test LS3-T3

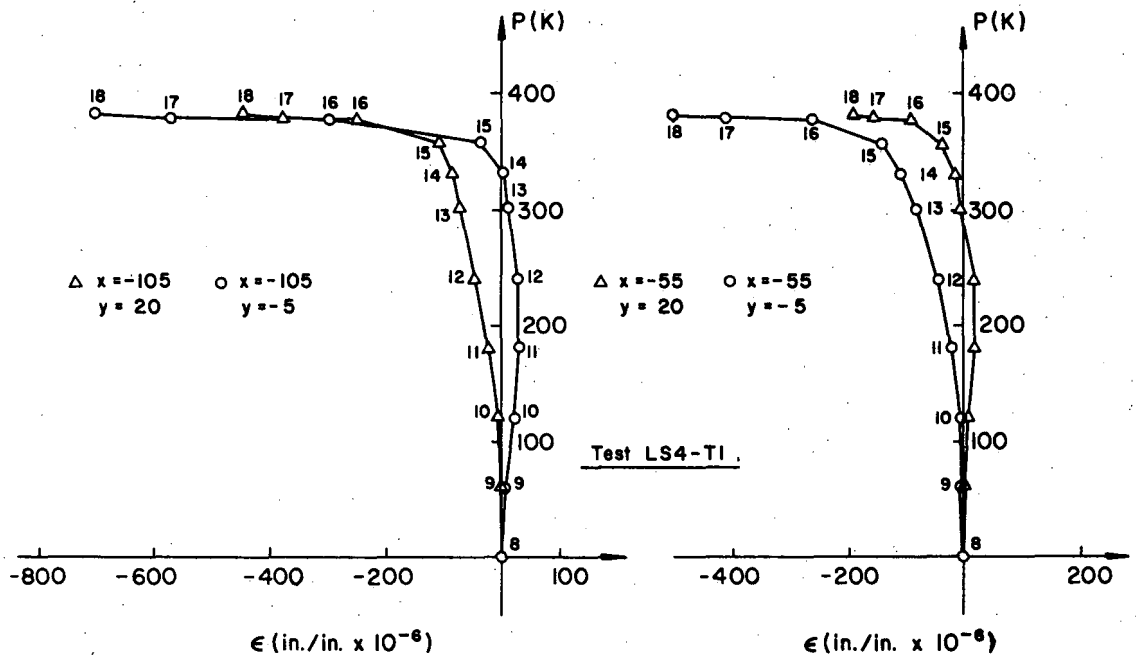


Fig. 3.42 Transverse Stiffener Axial Strains, Test LS4-T1

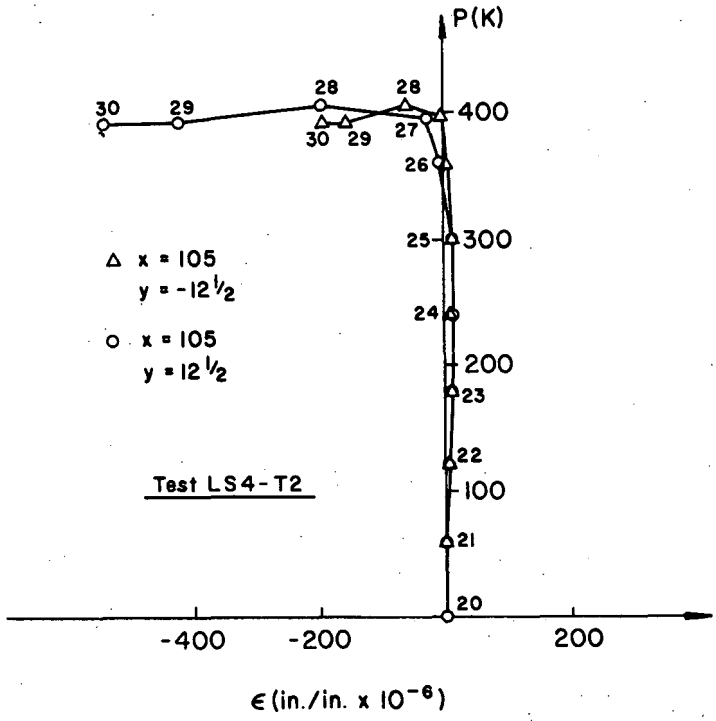


Fig. 3.43 Transverse Stiffener Axial Strains, Test LS4-T2

## REFERENCES


1. K. Basler and B. Thürlimann
STRENGTH OF PLATE GIRDERS IN BENDING, Proc., ASCE, Vol. 87, No. ST6, August, 1961

2. K. Basler
STRENGTH OF PLATE GIRDERS IN SHEAR, Proc., ASCE, Vol. 87, No. ST7, October, 1961

3. K. Basler
STRENGTH OF PLATE GIRDERS UNDER COMBINED BENDING AND SHEAR, Proc., ASCE, Vol. 87, No. ST7, October, 1961

4. K. Basler, B. T. Yen, J. A. Mueller and B. Thürlimann
WEB BUCKLING TESTS ON WELDED PLATE GIRDERS, Bulletin No. 64, Welding Research Council, New York, September, 1960

5. American Institute of Steel Construction, Inc.
MANUAL OF STEEL CONSTRUCTION, 6th Edition, 1963

6. P. B. Cooper
BENDING AND SHEAR STRENGTH OF LONGITUDINALLY STIFFENED PLATE GIRDERS, Fritz Engineering Laboratory Report No. 304.6, September, 1965

7. F. Stussi, C. Dubas and P. Dubas
LE VOILEMENT DE L'ÂME DES POUTRES FLÉCHIES, AVEC RAIDISSUER AU CINQUIÈME SUPÉRIEUR, Pub. IABSE, Vol. 17, 1957, p. 217 (THE BUCKLING DUE TO BENDING OF WEBS OF BEAMS HAVING STIFFENERS IN THE TOP FIFTH OF THE WEB)

8. Klöppel, K. and Scheer, J. S.
BEULWERTE AUSGESTEIFTER RECHTECKPLATTEN, Verlog von Wilhelm Ernst & Sohn, Berlin, 1960

9. American Association of State Highway Officials
STANDARD SPECIFICATIONS FOR HIGHWAY BRIDGES, 1961

10. Deuscher Normenausschuss
DIN 4114 (German Buckling Specifications), Blatt 1 und 2, Beuth-Vertrieb GmbH, Berlin and Cologne, July, 1952

11. British Standards Institution
BRITISH STANDARD 153 : STEEL GIRDER BRIDGES, Parts 3B and 4, British Standards House, London, 1958

12. K. Basler
FURTHER TESTS ON WELDED PLATE GIRDERS, Proc., AISC National Engineering Conference, 1960

13. P. B. Cooper
PLATE GIRDERS, Chapter 8 of "Structural Steel Design", The Ronald Press, 1964

14. Massonnet, C.
STABILITY CONSIDERATIONS IN THE DESIGN OF STEEL PLATE GIRDERS, Proc., ASCE, Vol. 86, No. ST1, January, 1960

## ACKNOWLEDGEMENTS

This report was prepared as part of a research project on longitudinally stiffened plate girders conducted in the Department of Civil Engineering, Fritz Engineering Laboratory, Lehigh University, Bethlehem, Pennsylvania. Professor William J. Eney is Head of the Department and Laboratory and Dr. Lynn S. Beedle is Director of the Laboratory.

The sponsors of the research project are the Pennsylvania Department of Highways, the U. S. Department of Commerce-Bureau of Public Roads, the American Iron and Steel Institute, and the Welding Research Council. The research work is supervised by the Lehigh University Welded Plate Girder Subcommittee of the Welding Research Council. The interest and financial support of the sponsors and encouragement of the Committee are gratefully acknowledged.

The authors wish to thank the Project Directors, Dr. Theodore V. Galambos and Dr. Alexis Ostapenko, for their suggestions and guidance in planning and conducting the tests and in preparing the report. Assistance during the testing programs was provided by Joseph A. Corrado and Kyle E. Dudley. Miss Marilyn Courtright typed the report, John M. Gera prepared the drawings, and Richard N. Sopko took the photographs of the test specimens.